UNI ITY
OF M GAN
SEP 1957
ENGINEERING
LIBRARY

JOURNAL OF FLUID MECHANICS

VOLUME 2 PART 6

AUGUST 1957

Printed and Published by

TAYLOR & FRANCIS LTD

RED LION COURT, FLEET STREET, LONDON, E.C.4

The JOURNAL OF FLUID MECHANICS exists for the publication of theoretical and experimental investigations of all aspects of the mechanics of fluids, and is issued in six parts per volume.

Editor:

Dr. G. K. BATCHELOR, Cavendish Laboratory, University of Cambridge, Cambridge, England.

Assistant Editors:

Dr. T. B. BENJAMIN, Dr. I. PROUDMAN.

Associate Editors:

Prof. G. F. CARRIER, Pierce Hall, Harvard University, Cambridge 38, Massachusetts, U.S.A.

Dr. W. C. GRIFFITH, Research and Development Laboratory, Missile Systems Division, Lockheed Aircraft Corporation, Palo Alto, California, U.S.A.

Prof. M. J. LIGHTHILL, Department of Mathematics, The University, Manchester, England.

Authors wishing to have papers published in the JOURNAL should communicate them to any one of the persons named above, choosing one in their own country where possible.

Authors are urged to ensure that their papers are written clearly and attractively, in order that their work will be readily accessible to readers.

Manuscripts should be typed in double spacing on one side of the paper only, with references listed at the end in alphabetical order of authors. Drawings should be done on a large scale in Indian ink on tracing cloth or drawing paper, captions being typed on a separate sheet. Proofs of papers from overseas will usually be despatched to authors by airmail. Authors are entitled to receive 50 offprints of a paper in the JOURNAL free of charge, and additional offprints can be purchased from the publisher.

PRICE £1 ($2.80) per part

Subscription, £5 10s. 0d. per volume of six parts, post free ($15.40 in U.S.A. and Canada)

Agents for U.S.A. and Canada:

Academic Press Inc., 111 Fifth Avenue, New York 3, N.Y., U.S.A.

The production of uniform shear flow in a wind tunnel

By P. R. OWEN and H. K. ZIENKIEWICZ
Mechanics of Fluids Department, University of Manchester

(*Received* 3 *May* 1957)

SUMMARY

A nearly uniform shear flow was obtained in the working section of a wind tunnel by inserting a grid of parallel rods with varying spacing.

The function of such a grid is to impose a resistance to the flow, so graded across the working section as to produce a linear variation in the total pressure at large distances downstream without introducing an appreciable gradient in static pressure near the grid. A method of calculating a suitable arrangement of the rods is described. Although this method is strictly applicable only to weakly sheared flows, an experiment made with a grid designed for a shear parameter as large as 0·45 gave results in close agreement with the theory. There was no evidence from the experiment of any large-scale secondary flow accompanying the shear—a danger inherent in an empirical attempt to grade the resistance of the grid—nor was any tendency observed for the shear to decay with increasing distance from the grid.

1. INTRODUCTION

A simple method of obtaining a two-dimensional shear flow $u(y)$ with vorticity ω_z in a wind tunnel is to insert near the beginning of the working section a grid of parallel rods in which the distance between adjacent rods varies in the y-direction, as sketched in figure 1. The effect of such an arrangement is clearly to produce a grading in the resistance of the grid which in turn gives rise to a non-uniform (irrotational) flow upstream of the grid and a non-uniform distribution of total pressure downstream of it. If it were possible to select a resistance grading such that the gradient of total pressure far downstream of the grid were constant, the vorticity ω_z would also be constant.

In principle it should not be difficult to devise empirically a grid which satisfies approximately the above condition on total pressure gradient (a remark on the feasibility of realizing it in practice is made in § 5), but such an approach carries with it the danger of introducing secondary vorticity components ω_x, ω_y since the variation of total pressure near the downstream face of the grid might include large static pressure gradients.

The method of grid design described in this paper has as its purpose the calculation of a resistance grading corresponding to a constant total

pressure gradient far downstream together with a predictable and, if possible, small static pressure gradient near the grid, and is applicable to weakly-sheared flows in the sense that the maximum change in velocity across the wind tunnel is small compared with the mean velocity.

On the basis of the method, a particular grid was designed and tested in a wind tunnel with a working section 20 in. square at a mean speed, near the tunnel axis, of approximately 75 ft. sec^{-1}. Static pressure and Pitot pressure traverses across the working section at a number of stations downstream of the grid revealed, over a large part of the area, an approximately linear velocity distribution, $u(y)$, which was almost invariant with both x and z. Furthermore, the static pressure was found to be sensibly constant over planes parallel to the grid at distances from it of one tunnel width and greater; the region in the immediate vicinity of the grid could not be explored with a conventional static probe for reasons explained in § 5.

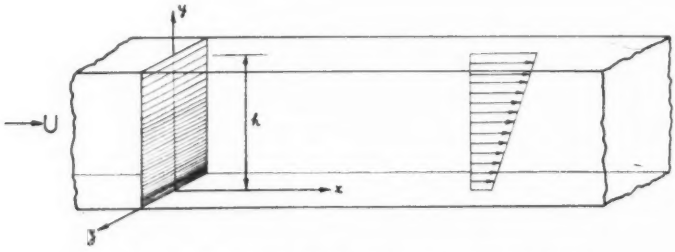

Figure 1. Arrangement of the grid and coordinate system.

One of the objects of producing a shear flow on a large scale is to examine the flow about bodies in a stream of uniform vorticity, and thereby to undertake the experimental counterpart of theoretical investigations made principally by Hawthorne & Martin (1955) and Lighthill (1956). It is hoped to report later on the results of these experiments.

2. Method of grid design

The wind tunnel may be treated as a long channel with walls $y = 0$, $y = h$, in which a grid is placed in the plane $x = 0$. At great distances upstream the velocity is uniform and has the value U; far downstream the velocity is again parallel to the walls and its magnitude is given by

$$u = U + \lambda(y - \tfrac{1}{2}h). \tag{1}$$

We suppose the fluid is inviscid and that $\lambda h/U$ is so small that the departure of any streamline from a straight line is correspondingly small. Accordingly, the stream function may be written

$$\begin{aligned} \psi &= Uy + \psi', && x < 0, \\ &= Uy + \tfrac{1}{2}\lambda(y^2 - hy) + \psi', && x > 0, \end{aligned} \tag{2}$$

where ψ', which is everywhere small compared with Uh and tends to zero as $x \to \pm\infty$, satisfies $\nabla^2\psi' = 0$. Appropriate solutions satisfying the boundary conditions

$$\frac{\partial\psi'(x,0)}{\partial x} = \frac{\partial\psi'(x,h)}{\partial x} = 0$$

for all x are

$$\frac{\psi'}{Uh} = \sum_{n=1}^{\infty} A_n e^{n\pi x/h}\sin(n\pi y/h), \qquad x < 0,$$

$$= \sum_{n=1}^{\infty} B_n e^{-n\pi x/h}\sin(n\pi y/h), \qquad x > 0. \tag{3}$$

The presence of the grid requires that (i) $\partial\psi/\partial y$ is continuous through $x = 0$, (ii) the velocity component $\partial\psi/\partial x$ obeys a certain refraction condition across $x = 0$, and (iii) the difference between the total pressures on a given streamline for large positive and negative values of x must be equal to the resistance per unit area imposed by the grid. To these may be added the condition that the static pressures far upstream and far downstream of the grid are independent of y.

Condition (i) leads to

$$\pi\sum_{n=1}^{\infty} nA_n\cos(n\pi y/h) - \pi\sum_{n=1}^{\infty} nB_n\cos(n\pi y/h) = \left(\frac{y}{h} - \frac{1}{2}\right)\frac{\lambda h}{U},$$

or, setting

$$\tfrac{1}{2}y(y-h) = h^2\sum_{n=1}^{\infty} C_n\sin(n\pi y/h),$$

$$A_n - B_n = C_n\lambda h/U. \tag{4}$$

The refraction condition (ii) requires the y-component of the velocity to change by a factor α in passing through the grid. α for a grid of uniform resistance is known to be $1{\cdot}1(1+K)^{-1/2}$, where K is the resistance coefficient (Taylor & Batchelor 1949), and it is unlikely that this value will be seriously in error for a grid with slightly graded resistance provided that K is given its local value. It follows that, if the resistance grading is represented by $K = K_0[1+\epsilon(y)]$, such that ϵ is small and $\int_0^h \epsilon\, dy = 0$,

$$\alpha = \frac{1{\cdot}1}{(1+K_0)^{1/2}}\left[1 - \frac{K_0\epsilon}{2(1+K_0)}\right] + O(\epsilon^2). \tag{5}$$

With α given by (5), the refraction condition is

$$\sum_{n=1}^{\infty} nB_n\sin(n\pi y/h) + (a+b\epsilon)\sum_{n=1}^{\infty} nA_n\sin(n\pi y/h) = 0,$$

which, noting that A_n and B_n are $O(\lambda h/U)$, reduces to

$$B_n + aA_n = 0 + O(\lambda h\epsilon/U), \tag{6}$$

where $a = 1{\cdot}1(1+K_0)^{-1/2}$.

Finally, we have to consider the change in total pressure along a streamline. According to the assumption of an inviscid fluid, the total pressure remains constant along streamlines upstream and downstream of the grid but, at the grid itself, there is a decrease in total pressure amounting to $K\frac{1}{2}\rho[u(0)]^2$. Hence,

$$p_0+\tfrac{1}{2}\rho U^2-p_1-\tfrac{1}{2}\rho[U+\lambda(y_1-\tfrac{1}{2}h)]^2=K\tfrac{1}{2}\rho[u(0)]^2, \tag{7}$$

where p_0 and p_1 are respectively the static pressures far upstream and far downstream of the grid. The streamline which has the ordinate y_1 for large x meets the grid at $y=y_0$, and the relation between y_0 and y_1 follows from (2);

$$y_1=y_0+\psi'(0,y_0)/U+O(\lambda\psi'/U^2). \tag{8}$$

Equation (8) implies that, to the first order in $\lambda h/U$ and ψ'/Uh, the x-component of the velocity at the grid is given by

$$u(0)=U+\lambda(y_0-\tfrac{1}{2}h)+\frac{\partial\psi'(0,y_0)}{\partial y}, \tag{9}$$

which, together with (7), leads to

$$\frac{p_0-p_1}{\frac{1}{2}\rho U^2}=K_0(1+\epsilon)+2\frac{\lambda h}{U}(1+K_0)\left(\frac{y_0}{h}-\frac{1}{2}\right)+\frac{2K_0}{U}\frac{\partial\psi'(0,y_0)}{\partial y}. \tag{10}$$

Since (p_0-p_1) is independent of y, (10) resolves into

$$\frac{p_0-p_1}{\frac{1}{2}\rho U^2}=K_0 \tag{11}$$

and

$$K_0\epsilon+2\frac{\lambda h}{U}(1+K_0)\left(\frac{y_0}{h}-\frac{1}{2}\right)+2\frac{K_0}{U}\frac{\partial\psi'(0,y_0)}{\partial y}=0. \tag{12}$$

The distribution $\epsilon(y_0)$ follows directly from (12) if we note from (3), (4) and (7) that

$$\frac{\partial\psi'(0,y_0)}{\partial y}=-\pi\lambda h^2\frac{a}{(1+a)}\sum_{n=1}^{\infty}nC_n\cos(n\pi y/h)=-\lambda h\frac{a}{(1+a)}\left(\frac{y_0}{h}-\frac{1}{2}\right); \tag{13}$$

hence,

$$\epsilon(y_0)=-2\frac{\lambda h}{U}\left(\frac{1}{K_0}+\frac{1}{1+a}\right)\left(\frac{y_0}{h}-\frac{1}{2}\right). \tag{14}$$

This result could have been arrived at without introducing the Fourier series, but the series representation (3) is useful for calculating streamlines and pressures away from the grid.

3. Pressures on the faces of the grid

Equations (9) and (13) demonstrate that, of the ultimate perturbation $\lambda(y-\frac{1}{2}h)$ to the velocity in the channel, a fraction $1/(1+a)$ appears at the grid and is produced irrotationally in the flow upstream. Clearly, as a approaches zero, a condition which could be realized by making K_0 very large, a progressively greater proportion of the velocity adjustment is achieved before the flow reaches the grid; consequently the static pressure on the downstream face of the grid must tend to a constant value consistent

with a uniform distribution of vorticity ω_z. (The static pressure on the *upstream* face will, of course, not be constant and we shall refer to its effect presently). Whilst the implication of this argument is clear enough as a criterion for avoiding the development of secondary circulation in the flow downstream of the grid, it is not very helpful in practice because there is always a limit to the value of the resistance beyond which a useful performance cannot be obtained from the wind tunnel in which the grid is placed.

To explore the possibility of a compromise between constancy of static pressure in the plane $x = +0$ and a tolerably small value of K_0—approximately 1, say—note that the pressure on the downstream face of the grid is given by

$$-C_p(+0, y_0) = \frac{p_0 - p(+0, y_0)}{\frac{1}{2}\rho U^2} = K_0 - \left(\frac{\lambda h}{U}\right)\frac{2a}{(1+a)}\left(\frac{y_0}{h} - \frac{1}{2}\right) + O\left(\frac{\lambda^2 h^2}{U^2}\right). \tag{15}$$

Although (15) shows that the pressure coefficient departs from a constant value only by $O(\lambda h/U)$ when K_0, and therefore a, are $O(1)$, it cannot be inferred immediately that such a pressure variation is acceptable unless the associated secondary vorticity, ω_x, is of a still smaller order of magnitude; for the primary (non-dimensional) vorticity $\omega_z h/U$ induced by the grid is itself only $O(\lambda h/U)$.

The development of secondary vorticity arises from the action of the pressure gradient $\partial p/\partial y$ on the fluid in the boundary layers on the tunnel walls at $z = \pm\frac{1}{2}h$. Such fluid, on account of its reduced velocity in the x-direction, more readily acquires a motion in the y-direction in response to the pressure gradient than the faster-moving fluid in the main stream. Once a cross-flow is well-established in the boundary layers a compensating flow must appear in the main stream in order to preserve continuity, and it follows that, if the maximum cross-flow velocity in the boundary layers is v', the secondary vorticity in the main stream will be $O(v'\delta/h^2)$, at most, where δ is the boundary layer thickness.

Now the maximum value of the pressure gradient $\partial p/\partial y$ is, from (15), $\rho U\lambda a/(1+a)$ on the downstream face of the grid, and it falls off with x like $e^{-\pi x/h}$. On the assumption of laminar boundary layers on the walls of the tunnel (it is known from experiments with curved pipes that the secondary flow in these circumstances is more powerful than when the flow is turbulent), a rough argument based on consideration of the balance between the flux of boundary-layer momentum in the y-direction and the combined forces due to the pressure gradient and skin friction indicates that the maximum value of v' attained some small distance downstream of the plane of the grid is $O(\lambda h)$. It follows that ω_x is $O(\lambda\delta/h)$ at most and, owing to the presence of the small factor δ/h, is of an order of magnitude smaller than ω_z. Since the boundary layers downstream of a grid are certain to be turbulent in any apparatus of useful dimensions, the mean resistance may safely be confined to values near 1.

Turning our attention to the flow upstream of the grid, we notice that any attempt to ameliorate the pressure gradient at $x > 0$ by increasing K_0 will result in an increased pressure gradient at $x < 0$, for the maximum values of $\partial p/\partial y$, which occur on the faces of the grid, are related by

$$\left(\frac{\partial C_p}{\partial y}\right)_{x=-0} = \frac{1}{a}\left(\frac{\partial C_p}{\partial y}\right)_{x=+0},$$

and so the danger of inducing a secondary circulation is merely transferred from $x > 0$ to the region $x < 0$. We have however already rejected the use of large K_0 on the grounds of wind tunnel performance, and it remains to consider the suitability of values of K_0 near 1. The problem can be disposed of quickly by appealing to the arguments of the preceding paragraph. The conclusions reached there hold equally well for the region $x < 0$, with the reservation that the increased severity of the transverse pressure gradient in the flow approaching the grid ($a < 1$ for $K_0 \doteqdot 1$) will be offset by the smaller boundary layer thickness on the vertical walls and by the attenuating action of the grid on any secondary vorticity that happened to develop.

4. Resistance grading

At large Reynolds numbers the resistance of a grid of rods in a uniform stream can be predicted with good accuracy if the drag coefficient based on the blocked area and the average interstitial velocity is taken to be 1 (Wieghardt 1953). For our present purpose it will be assumed permissible to adopt the same procedure for each portion of the grid, with the possible exception of places where the spacing changes rapidly with y, since the scale of variation in the y-direction of the velocity through the plane of the grid, $u(0)$, is much larger than the greatest spacing between adjacent rods. Accordingly, $K_0(1+\epsilon) = \xi(1-\xi)^{-2}$, where $\xi = d/s$; d is the diameter of each rod and the spacing is $s(y)$. With ϵ given by (14),

$$\frac{\xi}{(1-\xi)^2} = K_0\left[1 - 2\frac{\lambda h}{U}\left(\frac{1}{K_0} + \frac{1}{1+a}\right)\left(\frac{y}{h} - \frac{1}{2}\right)\right]. \tag{16}$$

It will be observed from (16) that the choice of K_0 is not entirely arbitrary, since for each value of K_0 there is a maximum value of $\lambda h/U$ which can be reached with a physically-realizable grid. This maximum, which is given in the following table, is governed by the condition that $\xi > 0$ at $y = h$.

K_0	0·2	0·4	0·6	0·8	1·0
$(\lambda h/U)_{\max}$	0·18	0·33	0·45	0·56	0·64

5. Experiment

A grid composed of parallel rods of 0·125 in. diameter was constructed according to (16) with $\lambda h/U = 0{\cdot}45$ and $K_0 = 1{\cdot}15$. A conservative choice of K_0, as compared with the values shown in the table above, was considered

desirable in order to avoid unduly rapid rates of change of the rod spacing with y near $y/h = 1$. The appropriate values of ξ are shown in figure 2, which also contains the values measured on the centre-line, $z = 0$, of the grid after it was built.

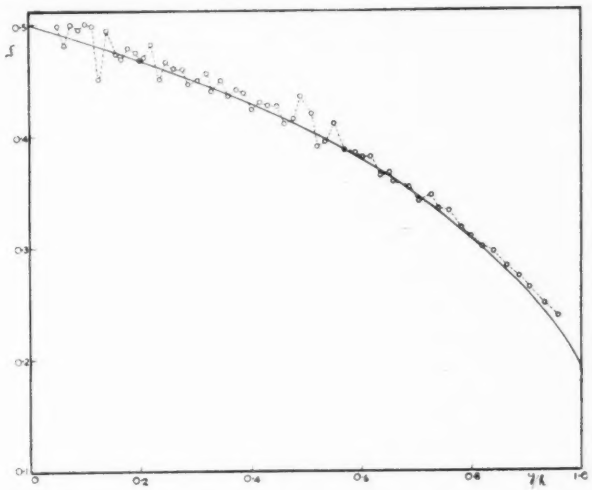

Figure 2. Spacing of the rods; ——— design values of ξ, – – o – – o – – measured values on the grid centre-line.

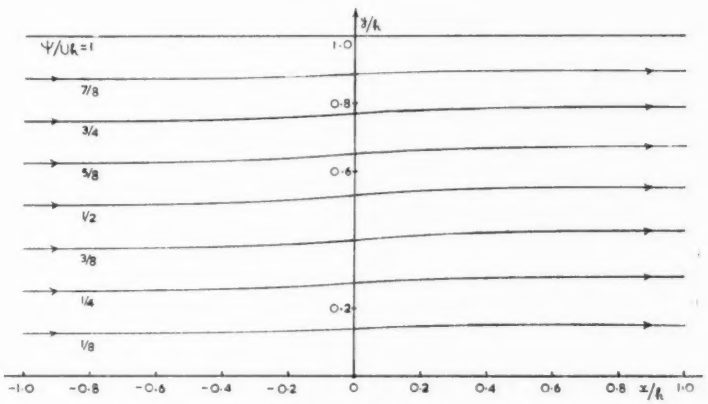

Figure 3. Calculated streamline pattern for $\lambda h/U = 0{\cdot}45$ and $K_0 = 1{\cdot}15$.

The grid was placed at the entrance to the working section, 20 in. square, of the low-turbulence wind tunnel at the Mechanics of Fluids Laboratory. Traverses across the working section in planes parallel to the grid at a number of distances from it were made with Pitot and static tubes of 1 mm outside diameter at a mean windspeed U of roughly 75 ft. sec^{-1}.

No variation in static pressure could be detected from the traverses, which were confined to distances greater than approximately one tunnel height from the grid. The grid could not be approached much more closely with a conventional static probe owing to an appreciable inclination and curvature of the streamlines, the predicted pattern of which is shown in figure 3.

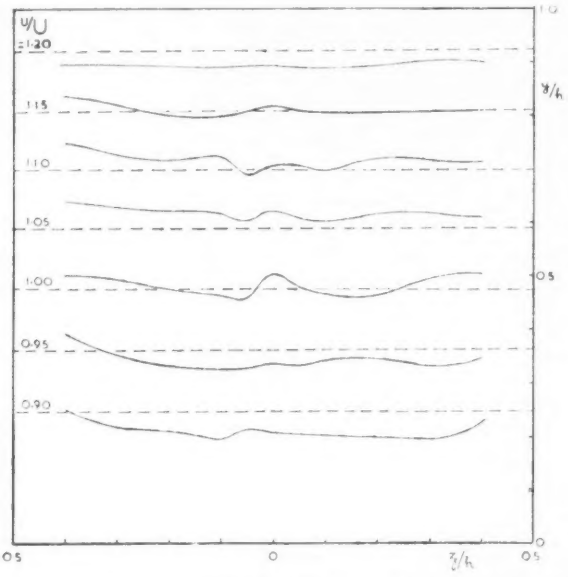

Figure 4. Velocity contours in the plane $x/h = 3$; ——— measured, – – – – – calculated.

The contours of u/U as deduced from the Pitot and static pressure traverses in a plane parallel to the grid and 5 ft. ($x/h = 3$) downstream of it are shown in figure 4. The absence of any systematic departure from lines parallel to the z-axis, together with the previously-mentioned fact that the static pressure is constant over the region, suggests that no secondary flow was present on a large scale.

The profiles of u/U in the plane of symmetry of the tunnel, $y = 0$, at distances of 2, 5 and 7 ft. from the grid ($x/h = 1{\cdot}2$, $3{\cdot}0$, $4{\cdot}2$) are presented in figure 5. The most striking feature of this figure is the close agreement between the measured velocity distribution and that predicted by the theory: an agreement which is remarkable in view of the fact that the grid was designed for a value of $\lambda h/U$ of 0·45, which could hardly be accepted as small enough to come within the scope of a linear theory. To be sure, the presumed effects of neglecting squares and higher powers of $\lambda h/U$ can be interpreted in the experimental velocity profile as a deficit in the average rate of shear together with a small departure from linearity, although the latter effect is equally likely to be due to an inadequacy in the method of relating

the spacing of the rods to the local resistance. (The curvature of the velocity profile in figure 5 is most marked in the interval $0{\cdot}70 < y/h < 0{\cdot}95$, where according to figure 2, ξ changes rapidly with y/h.)

The small-scale irregularities in the velocity profile, which were found to be repeatable in the experiments, can be attributed to inaccuracies in the manufacture of the grid, as displayed in figure 2, and a detailed examination of the measurements (not all of which, for the sake of clarity, are reproduced in figure 5) suggested that the small amplitude waviness

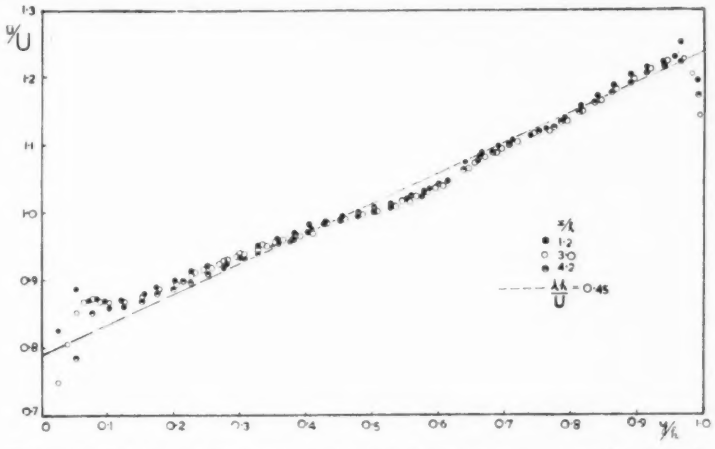

Figure 5. Velocity profiles measured in the plane of symmetry of the tunnel.

of the velocity profile in the region $y/h < 0{\cdot}5$ could be associated with the corresponding abrupt fluctuations in ξ. In particular, the pronounced dip in the velocity profile near $y/h = 0{\cdot}5$ might be caused by the error in ξ at roughly the same value of y/h; for it is easily shown that the change in u/U brought about by a small change in ξ in the interval

$$y - \tfrac{1}{2}\Delta y < y < y + \tfrac{1}{2}\Delta y$$

is given by*

$$\Delta\xi = -\frac{1}{K_0^2}\left(1+\frac{K_0}{1+a}\right)\left(\frac{1+2K_0}{(1+4K_0)^{1/2}}-1\right)\frac{\Delta u}{U}, \tag{17}$$

provided that outside the interval ξ is altered by a constant amount so as to preserve the condition $\int_0^h \epsilon\, dy = 0$. In the present case, with $K_0 = 1{\cdot}15$, $a = 0{\cdot}75$ and $\Delta\xi \doteqdot 0{\cdot}015$, (17) gives $\Delta u/U \doteqdot -0{\cdot}03$, which is near to the

* This relation offers the possibility of an iterative method of designing the grid, by adjusting ξ to compensate for the differences between the required velocity profile and that observed in an initial experiment. Such complication was not considered necessary for the case considered here, although in choosing a design value of $\lambda h/U$ as large as 0·45 we were anticipating an iterative approach.

observed amplitude of the dip ($\Delta u/U \doteqdot -0{\cdot}02$). Closer agreement could not be expected because the error $\Delta\xi$, being caused by a sag in some of the rods rather than a bodily displacement, is not independent of z, and the resulting distortion of the flow from that of nearly-uniform shear is essentially three-dimensional and must resemble the effect of a wake embedded in the stream. Indeed, a comparison between the observed velocity profiles at $z/h = 0$ and $z/h = -0{\cdot}2$ displayed in figure 6 for $x/h = 3$ shows that the dip had almost disappeared at $z/h = -0{\cdot}2$ (4 in. from the central plane of the tunnel).

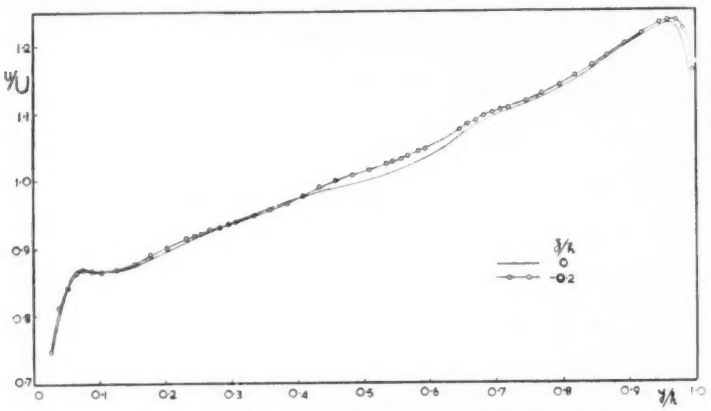

Figure 6. Velocity profiles for $z = 0$ and $z/h = -0{\cdot}2$ measured at $x/h = 3$.

The above calculation provides a stricture on the remark made in the Introduction that it might not be difficult (in principle) to devise empirically the correct spacing between the rods, because the misalignment that gave rise to the error 0·015 in ξ amounted only to 0·02 in. The chance of adjusting by experiment the positions of 62 rods, as used here, to an accuracy significantly greater than 0·02 in. seems very remote!

The velocity profiles of figure 5 exhibit complete departure from linearity near the walls, a behaviour evidently to be associated with the presence of the boundary layers. In this respect, two points require comment. In the first place, near each wall the velocity reaches a distinct peak which tends to subside with increasing distance from the grid. Secondly, the peak near $y = h$ occurs closer to the wall than that near $y = 0$. The appearance of these velocity peaks is due to the accelerating action of the pressure drop across the grid on the fluid in the boundary layer which, by virtue of its reduced velocity, suffers a smaller change in total pressure on passing through the grid than fluid in the main stream. Since the change in total pressure diminishes progressively as the wall is approached, whereas the static pressure is constant, the velocity in the boundary layer would, in the absence of shearing stresses, increase towards the wall. This tendency is however resisted by the shearing stresses and wall friction, with the result that a maximum velocity occurs in the outer part of the

boundary layer. With increasing distance from the grid, the shearing stresses smooth out the velocity peak, as can be seen in figure 5. The difference between the positions of the velocity maxima on the top and bottom walls is obviously a consequence of the difference in boundary layer thickness; for the boundary layer on the upper wall is subjected to a favourable pressure gradient whereas the pressure gradient on the lower wall is adverse, as is evident from the calculated wall pressure distribution shown in figure 7. The observed difference in boundary layer thickness on the upper and lower walls agreed quite well with a rough calculation based on Truckenbrodt's method (Schlichting 1955) using the pressure distributions of figure 7.

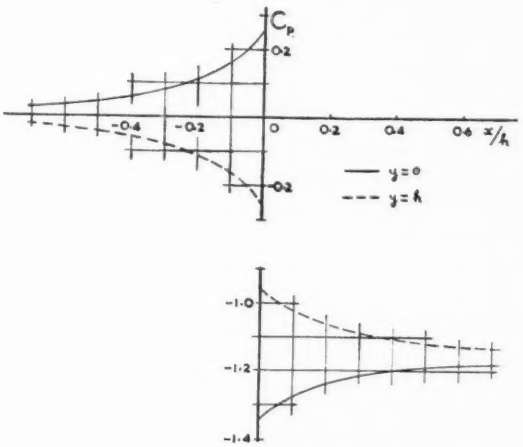

Figure 7. Calculated pressure distributions on the top and bottom walls of the tunnel; $\lambda h/U = 0{\cdot}45$, $K_0 = 1{\cdot}15$.

A final remark may be made on figure 5. Ostensibly there is no systematic change in the rate of shear between $x/h = 1{\cdot}2$ and $x/h = 4{\cdot}2$, and even the small irregularities in the velocity profile appear to suffer no appreciable decay. This is not entirely surprising, because a uniform shear flow would be expected to persist almost indefinitely if, as is likely, the turbulence generated at the grid gives rise to an approximately constant eddy viscosity. All modification to the rate of shear would then be confined to regions excluded from the action of a uniform shearing stress, that is, to the boundary layers on the tunnel walls, which only gradually encroach on the main stream.

References

Hawthorne, W. R. & Martin, M. E. 1955 *Proc. Roy. Soc.* A, **232**, 184.

Lighthill, M. J. 1956 *J. Fluid Mech.* **1**, 31.

Schlichting, H. 1955 *Boundary Layer Theory*. London: Pergamon Press.

Taylor, G. I. & Batchelor, G. K. 1949 *Quart. J. Mech. Appl. Math.* **2**, 1.

Wieghardt, K. E. G. 1953 *Aero. Quart.* **4**, 186.

An exact solution for progressive capillary waves of arbitrary amplitude

By G. D. CRAPPER
Department of Mathematics, University of Manchester

(*Received* 4 *March* 1957)

SUMMARY

An exact solution is found in a fairly simple form for two-dimensional progressive waves of arbitrary amplitude on a fluid of unlimited depth, when only surface tension and not gravity is taken into account as the restoring force. The calculated wave forms are exhibited graphically for various amplitudes, and the relation between wave velocity and amplitude is plotted. The wave of greatest height occurs when the vertical distance between trough and crest is 0·730 wavelengths (compared with 0·142 for gravity waves). Higher waves are prevented from appearing by the enclosing of air bubbles in the troughs.

1. INTRODUCTION

Periodic gravity waves of finite amplitude have been investigated by Stokes (1847; 1880, pp. 197 & 314; see also Lamb 1932, § 250) and others, and a good approximate solution has been found. The gravity wave of greatest height has also been determined (Stokes 1880, p. 225). It is therefore interesting to see if analogous solutions can be obtained for purely capillary waves, for which gravity is neglected; it is particularly interesting as a first step towards investigating the problem of waves of finite amplitude under the combined effects of gravity and surface tension.

Capillary waves are found to be remarkable in that an exact solution exists for arbitrary amplitude. The case where the fluid has infinite depth was considered first, and, following Stokes, a series approach was made. Inspection revealed regularities in the coefficients, however, and the series obtained by assuming that these regularities continued in the higher terms was found to have a sum in closed form. This sum was then shown to be an exact solution. From this original investigation the present method, leading directly to the solution, was evolved. The present method indicates that there is also an exact solution if the fluid has finite uniform depth. The analysis is, however, rather complicated, involving elliptic functions, and the solution is not considered worth evaluating in detail.

The solution for infinite depth shows that the wave velocity given by the theory of waves of infinitesimal amplitude (Lamb 1932, § 265 & § 266) is accurate only for zero amplitude and that, if the wavelength is fixed, the velocity decreases as the amplitude increases. This behaviour is exactly

opposite to that of gravity waves. The waves themselves are very rounded in section, and the wave of greatest height is reached when the surface bends back to touch itself, enclosing a bubble of air.

2. Equations of motion in the (ϕ, ψ)-plane

Our investigation will be confined to two-dimensional travelling waves on the surface of an ideal fluid which has infinite depth. It is convenient to choose Cartesian axes with x measured horizontally to the left and y vertically downwards. To make the flow steady we bring the waves to rest by superimposing a uniform velocity on the system, and therefore we assume that the undisturbed fluid (that is, the fluid at great depths) is moving in the positive x-direction with velocity c, the wave velocity.

If the motion is generated from rest, the flow must be irrotational, and so the equation of motion is

$$\frac{\partial^2\phi}{\partial x^2} + \frac{\partial^2\phi}{\partial y^2} = 0, \tag{1}$$

where ϕ is the velocity potential of the flow. The stream function ψ also satisfies this equation.

In a steady flow the surface is a streamline, say $\psi = 0$, and Bernoulli's equation holds, so we have

$$p/\rho + \tfrac{1}{2}q^2 = \tfrac{1}{2}c^2. \tag{2}$$

Here p represents the difference of pressure from its hydrostatic value; the constant on the right is $\frac{1}{2}c^2$ because at great depths, where $q = c$, this difference is zero. Surface tension creates a pressure difference across the surface which is given by

$$p - p_0 = T/R, \tag{3}$$

where p is the pressure in the fluid at the surface, p_0 is the 'atmospheric' pressure, T is the surface tension, and R is the radius of curvature of the surface, counted positive when the centre of curvature lies inside the fluid. The use of p to represent the absolute pressure at the surface as well as its difference from the hydrostatic value is permissible since gravity is neglected as a restoring force. Now when R is positive, d^2y/dx^2 is positive, and so

$$\frac{1}{R} = \frac{d^2y/dx^2}{\{1+(dy/dx)^2\}^{3/2}}. \tag{4}$$

The boundary condition is therefore

$$\frac{T}{\rho}\,\frac{d^2y/dx^2}{\{1+(dy/dx)^2\}^{3/2}} + \tfrac{1}{2}q^2 = \tfrac{1}{2}c^2 \quad \text{on } \psi = 0. \tag{5}$$

As the fluid is of infinite depth there are the further conditions

$$\left.\begin{aligned} \frac{\partial\phi}{\partial x} &= \frac{\partial\psi}{\partial y} \to c, \\ \frac{\partial\phi}{\partial y} &= -\frac{\partial\psi}{\partial x} \to 0, \end{aligned}\right\} \quad \text{as } y \to \infty. \tag{6}$$

The problem as formulated is very complicated, but it becomes much simpler on taking new independent variables (ϕ, ψ) and new dependent variables (τ, θ), where $\tau = \log q$ and $(q\cos\theta, q\sin\theta)$ are the (x, y)-components of the velocity of the fluid.

On any streamline

$$\frac{1}{R} = \frac{d\theta}{ds}, \tag{7}$$

where ds is an elementary arc of the streamline, so

$$\frac{1}{R} = q\left(\frac{\partial\theta}{\partial\phi}\right)_{\psi=\text{const.}}, \tag{8}$$

and we can write (5) as

$$\frac{T}{\rho} q \frac{\partial\theta}{\partial\phi} + \tfrac{1}{2}q^2 = \tfrac{1}{2}c^2 \quad \text{on } \psi = 0. \tag{9}$$

This can be simplified further if we take $T/\rho c^2$ as unit of length and c as unit of velocity, and this gives

$$e^{\tau}\frac{\partial\theta}{\partial\phi} + \tfrac{1}{2}e^{2\tau} = \tfrac{1}{2} \quad \text{on } \psi = 0. \tag{10}$$

Thus, the boundary condition in the (ϕ, ψ)-plane is

$$\frac{\partial\theta}{\partial\phi} = -\sinh\tau \quad \text{on } \psi = 0. \tag{11}$$

If $w = \phi + i\psi$ and $z = x + iy$,

$$\frac{dw}{dz} = qe^{-i\theta}, \tag{12}$$

and

$$\log\left(\frac{dw}{dz}\right) = \tau - i\theta. \tag{13}$$

These must be regular functions, so we have, equivalent to the original equation of motion (1),

$$\frac{\partial^2\tau}{\partial\phi^2} + \frac{\partial^2\tau}{\partial\psi^2} = 0, \tag{14}$$

and for the same reason we can use the Cauchy–Riemann equations to write (11) as

$$\frac{\partial\tau}{\partial\psi} = -\sinh\tau \quad \text{on } \psi = 0. \tag{15}$$

In the new units $q \to 1$ as $y \to \infty$, so that the conditions (6) become

$$\tau \to 0 \quad \text{and } \theta \to 0 \quad \text{as } \psi \to \infty. \tag{16}$$

3. General solution for τ

To solve this non-linear problem we look for a solution of (14) which satisfies the equation

$$\frac{\partial\tau}{\partial\psi} = -f(\psi)\sinh\tau \tag{17}$$

everywhere in the flow, for some function $f(\psi)$. Such a solution will satisfy the boundary condition (15) provided that

$$f(0) = 1. \tag{18}$$

We can integrate (17) directly:

$$\operatorname{logtanh} \tfrac{1}{2}\tau = F(\psi) + G(\phi), \tag{19}$$

where

$$\frac{\partial}{\partial \psi} F(\psi) = -f(\psi) \tag{20}$$

and $G(\phi)$ is arbitrary, or

$$\tau = \log\left\{\frac{X(\psi) + Y(\phi)}{X(\psi) - Y(\phi)}\right\}, \tag{21}$$

where

$$X(\psi) = e^{-F(\psi)}, \tag{22}$$

and

$$Y(\phi) = e^{G(\phi)}. \tag{23}$$

Functions $X(\psi)$ and $Y(\phi)$ can now be determined so that Laplace's equation (14) is satisfied. For this to be so we must have

$$2\{(X'(\psi))^2 + (Y'(\phi))^2\} + \{X^2(\psi) - Y^2(\phi)\}\left\{\frac{Y''(\phi)}{Y(\phi)} - \frac{X''(\psi)}{X(\psi)}\right\} = 0. \tag{24}$$

Differentiating this with respect to ϕ and then with respect to ψ gives

$$(X^2(\psi))'\left(\frac{Y''(\phi)}{Y(\phi)}\right)' + \left(\frac{X''(\psi)}{X(\psi)}\right)'(Y^2(\phi))' = 0, \tag{25}$$

or

$$(X^2(\psi))'\Big/\left(\frac{X''(\psi)}{X(\psi)}\right)' + (Y^2(\phi))'\Big/\left(\frac{Y''(\phi)}{Y(\phi)}\right)' = 0. \tag{26}$$

Here each term must be merely a constant, say

$$(X^2(\psi))' = h\left(\frac{X''(\psi)}{X(\psi)}\right)' \tag{27}$$

and

$$(Y^2(\phi))' = -h\left(\frac{Y''(\phi)}{Y(\phi)}\right)'. \tag{28}$$

Integrating, we have

$$X^2(\psi) = h\frac{X''(\psi)}{X(\psi)} + l, \tag{29}$$

$$Y^2(\phi) = -h\frac{Y''(\phi)}{Y(\phi)} + m, \tag{30}$$

where l, m are arbitrary constants, and (24) reduces to

$$2(X'(\psi))^2 - X(\psi)X''(\psi) + m\frac{X''(\psi)}{X(\psi)} + 2(Y'(\phi))^2 - Y(\phi)Y''(\phi) + l\frac{Y''(\phi)}{Y(\phi)} = 0. \tag{31}$$

Hence

$$2(X'(\psi))^2 - X(\psi)X''(\psi) + m\frac{X''(\psi)}{X(\psi)} = n, \tag{32}$$

$$2(Y'(\phi))^2 - Y(\phi)Y''(\phi) + l\frac{Y''(\phi)}{Y(\phi)} = -n, \tag{33}$$

where, again, n is a constant.

From (29)
$$X''(\psi) = \frac{X(\psi)}{h}(X^2(\psi) - l), \tag{34}$$

and from (32)
$$2(X'(\psi))^2 = n + \frac{1}{h}(X^2(\psi) - l)(X^2(\psi) - m). \tag{35}$$

But differentiating (35) gives

$$X''(\psi) = \frac{X(\psi)}{2h}(X^2(\psi) - l + X^2(\psi) - m), \tag{36}$$

and therefore
$$l = m, \tag{37}$$

$$2(X'(\psi))^2 = n + \frac{1}{h}(X^2(\psi) - l)^2, \tag{38}$$

and similarly
$$2(Y'(\phi))^2 = -n - \frac{1}{h}(Y^2(\phi) - l)^2. \tag{39}$$

Thus the general solutions for $X(\psi)$ and $Y(\phi)$ satisfy

$$(X'(\psi))^2 = a_1 + a_2 X^2(\psi) + a_3 X^4(\psi), \tag{40}$$

$$(Y'(\phi))^2 = -a_1 - a_2 Y^2(\phi) - a_3 Y^4(\phi), \tag{41}$$

where a_1, a_2, a_3 are any constants.

The quadratic case ($a_3 = 0$) has been found to satisfy our requirements for fluid of infinite depth, but inspection of the full quartic has shown that it will give a solution when the fluid depth is finite. It has already been pointed out, however, that the analysis needed is too elaborate to make this solution worthwhile.

4. Details of solution

If we put $a_3 = 0$ in (40) and (41) we have

$$X(\psi) = (a_1/a_2)^{1/2}\sinh(\pm\psi a_2^{1/2} + C), \tag{42}$$

$$Y(\phi) = i(a_1/a_2)^{1/2}\sin(\pm\phi a_2^{1/2} + D), \tag{43}$$

where C, D are constants of integration. Clearly $\{Y(\phi)/X(\psi)\} \to 0$ as $\psi \to \infty$, so that the condition $\tau \to 0$ (16) is satisfied.

From (20) and (22),

$$f(\psi) = \frac{\partial}{\partial\psi}\log X(\psi) \tag{44}$$

$$= \pm k\coth(\pm k\psi + C), \tag{45}$$

writing k for $a_2^{1/2}$, and hence the boundary condition $f(0) = 1$ determines C:

$$C = \pm\{\log(\pm i/A)\}, \tag{46}$$

where
$$A^2 = \frac{k-1}{k+1}. \tag{47}$$

Now, by (21), (42) and (43),

$$\tau = \log\left\{\frac{\sinh(\pm k\psi + C) + \sinh(\pm ik\phi + iD)}{\sinh(\pm k\psi + C) - \sinh(\pm ik\phi + iD)}\right\} \tag{48}$$

$$= \log\frac{\tanh P}{\tanh Q}, \tag{49}$$

where

$$\left.\begin{aligned} P &= \tfrac{1}{2}(\pm k\psi + C \pm ik\phi + iD), \\ Q &= \tfrac{1}{2}(\pm k\psi + C \mp ik\phi - iD). \end{aligned}\right\} \tag{50}$$

Hence,

$$\frac{\partial\tau}{\partial\psi} = \pm\tfrac{1}{2}k\frac{\operatorname{sech}^2 P}{\tanh P} \mp \tfrac{1}{2}k\frac{\operatorname{sech}^2 Q}{\tanh Q} = \frac{\partial\theta}{\partial\phi}, \tag{51}$$

so that

$$\theta = i\log(\coth P \coth Q) \tag{52}$$

and $\theta \to 0$ as $\psi \to \infty$. Thus

$$\log\frac{dw}{dz} = \log\coth^2 Q, \tag{53}$$

and hence

$$\frac{dw}{dz} = \left(\frac{e^{\mp ikw + C - iD} - 1}{e^{\mp ikw + C - iD} + 1}\right)^2. \tag{54}$$

From (46),

$$e^C = \pm i/A \quad \text{or} \quad \mp iA, \tag{55}$$

and, as it only amounts to adding a constant to ϕ, it is permissible to put $D = \frac{1}{2}\pi$. Then we find that both the alternatives (55) lead to

$$\frac{dz}{dw} = \left(\frac{1 \mp Ae^{ikw}}{1 \pm Ae^{ikw}}\right)^2. \tag{56}$$

Taking the alternative sign is equivalent to adding a constant π/k to w (i.e. to ϕ), so the solution is unique:

$$z = w - \frac{4i}{k}\frac{1}{1 + Ae^{ikw}} + \frac{4i}{k}. \tag{57}$$

The constant has been chosen to make $z = w$ when $A = 0$. Returning to the original length and velocity units, we get

$$z = \frac{w}{c} - \frac{4i}{k}\frac{1}{1 + Ae^{ikw/c}} + \frac{4i}{k}. \tag{58}$$

If w is increased by $2\pi c/k$, the only effect is to increase z by $2\pi/k$, so we have, for the wavelength λ,

$$\lambda = 2\pi/k$$

$$= 2\pi\left(\frac{1 - A^2}{1 + A^2}\right)\frac{T}{\rho c^2}. \tag{59}$$

Hence

$$c = \left(\frac{2\pi T}{\lambda\rho}\right)^{1/2}\left(\frac{1 - A^2}{1 + A^2}\right)^{1/2}, \tag{60}$$

and

$$\frac{z}{\lambda} = \alpha - \frac{2i}{\pi}\frac{1}{1 + Ae^{2\pi i\alpha}} + \frac{2i}{\pi}, \tag{61}$$

where
$$\alpha = w/c\lambda, \tag{62}$$
and the range $0 \leqslant \alpha \leqslant 1$ is one wavelength. On the surface $\psi = 0$, $\alpha = (\phi/c\lambda)$ and
$$\left.\begin{aligned} \frac{x}{\lambda} &= \alpha - \frac{2}{\pi}\frac{A\sin 2\pi\alpha}{1+A^2+2A\cos 2\pi\alpha}, \\ \frac{y}{\lambda} &= \frac{2}{\pi} - \frac{2}{\pi}\frac{1+A\cos 2\pi\alpha}{1+A^2+2A\cos 2\pi\alpha}. \end{aligned}\right\} \tag{63}$$
From these relations it is easily seen that, if a is the amplitude of the wave, defined as the vertical height between trough and crest, then
$$\frac{a}{\lambda} = \frac{4A}{\pi(1-A^2)}, \tag{64}$$
or
$$A = \frac{2\lambda}{\pi a}\left\{\left(1+\frac{\pi^2a^2}{4\lambda^2}\right)^{1/2} - 1\right\}. \tag{65}$$

5. Results

The full equation of the surface, in terms of the parameter α, is
$$\frac{z}{\lambda} = \alpha - \frac{2i}{\pi}\left[1+\frac{2\lambda}{\pi a}\left\{\left(1+\frac{\pi^2a^2}{4\lambda^2}\right)^{1/2} - 1\right\}e^{2\pi i\alpha}\right]^{-1} + \frac{2i}{\pi}. \tag{66}$$

Preliminary calculations showed that for large enough values of a/λ, the wave surface crosses itself, and this suggested that the wave of greatest height would occur at the value of a/λ for which the surface was tangent to itself.

For this to be possible we must have $x = 0$ for $\alpha \neq 0$; i.e.
$$1 + A^2 + 2A\cos 2\pi\alpha = \frac{4A\sin 2\pi\alpha}{2\pi\alpha}, \tag{67}$$
or
$$A^2 - 2Af(2\pi\alpha) + 1 = 0, \tag{68}$$
where
$$f(t) = \frac{2\sin t}{t} - \cos t, \tag{69}$$
and we want the least value of a/λ for which this condition is satisfied; i.e.
$$A = f(t_0) - \{(f(t_0))^2 - 1\}^{1/2}, \tag{70}$$
where $f(t_0)$ is the minimum value of $f(t)$. This gives for the wave of greatest height
$$a/\lambda = 0{\cdot}730. \tag{71}$$
By contrast, the gravity wave of greatest height has $a/\lambda = 0{\cdot}142$ (Michell 1893).

An interesting point to notice is that the surface $\psi = 0$ for waves with amplitude corresponding to $A = A_1$ is the streamline $\psi = \text{const.}$, given by
$$A_2 e^{-2\pi\psi/c\lambda} = A_1 \tag{72}$$
for waves with amplitude corresponding to $A = A_2$ ($A_2 > A_1$). This fact simplifies the computation because the streamlines for the wave of greatest height, shown in figure 1, are themselves surface shapes for the

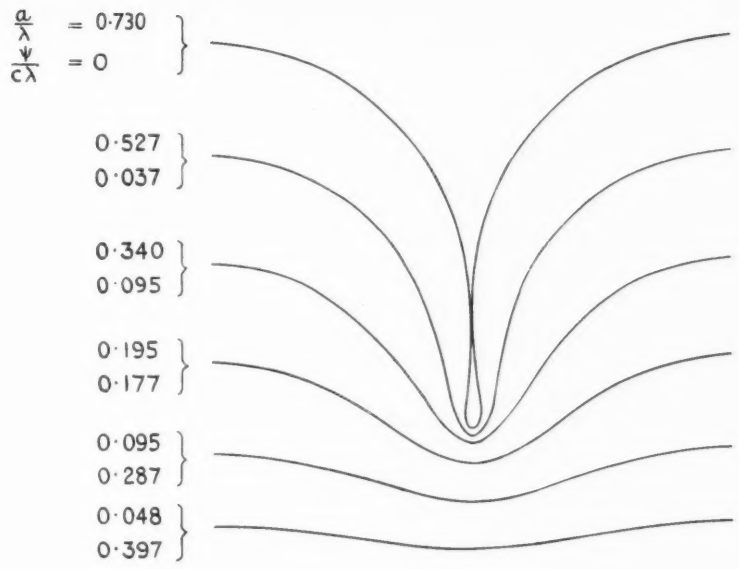

Figure 1. Streamlines for the wave of greatest height. Each line is itself the surface shape for the stated value of a/λ, and if any particular one is taken as surface those below it are still streamlines.

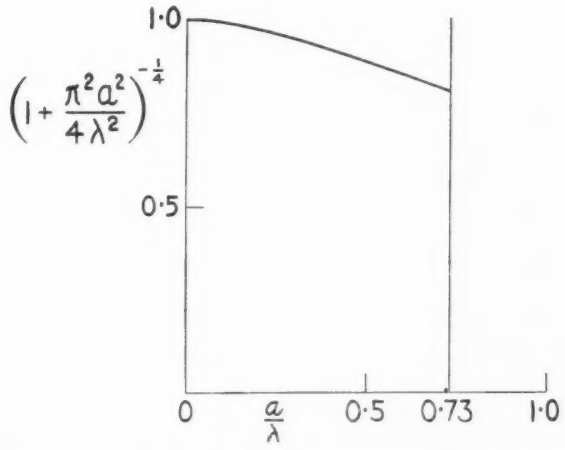

Figure 2. Ratio of wave velocity for amplitude a to wave velocity for zero amplitude for waves of length λ.

stated values of (a/λ), and if any particular line is taken as surface, those below it are still streamlines. The almost circular shape of the crests in figure 1 is to be expected in what the streamlines indicate to be a region of slow flow, since here surface tension is the dominating force.

Finally we have, from (60) and (64),

$$c = \left(\frac{2\pi}{\lambda}\,\frac{T}{\rho}\right)^{1/2}\left(1+\frac{\pi^2 a^2}{4\lambda^2}\right)^{-1/4}. \tag{73}$$

The function $(1+\pi^2a^2/4\lambda^2)^{-1/4}$, which shows how the wave velocity falls away from the value given by linear theory as the amplitude increases, is drawn in figure 2.

The author is greatly indebted to Professor M. J. Lighthill for much valuable help with the research and preparation of the paper, and to the Department of Scientific and Industrial Research for a maintenance grant.

References

Lamb, H. 1932 *Hydrodynamics*, 6th Ed. Cambridge University Press.

Michell, J. H. 1893 *Phil. Mag.* (5), **36**, 430.

Stokes, G. G. 1847 *Trans. Camb. Phil. Soc.* **8**, 441.

Stokes, G. G. 1880 *Mathematical and Physical Papers*, Vol. 1. Cambridge University Press.

The flow past a rapidly rotating circular cylinder in a uniform stream

By D. W. MOORE
Jesus College, Cambridge

(*Received* 5 *April* 1957)

SUMMARY

A circular cylinder is rotating in a uniform stream of viscous liquid, the circumferential velocity of the cylinder being much greater than that of the uniform stream. It is shown that the effect of the uniform stream can be regarded as a small perturbation of the rotary flow due to the cylinder, and that a uniformly valid first approximation to the flow field can be obtained in this way. This approximate solution has the interesting property that the circulation about any circular contour concentric with the cylinder is the same. The lift on the cylinder is shown to be that given by the classical formula, and the drag force is zero to the order of the approximation considered.

1. INTRODUCTION

In inviscid fluid theory an important type of two-dimensional flow is that generated when an infinite cylinder is placed in a uniform stream, with its generators normal to the plane of flow. Since the space outside the cylinder is doubly connected the velocity potential is determined only if the circulation $K = \int_\Gamma \mathbf{u}.d\mathbf{l}$ is specified about some contour Γ encircling the cylinder. The cylinder is then found to experience a force of magnitude $K\rho U$ per unit length perpendicular to the direction of the uniform stream, where ρ is the fluid density, and U is the velocity of the uniform stream. This result is due to Kutta (1910). Taylor (1925) showed that this same formula for the force on the cylinder is valid for a viscous fluid, provided that K is defined by a contour which is everywhere distant from the cylinder, and which crosses the cylinder's wake normally. This result explained the experimental work of Bryant & Williams (1925), who had compared the measured value of the lift with the value obtained from the inviscid formula by inserting the measured value of K.

To determine the value of K for given boundary conditions on the cylinder it is necessary to take the viscosity of the fluid into account. Sometimes this can be done without reference to the detailed viscous flow pattern. In the case of a slender aerofoil terminating in a cusp, for instance, the well-known Kutta–Joukowski condition, that K must be chosen so that the velocity of the potential flow is finite at the cusp, is a very plausible version of the requirement that steady viscous flow should be possible in the boundary layers near the cusp. In general, however, it is not possible

to determine K without solving the Navier–Stokes equations for the flow, and it is with one such case that the present paper is concerned.

The problem considered is that of a circular cylinder of radius a rotating with a circumferential velocity V in a uniform stream of velocity U. The viscous stresses set up by the cylinder's rotation induce a circulation in the fluid, and the cylinder experiences a transverse force in accordance with the general theory mentioned above. The existence of this force was discovered by Magnus in 1852, and the phenomenon is now usually known as the 'Magnus Effect'.

When the Reynolds number Va/ν is large the viscous forces may be expected to be small outside the boundary layer, and therefore the well-known inviscid theory will apply outside the boundary layer. The flow pattern given by the inviscid theory depends critically on the ratio $2\pi Ua/K$. If this ratio exceeds $\frac{1}{2}$ there are two stagnation points on the circumference of the cylinder. If $2\pi Ua/K < \frac{1}{2}$, on the other hand, there are no stagnation points on the cylinder, and there is a region of closed streamlines near the cylinder. In this case, closed boundary layers of a well-behaved type might be expected to form if the Reynolds number of the flow were large. If the circulation is produced solely by the cylinder's rotation it is plausible to assume that K is $O(aV)$, so that if U/V is small closed boundary layers may be expected to be formed. These are observed experimentally when $U/V < \frac{1}{4}$ (Prandtl & Tietjens 1936, plate 7). Wood (1957) has considered this case from a boundary layer point of view, by expanding the velocity in the boundary layer in powers of U/V and substituting this expansion into the boundary layer equations.

In the case $U/V = 0$ the problem has a simple exact solution for all values of R, and it is reasonable to expect that when $U/V \ll 1$ a solution might be obtained, for all values of R, by regarding the uniform stream as producing a small perturbation of this exact solution. It is the purpose of the present paper to examine this approximation. Since the perturbation velocity becomes comparable with the velocity of the basic flow at a great distance from the cylinder, the perturbation method is obviously in danger of being invalid in this region of the flow. In § 2 it is shown that this difficulty can be overcome by using two approximations, one appropriate to the region near the cylinder, and one appropriate to large distances from the cylinder. In particular a uniformly valid first approximation to the velocity distribution can be found for all values of the Reynolds number, and a uniformly valid second approximation to the velocity distribution is found when the Reynolds number is greater than $\sqrt{48}$. Further approximations are not obtained explicitly, but their general nature can be inferred, and their relation to Wood's expansion elucidated.

The remainder of the paper is concerned mainly with the first approximation; the nature of the flow pattern, and the forces on the cylinder, being considered in § 3 and § 4, respectively. It appears that, to the first order in U/V the circulation round every *circular* contour concentric with the cylinder is the same. Thus, to this order, either the circulation at the

cylinder's circumference, or round a contour very distant from the cylinder can be inserted in the formula for the lift. This is verified in § 4 by a direct calculation of the lift. The drag force is also calculated, and is shown to be zero to this order in U/V. The results provided by a second approximation are also considered briefly in § 3 and § 4. In particular, the circulation round a distant contour is determined, and, in the limit of infinite Reynolds numbers, is shown to be the same as that predicted by Wood from boundary layer considerations.

2. The first approximation

Using polar coordinates (ar, θ) with the origin at the centre of the cylinder, and the line $\theta = 0$ in the direction of the uniform stream, the equation for the stream function $Va\psi$ is

$$\nabla^4\psi = R\left[\frac{1}{r}\frac{\partial\psi}{\partial\theta}\frac{\partial}{\partial r}(\nabla^2\psi) - \frac{1}{r}\frac{\partial\psi}{\partial r}\frac{\partial}{\partial\theta}(\nabla^2\psi)\right], \tag{1}$$

where, it will be remembered, $R = Va/\nu$ is the Reynolds number based on the circumferential speed of the cylinder. The boundary conditions to be satisfied by ψ are,

$$\psi = 0, \qquad \frac{\partial\psi}{\partial r} = -1, \qquad \text{at } r = 1, \tag{2}$$

$$\psi \sim \epsilon r\sin\theta \quad \text{as } r \to \infty, \tag{3}$$

where $\epsilon = U/V$ is the small expansion parameter.

When $\epsilon = 0$, the relevant exact solution of (1) is the irrotational purely rotary flow

$$\psi_0 = -\log r. \tag{4}$$

Here, in accordance with the ideas discussed in § 1, an approximate solution of the form

$$\psi = \psi_0 + \epsilon\psi_1 \tag{5}$$

is sought. The function ψ_1 must satisfy the boundary conditions

$$\psi_1 = \frac{\partial\psi_1}{\partial r} = 0 \quad \text{at } r = 1, \tag{6}$$

$$\psi_1 \sim r\sin\theta \quad \text{as } r \to \infty. \tag{7}$$

If terms in ϵ^2 are neglected, substitution of (5) in the exact flow equation (1) shows that ψ_1 satisfies the equation

$$\nabla^4\psi_1 - \frac{R}{r^2}\frac{\partial}{\partial\theta}(\nabla^2\psi_1) = 0. \tag{8}$$

The general solution of (8) can be obtained by assuming that it may be represented by a Fourier series

$$\psi_1 = \sum_{-\infty}^{+\infty} f_n(r)e^{ni\theta}; \tag{9}$$

this is suggested by the fact that ψ_1 must be a single-valued function of θ. Fortunately, it is found that the boundary conditions (2) and (3) can be satisfied by taking only the terms for $n = \pm 1$, so that convergence questions

do not arise. It is then easily found that

$$\psi_1 = \mathscr{R}\{e^{i\eta}[-i(r-r^{-1}) - Fr^{-1} + Fr^{(2-p+iq)}]\}. \tag{10}$$

In this solution

$$F = \frac{q+(3-p)i}{q^2+(3-p)^2} \tag{11}$$

and p and q are real constants given by

$$p, -q = [\tfrac{1}{2}\{\sqrt{(1+R^2)} \pm 1\}]^{1/2}. \tag{12}$$

A description of the flow pattern represented by (10) will be given in § 3; the remainder of the present section is concerned with the validity of the approximations leading to this solution.

The exact solution of (1), (2) and (3) is, of course, unknown, so that the validity of (10) must be considered by indirect methods. Thus if (10) is substituted into (1), the value of the terms that are neglected when (8) is derived can be calculated; and the magnitude of these neglected terms compared with the magnitude of the retained terms determines whether or not the approximation is consistent. It must be emphasized that this procedure cannot rigorously establish the validity of the approximation; for if the approximation is invalid it cannot be used to calculate the neglected terms, and the procedure fails. However, since the approximation is physically plausible, it seems reasonable to accept it as valid if the procedure should show it to be consistent.

The exact equation for ψ_1 is

$$\nabla^4\psi_1 - \frac{R}{r^2}\frac{\partial}{\partial\theta}(\nabla^2\psi_1) = R\epsilon\left[\frac{\partial\psi_1}{\partial\theta}\frac{1}{r}\frac{\partial}{\partial r}(\nabla^2\psi_1) - \frac{\partial\psi_1}{\partial r}\frac{1}{r}\frac{\partial}{\partial\theta}(\nabla^2\psi_1)\right], \tag{13}$$

where the second term on the left-hand side is the retained inertia term, and the right-hand side consists of the previously neglected inertia terms. When $r = O(1)$ the retained inertia term is obviously dominant. At large values of r, however, one finds, on inserting (10) into this equation, that the retained inertia term is $O(r^{-p-2})$ whilst the largest neglected inertia term is $O(\epsilon r^{-p-1})$. Thus the approximation breaks down when $r = O(1/\epsilon)$, and since the outer boundary condition (7) must be applied, the validity of the solution (10) requires further justification, even when $r \ll 1/\epsilon$.

Now when $r = O(1/\epsilon)$ the contributions to the velocity from both the basic rotary flow and the uniform stream are $O(\epsilon)$, and it is reasonable to suppose that the exact solution has this same property. If, then, the equation (8) is solved subject to the exact boundary conditions on the cylinder and the order of magnitude conditions on the velocity when $r = O(1/\epsilon)$ one finds that the solution must be of the form $C\psi_1$ where C is a constant of order unity and ψ_1 is given by (10). In order to proceed any further the nature of the flow in the region $O(1) < \epsilon r < \infty$ must be examined. Now the rotational part of the velocity distribution corresponding to this solution is $O(\epsilon^p)$ when $r = O(1/\epsilon)$ where, from (12), p is always greater than unity and increases with R. Hence, with the mild assumption that the order of magnitude of the vorticity does not increase with r in the outer region, the

flow in this region is, to a first approximation, irrotational. The problem in the outer region is therefore that of finding an irrotational stream function which satisfies the boundary conditions

$$\psi \sim \rho \sin\theta \quad \text{as } \rho = \epsilon r \to \infty, \tag{14}$$

$$\psi \sim C(\log\epsilon - \log\rho + \rho\sin\theta + o(\rho)) \quad \text{as } \rho \to 0. \tag{15}$$

Equation (15) is the condition that the inner and outer solutions should match. Clearly a solution is possible only if $C = 1$, and the unique outer solution is then

$$\psi = -\log r + \epsilon r \sin\theta. \tag{16}$$

Thus, subject to the assumed conditions on the orders of magnitude of the velocity and vorticity distributions, it has been established that (10) provides a first approximation to the velocity distribution throughout the whole flow field. It should be noted, however, that this solution provides an approximation to the vorticity distribution only when $r < O(1/\epsilon)$.

It is clear that, in general, one cannot obtain a better approximation to ψ without taking account of viscous effects in the outer region. A method of obtaining outer expansions which included the effects of viscosity was considered recently by Proudman & Pearson (1957), and it is reasonable to suppose that their technique could be applied to this case*. However, when $p > 2$, the discussion of the rotational term given above shows that it is $O(\epsilon^2)$ in the outer region, so that the flow in the outer region is irrotational to a second approximation. In this case one seeks a second approximation in the inner region by writing

$$\psi = \psi_0 + \epsilon\psi_1 + \epsilon^2\psi_2, \tag{17}$$

and neglecting terms in ϵ^3 when (17) is substituted into (1). One finds that ψ_2 must satisfy the equation

$$\nabla^4\psi_2 - \frac{R}{r^2}\frac{\partial}{\partial\theta}(\nabla^2\psi_2) = R\left[\frac{\partial\psi_1}{\partial\theta}\frac{1}{r}\frac{\partial}{\partial r}(\nabla^2\psi_1) - \frac{\partial\psi_1}{\partial r}\frac{1}{r}\frac{\partial}{\partial\theta}(\nabla^2\psi_1)\right]. \tag{18}$$

The general solution of (18) can be effected by expanding ψ_2 as a complex Fourier series. One then imposes the exact boundary conditions

$$\psi_2 = \frac{\partial\psi_2}{\partial r} = 0, \quad \text{at } r = 1, \tag{19}$$

and the order of magnitude requirement that the vorticity corresponding to this solution should be $O(\epsilon^3)$ when $r = O(1/\epsilon)$. These conditions show that the most general form ψ_2 can have is

$$\psi_2 = \lambda\psi_1 - f'(1)\log r - f(1) + f(r) + \mathscr{R}\{e^{2i\theta}[\alpha r^2 + \beta r^{-2} + \gamma r^{\delta} + g(r)]\}. \tag{20}$$

In (20), $f(r)$ and $g(r)$ are known functions arising from the inhomogeneous

* Filon (1928) considered some general properties of the flow at great distances for a cylinder when circulation is present, but did not consider the possibility of matching his solutions to an inner expansion.

part of (18), and α, β, λ, and γ are unknown constants satisfying the equations

$$\left.\begin{aligned} \alpha+\beta+\gamma+g(1) &= 0, \\ 2\alpha-2\beta+\delta\lambda+g'(1) &= 0. \end{aligned}\right\} \tag{21}$$

The constant δ is the value of $2+(4+2iR)^{1/2}$ whose real part is negative. The most general form that the expansion in the irrotational outer region can assume is

$$\psi = \log\epsilon+(-\log\rho+\rho\sin\theta)+\epsilon\mathscr{R}[A(\log\epsilon-\log\rho)+Be^{i\theta}/\rho+Ce^{2i\theta}/\rho^2+\ldots]+ \\ +\epsilon^2\mathscr{R}[A'(\log\epsilon-\log\rho)+B'e^{i\theta}/\rho+C'e^{2i\theta}/\rho^2+\ldots]. \tag{22}$$

If one puts $r=\rho/\epsilon$ in (20) and imposes the condition that the expansions (17) and (22) should match when $\rho\to 0$, one finds that

$$\left.\begin{aligned} \lambda &= 0, \qquad \alpha = 0, \\ A &= B = C = \ldots = 0, \\ A' &= f'(1), \qquad B' = C' = \ldots = 0. \end{aligned}\right\} \tag{23}$$

Thus ψ_2 is uniquely determined, and the outer expansion is now

$$\psi = \log\epsilon+(-\log\rho+\rho\sin\theta)+\epsilon^2 f'(1)(\log\epsilon-\log\rho). \tag{24}$$

The calculation of the functions $f(r)$ and $g(r)$ is straightforward, but rather lengthy, and details will not be given.

The solution just obtained is valid only when $p>2$, or from (12), $R>\sqrt{48}$. The determination of the second approximation would, as has been remarked, require the consideration of a viscous outer expansion if this condition were not satisfied, but in view of the greater practical interest in higher Reynolds numbers this is not attempted.

As R is still further increased the vorticity in the outer region decreases in order of magnitude, and one can find progressively more terms of an inner expansion in powers of ϵ. Eventually in the limit of infinite Reynolds number, one would arrive at the situation considered by Wood (1957) in which one expands the velocity in powers of ϵ and determines the coefficients by substitution in the boundary layer equations. It is not clear that in the case of finite Reynolds numbers the inner expansion will be a power series in ϵ, as it may well contain terms of the type $\epsilon^n(\log\epsilon)^m$.

3. The nature of the flow pattern

The flow field surrounding the rotating cylinder presents some interesting features, and it will be discussed in this section on the basis of the approximations obtained in § 2.

The first step in elucidating the flow pattern is to calculate the circulation about a circular contour of radius r, concentric with the cylinder. This is given by the formula

$$K(r) = -Var\int_0^{2\pi}\frac{\partial}{\partial r}(\psi_0+\epsilon\psi_1)\,d\theta, \tag{25}$$

and on inserting the expressions given in § 2 for the functions ψ_0 and ψ_1 one finds that ψ_1 makes no contribution to the integral, so that

$$K(r) = 2\pi Va. \tag{26}$$

Thus the circulation about all circular contours concentric with the cylinder is the same, and is equal to the circulation at the circumference of the cylinder. By Stokes's theorem, this implies that the net amount of vorticity contained between any two such circles is zero. It is interesting to recall that Taylor (1925) made the hypothesis that the net amount of vorticity in the wake contained between lines perpendicular to the wake was zero.

If $p > 2$, the second approximation derived in § 2 can be used to calculate the circulation. It is found that in the inner region

$$K(r) = 2\pi Va[1 + \epsilon^2 f'(1) - rf'(r)] \tag{27}$$

and that in the outer region

$$K(r) = 2\pi Va[1 + \epsilon^2 f'(1)]. \tag{28}$$

The function $f(r)$ is given by

$$f(r) = R\mathscr{R}\left[\frac{2ir^{\sigma+\bar{\sigma}}}{(\sigma+\bar{\sigma})^2(\sigma+\bar{\sigma}-2)(\sigma+1)} - \frac{ir^{\bar{\sigma}+1}}{(\bar{\sigma}+1)^2} + \frac{ir^{\bar{\sigma}+1}(\sigma-1)}{(\bar{\sigma}-1)(\bar{\sigma}-3)(\sigma+1)}\right], \tag{29}$$

where $\sigma = 2-p+iq$, and the overbar denotes the complex conjugate. Thus the circulation at very large distances is constant, and is given by

$$K = 2\pi Va\left[1 + \frac{\epsilon^2 q(3p-5)}{2(p^2-1)(p^2-3p+4)}\right]. \tag{30}$$

It may be shown from (12) that

$$p, -q \sim (\tfrac{1}{2}R)^{1/2} \quad \text{as } R \to \infty, \tag{31}$$

and so one finds that

$$K \to 2\pi Va(1-3\epsilon^2) \quad \text{as } R \to \infty. \tag{32}$$

The result (32) was obtained by Wood (1957) from boundary layer considerations.

A first approximation to the distribution of the vorticity ζ can be calculated from (10):

$$\zeta = -\epsilon Va^{-1}\mathscr{R}\{r^{-p+iq}e^{i\theta}F[(2-p+iq)^2-1]\}. \tag{33}$$

The result assumes a simpler form when R is large compared with unity. It is then found that

$$\zeta \sim Ua^{-1}R^{1/2}r^{-\sqrt{(\frac{1}{2}R)}}\cos(\tfrac{3}{4}\pi + \theta - (\tfrac{1}{2}R)^{1/2}\log r). \tag{34}$$

This expression shows that the vorticity suffers a rapid oscillatory decay as the wall of the cylinder is left, and that it is effectively confined to a boundary layer of thickness $O(aR^{-1/2})$. Wood (1957) has shown that this oscillatory character is an inherent property of closed boundary layers.

A closer examination of (10) throws further light on the nature of the flow pattern. The first term is simply the potential flow around the cylinder induced by the uniform stream. The second and third terms arise from the

viscosity of the fluid. At large Reynolds numbers, the third term decays rapidly as r increases, and corresponds to a thin, closed, boundary layer attached to the cylinder. The second term, on the other hand, decays only as fast as r^{-1}, and corresponds to an irrotational secondary flow induced by the normal velocities at the outer edge of the boundary layer. The character of this secondary flow is made clear by writing down the stream function from which it can be derived. When R is large compared with unity this stream function is

$$\psi' \sim Uar^{-1}R^{-\frac{1}{2}}\cos(\theta+\tfrac{1}{4}\pi). \tag{35}$$

This secondary flow, like all such flows, is irrotational, and decreases in magnitude as $R \to \infty$. The inflow into the boundary layer is shown diagrammatically in figure 1.

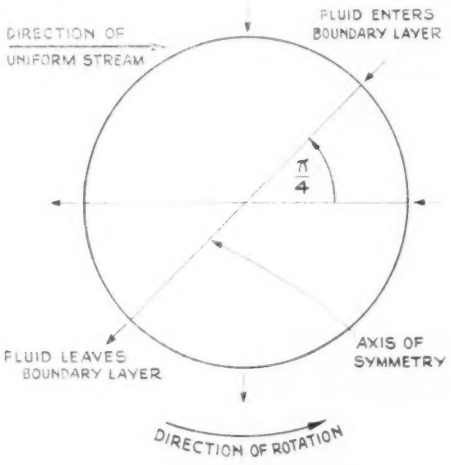

Figure 1. The distribution of inflow velocity into the boundary layer.

The mechanism producing the secondary flow is of the same general type as is found in other rotary flows. The viscous forces modify the velocity of a given fluid particle, so that the centrifugal force due to the curvature of the streamlines no longer balances the normal pressure gradient. There seems to be no obvious physical reason for the angular distribution of the flow, particularly the symmetry about the line $\theta = \frac{1}{4}\pi$.

It appears, then, that at large Reynolds numbers the flow pattern outside the boundary layer is very nearly that predicted by the inviscid theory. More precisely, at any point outside the boundary layer,

$$\text{(viscous stream function)} = \text{(inviscid stream function)} + O(R^{-\frac{1}{2}}). \tag{36}$$

In particular, there is no wake; a fact which will be found to have important consequences for the drag force experienced by the cylinder.

The formation of a boundary layer as $R \to \infty$, with the corresponding occurrence of large velocity gradients, may make some of the terms neglected in the derivation of (8) of comparable order to those retained. Inspection of the exact equation (13) for ψ_1 reveals that the terms retained are $O(\psi\epsilon/\delta^4)$ whilst the largest neglected terms are $O(\psi^2\epsilon^2 R/\delta^3)$, where δ is the dimensionless boundary layer thickness. In the boundary layer $\psi = O(R^{-1/2})$ and $\delta = O(R^{-1/2})$, so that the retained terms are $O(\epsilon R^{3/2})$ and the largest neglected terms are $O(\epsilon^2 R^{3/2})$. Thus the neglected terms are still smaller than those retained by a factor ϵ, and the validity of the approximation is unaffected by the presence of a boundary layer.

4. The forces experienced by the cylinder

The solution obtained in § 2 can be used to calculate the forces exerted on the cylinder by the fluid.

It may be shown that on the surface of the cylinder

$$p_{r\theta} = -\frac{\mu V}{a}\frac{\partial}{\partial r}\left(\frac{1}{r}\frac{\partial \psi}{\partial r}\right)_{r=1} \tag{37}$$

and

$$p_{rr} = -p(1,\theta), \tag{38}$$

where $p(1,\theta)$ satisfies the equation

$$\frac{\partial p(1,\theta)}{\partial \theta} = -\frac{\mu V}{a}\left(\frac{\partial^3 \psi}{\partial r^3} + \frac{\partial^2 \psi}{\partial r^2} + 1\right)_{r=1}. \tag{39}$$

If the solution $\psi_0 + \epsilon\psi_1$ found in § 2 is used to calculate these stresses, the force (X, Y) acting on the cylinder can be determined by integration, and one finds that

$$X = 0, \tag{40}$$

$$Y = -2\pi a V \rho U. \tag{41}$$

Thus the drag force is zero to the order of the approximation considered. This is perhaps a surprising result, but it follows from the character of the flow at large distances from the cylinder. There is no wake in this flow, since the boundary layers are closed, and consequently the flow at great distances is (to this order) everywhere irrotational. It follows from momentum considerations (Taylor 1925) that the drag force is zero.

The result (41) for the lifting force is also in agreement with Taylor's conclusions (discussed in § 1), since, as was shown in § 3, the circulation is $2\pi a V$ to the first order.

The above results have been derived from the first approximation $\psi_0 + \epsilon\psi_1$ which, as was shown in § 2, provides a valid approximation to the flow pattern for $R > 0$. If attention is restricted to the case $p > 2$, the second approximation to the flow field can be inserted in the above expressions for the stresses, and the total force on the cylinder recalcuated. One finds that the second approximation makes no contribution to either X or Y, so that

$$X = O(\epsilon^3), \tag{42}$$

$$Y = -2\pi a V \rho U\{1 + O(\epsilon^2)\}. \tag{43}$$

The result (42) is not surprising in view of the argument given above, and (43) is in agreement with the value obtained when the circulation at large distances calculated in § 3 is inserted in Taylor's formula for the lift. Unfortunately the measurements that have been made of the forces experienced by a rotating circular cylinder (Goldstein 1938, pp. 545–548) have been made at high Reynolds numbers where the stability of the flow is in doubt, so that no comparison of the above theory with experiment seems to be possible.

The viscous dissipation in the boundary layer absorbs the work which must be done against the torque to maintain the cylinder's rotation. The torque G can be calculated from (37), and, using the second approximation one finds that

$$G(R) = -4\pi\mu aV\left[1+\frac{\epsilon^2R^2}{4p(p^2-1)}\right]. \tag{44}$$

For large values of R, p may be replaced by its asymptotic expression, and

$$G \sim -4\pi\mu aV(1+\tfrac{1}{2}\sqrt{2}\epsilon^2R^{1/2}). \tag{45}$$

The author is indebted to Dr I. Proudman for his encouragement and advice, to Mr J. R. A. Pearson for some stimulating discussions on the nature of the approximations, and to Mr M. B. Glauert for some valuable comments on an earlier draft of this paper. During the period of preparation of this paper the author was in receipt of a maintenance allowance from the Department of Scientific and Industrial Research.

References

Bryant, L. W. & Williams, G. H. 1925 *Phil. Trans.* A, **225**, 199.

Filon, L. N. G. 1928 *Phil. Trans.* A, **227**, 93.

Goldstein, S. (Ed.) 1938 *Modern Developments in Fluid Dynamics.* Oxford: Clarendon Press.

Kutta, W. M. 1910 *S. B. bayer. Akad. Wiss.* (Abh. 2), 1.

Magnus, G. 1853 *Poggendorf's Ann. Phys. Chem.* **88**, 1.

Prandtl, L. & Tietjens, O. G. 1936 *Applied Hydro- and Aero-Mechanics.* New York: McGraw-Hill.

Proudman, I. & Pearson, J. R. A. 1957 *J. Fluid Mech.* **2**, 237.

Taylor, G. I. 1925 *Phil. Trans.* A, **225**, 238.

Wood, W. W. 1957 *J. Fluid Mech.* **2**, 77.

Experiments on the onset of wave formation on a film of water flowing down a vertical plane

By A. M. BINNIE
Trinity College, Cambridge

(*Received* 16 *March* 1957)

SUMMARY

The supply of water to the outside of a long vertical tube was adjusted until the water film was seen to be only just disturbed by a train of travelling waves. Under these conditions the Reynolds number, defined as the discharge per unit width divided by the kinematic viscosity, was 4·4. The wave train was slightly irregular, and average values of the length and velocity of the waves were about 0·45 in. and $5\frac{1}{2}$ in./sec, the temperature being 19° C.

1. INTRODUCTION

When a thin sheet of water passes over a smooth inclined plane, such as a slab of rock or a tarred road, its surface is sometimes disturbed by travelling waves even in the absence of wind. These roll waves, as they are often termed, occur with their crests normal to the direction of streaming, and photographs of those produced in highly turbulent form in an embanked torrent of uniform slope and cross-section were published by Cornish (1934, plates 21–23). Under laboratory conditions in still air numerous experiments have been made, mostly on vertical surfaces, and the observations can be recorded in terms of the Reynolds number R defined by $R = Q/\nu$, where Q is the discharge per unit width of the stream and ν is the kinematic viscosity of the liquid. If the slope is vertical and the liquid is water, the film to be examined is very thin and the experimental difficulties are considerable. In vertical flow the motion is not obviously turbulent below about $R = 250$, and over most of this range the surface of the liquid is agitated by irregular ripples, single photographs of which were published by Grimley (1945). Dukler & Bergelin (1952), after giving a detailed survey of the experimental literature, reported their measurements of ripple profiles at Reynolds numbers down to about 196 which showed steep-fronted slopes with heights that exceeded the mean film thickness. But most of the investigations have been concerned with finding the minimum Reynolds number at which waves can be observed. The results show a marked scatter. Friedman & Miller (1941) gave $R = 6{\cdot}25$ as the limit, and Grimley's value (1945) was 6·2, but his photograph obtained at $R = 6{\cdot}65$ showed waves that were apparently rather large as well as irregular. On the other hand Kirkbride's result (1934) was 2.

In the next section an account is given of an attempt to determine not only the smallest Reynolds number at which waves could be seen under good conditions of illumination but also the velocity and length of these waves. The liquid used was water, which was caused to flow down the outside of a long vertical glass tube. The thickness of the film was so small in comparison with the radius of the tube that the motion could be taken to be the same as that down a plane surface.

2. Description of experiments

The apparatus, which is shown in diagrammatic elevation in figure 1 (plate 1), was built round a fixed 5 ft. length of Truebore glass pipe of outside diameter 1·045 in. Distilled water passed from an elevated reservoir through a control valve and two alternative Rotameters into the upper Perspex chamber. A hole in the thick base of this chamber was slightly larger than the glass tube, and it could be centred by four adjusting screws threaded in the wall and pressing against the glass tube. In this way the water was delivered to the outside of the tube in as uniform a stream as possible. At the bottom the water was caught in another chamber and fell into a lower reservoir whence it was returned to the upper by a pump. The two chambers were joined by a Perspex pipe, held in position by rubber tubing. The pipe served as a dust cover to the working section, and in it a large window was cut which was removed only when photography was actually in progress. Four sprays were added at the extreme top of the working section so that, when required, the surface of the working section could be thoroughly wetted. They were supplied from a branch on the delivery side of the pump. For observation by eye, illumination at about 30° incidence at the middle of the working section was provided by bulbs and reflectors. A closely-fitting cylinder of glossy white paper was pushed down the inside of the glass tube; and when the waves were small, only their shadows on this paper were visible. The wave system extended all down the tube, and the motion appeared to be independent of the distance from the top. In spite of the care taken with cleaning and with precautions against the entry of dust, much experience with the apparatus was required before it would operate consistently at very low velocities.

The whole of the photographic work was very kindly carried out by Dr R. H. J. Brown, who used the repetitive flash apparatus that he has already described in detail (1952). Here it is sufficient to state that the flash duration of the lamp was about 10 microseconds, and that up to 95 pictures per second could be taken; thus the range of his apparatus was amply sufficient to meet the requirements of the present problem. The focused beam from the lamp was directed upwards at about 20° incidence, and it also illuminated a clock and a vertical scale placed close to the working section, which was photographed horizontally.

The procedure, when the final photographs were taken, was as follows. After the apparatus had been running at a moderate velocity for half an hour, the pump was stopped and the discharge slowly reduced while the tube

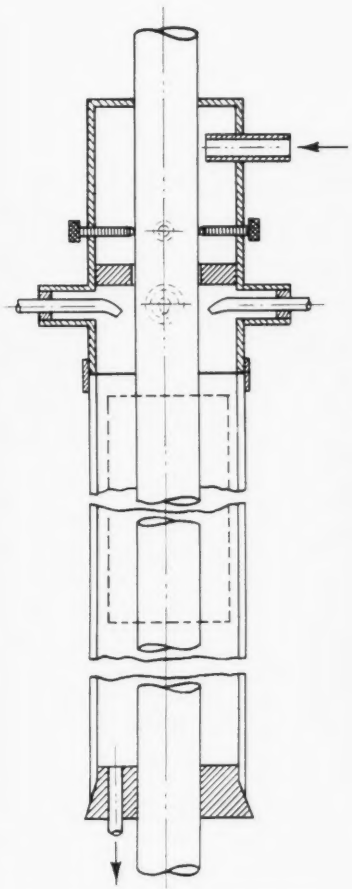

Figure 1. Elevation of apparatus.

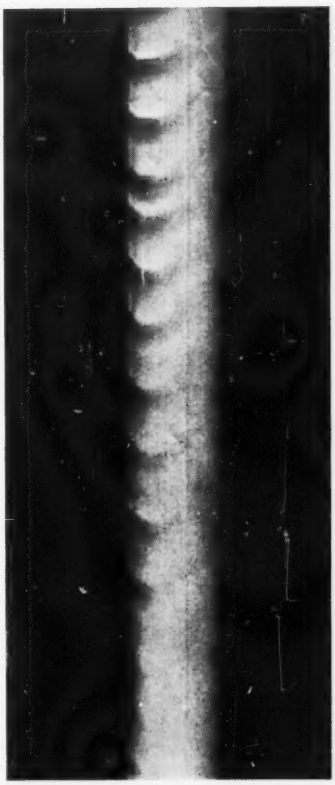

Figure 2. Shadow of limiting train of waves.

was repeatedly re-centred to produce waves of apparently the same amplitude all round the periphery. At the lowest velocity tried, waves could barely be seen on the front of the tube and over some but not all of the remainder of the periphery. The discharge was then very slightly increased, causing waves all round; and thus it was checked that the waveless zone had not dried off. When the velocity was again reduced to its previous value, it was seen that the wave pattern was the same as before. After this process of raising and lowering the flow had been carried out several times, it was thought that the minimum condition had been attained. The eye could just perceive a continuous stream of waves with horizontal crests, all moving with the same velocity but having slightly different lengths. Occasionally a larger and faster wave appeared that passed through the procession without permanently disturbing it. Two bursts of exposures were then taken and the flow determined by diverting and weighing the discharge from the base of the apparatus. The discharge per inch width of the tube circumference was $6{\cdot}9 \times 10^{-3}$ in.^{3}/sec at a temperature 19° C, thus $R = 6{\cdot}9/1{\cdot}58 = 4{\cdot}4$.

Eighty-three pictures were obtained at intervals of 0·047 sec, and they were examined with the aid of a projector. The specimen, reproduced in figure 2 (plate 1), shows one of the most regular wave trains that were photographed. Measurements were confined to the top 3 in. of the field of view, about 12 in. below the start of the working section, because there the shadows were most sharply defined and the distortion due to lack of parallelism in the light beam was least. The progress of typical single waves could be traced without difficulty on successive pictures because of the slight irregularities in the wave spacing, and recognition was helped by small density variations in some of the shadows, which suggested departure from the simple sinusoidal profile. Five crests followed in this way were found to travel 1·57, 1·53, 1·62 in. in 6 frames and 1·83, 1·87 in. in 7 frames, giving velocities 5·6, 5·4, 5·7, 5·6, 5·7 in./sec. In one picture all the waves had lengths between 0·45 and 0·5 in., except for one that was only 0·31 in. from its follower. A train of four equally spaced crests, occupying a distance 1·30 in., moved 1·60 in. in 6 frames, thus the wavelength was 0·43 in. and the velocity 5·7 in./sec. Average values of the length and velocity were therefore about 0·45 in. and 5½ in./sec.

In addition to Dr R. H. J. Brown, whose help is described above, I have also to thank Professor T. R. C. Fox for the loan of the hydraulic apparatus and Professor J. M. Kay for assistance in the early stages of the work.

References

Brown, R. H. J. 1952 *Photographic J.* **92B,** 130.
Cornish, V. 1934 *Ocean Waves.* Cambridge University Press.
Dukler, A. E. & Bergelin, O. P. 1952 *Chem. Engng Progress* **48,** 557.
Friedman, S. L. & Miller, C. O. 1941 *Industr. Engng Chem.* **33,** 885.
Grimley, S. S. 1945 *Trans. Inst. Chem. Engrs* **23,** 228.
Kirkbride, C. G. 1934 *Industr. Engng Chem.* **26,** 425.

Wave formation in laminar flow down an inclined plane

By T. BROOKE BENJAMIN

Department of Engineering, University of Cambridge

(*Received* 25 *March* 1957)

SUMMARY

This paper deals theoretically with a problem of hydrodynamic stability characterized by small values of the Reynolds number R. The primary flow whose stability is examined consists of a uniform laminar stream of viscous liquid running down an inclined plane under the action of gravity, being bounded on one side by a free surface influenced by surface tension. The problem thus has a direct bearing on the properties of thin liquid films such as have important uses in chemical engineering.

Numerous experiments in the past have shown that in flow down a wall the stream is noticeably agitated by waves except when R is quite small; on a vertical water film, for instance, waves may be observed until R is reduced to some value rather less than 10. The present treatment is accordingly based on methods of approximation suited to fairly low values of R, and thereby avoids the severe mathematical difficulties usual in stability problems at high R. The formulation of the problem resembles that given by Yih (1954); but the method of solution differs from his, and the respective results are in conflict. In particular, there is disagreement over the matter of the stability of a strictly vertical stream at very small R. In contrast with the previous conclusions, it is shown here that the flow is always unstable: that is, a class of undamped waves exists for all finite values of R. However, the rates of amplification of unstable waves are shown to become very small when R is made fairly small, and their wavelengths to become very large; this provides a satisfactory explanation for the apparent absence of waves in some experimental observations, and also for the wide scatter among existing estimates of the 'quasi-critical' value of R below which waves are undetectable. In view of the controversial nature of these results, emphasis is given to various points of agreement between the present work and the established theory of roll waves; the latter theory gives a clear picture of the physical mechanism of wave formation on gravitational flows, and in its light the results obtained here appear entirely reasonable.

The conditions governing neutral stability are worked out to the third order in a parameter which is shown to be small; but a less accurate approximation is then justified as an adequate basis for an easily workable theory providing a ready check with experiment.

This theory is used to predict the value of R at which observable waves should first develop on a vertical water film, and also the length and velocity of the waves. These three predictions are compared with the experimental results found by Binnie (1957), and are substantially confirmed.

1. Introduction

The flow of liquid in a thin film down a solid wall may often be observed in everyday life, as when rain water runs in a sheet down a window pane, or when paint, or mayonnaise, drains from some solid object which has been dipped in the liquid. It is also a subject of practical importance in chemical engineering, and has been studied by many experimental workers concerned with that field (e.g. Kirkbride 1934; Friedman & Miller 1941; Grimley 1945; Dukler & Bergelin 1952). The character of the flow has been shown to depend largely on the Reynolds number $R = Q/\nu$, where Q is the rate of volume flow per unit span of the stream and ν the kinematic viscosity (= viscosity μ/density ρ), although the influence of surface tension clearly may be important in most of the cases studied. In flow down a vertical plane, for example, the motion is apparently turbulent when R is greater than about 300 (Jeffreys 1925). When R is less than this, the mean flow is evidently governed by a law of laminar friction, and the mean depth is found to be approximately that given by the simple theory due to Nusselt (1916) and Jeffreys (1925) which assumes a uniform flow. Nevertheless, waves are to be observed on the free surface throughout almost the entire range of laminar flow, the possible exception being when R is reduced below a certain small value which may be about 4 if the liquid is water.

The apparent absence of waves on very thin films has led several investigators to assume that, for the flow down a vertical plane, there exists a critical value of R below which uniform laminar flow is entirely stable: that is, the flow is in a condition where small disturbances of every kind are suppressed. The well-proven significance of the Reynolds number in its more familiar contexts has undoubtedly encouraged this belief. Indeed, numerous estimates of the supposed critical Reynolds number have been stated (see Binnie (1957) for a review of some of them). On the theoretical side the work of Kapitza (1948) led to an estimate of 5·8 for the critical value, and that of Yih (1954) gave about 1·5.

In the present paper it will be argued that a critical Reynolds number in the usual sense does *not* exist for the particular case of uniform flow down a vertical plane. In other words, for all finite Reynolds numbers there is a class of wave-like disturbances which undergo unbounded amplification according to a linearized theory. The presence or absence of surface tension does not alter this general conclusion. The theory is, however, far from being incompatible with the various experiments seeming to indicate a critical Reynolds number, since an alternative explanation is readily forthcoming for the absence of observable waves. In fact the new explanation demonstrates a unity among various experimental results where

the respective values of the supposed critical Reynolds number are conflicting. On the other hand, it is necessary to dispute previous theoretical work on this subject.

The problem to be considered could be adapted to a simplified treatment akin to the usual theory of 'roll waves' on turbulent streams. In the latter only the 'overall' features of the flow are considered: that is, the frictional force against the stream is taken to vary in some prescribed way with the local depth and mean velocity and to be independent of the finer details of the motion, while the action of gravity (whose component perpendicular to the flow tends to keep the free surface flat) is expressed in a momentum equation based on the mean velocity. In his theory of roll-wave formation, Dressler (1952) derived a stability condition for a generalized law of friction, which extends to the example of laminar flow in question here. Thus, as the terms representing the restoring forces can easily be modified to encompass surface tension as well as gravity, immediate use may be made of his result to estimate when waves should appear. In § 5 of this paper the result following from Dressler's theory is shown to correspond to a limiting case of the present theory; but it is appropriate to note here that an approach to the problem directly by way of Dressler's work effectively demonstrates the instability inherent at all Reynolds numbers when the plane is vertical. This is particularly encouraging since roll-wave theory keeps a much closer connection with physical reasoning than is possible in the present treatment.

Since the primary (waveless) flow is laminar and completely known, the stability problem can be formulated mathematically in a more precise way than that of roll-wave theory. The formulation is made in the well-known manner which has been extensively used for stability problems concerned with laminar flows between fixed boundaries (cf. Lin 1955). It is implicitly assumed that the Fourier components of an arbitrary small disturbance are dynamically independent; thus the solution for a wave of arbitrary period and velocity constitutes a complete solution. The equations of motion for a wave of small amplitude are then set up, together with appropriate boundary conditions; this defines a characteristic-value problem leading to a relationship among the essential parameters of the primary flow and the wave. There is particular interest in the conditions under which the wave is propagated unchanged (i.e. its velocity is a real constant), since these refer to the dividing line between stability and instability. These few sentences merely outline a very well-known type of problem, and we may refer to the book by Lin (1955) for an extensive account of the subject. The novelties of the present application are, first, the introduction of boundary conditions appropriate to a free surface under the action of gravity and surface tension, and, second, the use of a method of approximate solution suited to fairly small Reynolds numbers. The latter avoids the serious difficulties which beset many of the well-known problems of hydrodynamic stability, in which instability is expected only for large Reynolds numbers (Lin 1955, p. 7). Furthermore, in a later part of this

paper justification is found for throwing off most of the weight of an analysis along the usual lines of stability theory, and hence proceeding with an easily workable approximation which is able to give a satisfactory account of all the main features of wave formation in practice. A rather similar formulation of this problem has already been given by Yih (1954), except that no account was taken there of surface tension; however, since the present method of solution is different and the results entirely so, there seems to be sufficient reason for setting out the argument completely from the beginning.

The analysis will be restricted to two-dimensional wave disturbances in a vertical plane (x, y). This simplification may be justified by appeal to the well-known argument first given by Squire (1933; restated by Lin 1955, §3.1) in connection with the problem of disturbed flow between parallel planes. He pointed out that any three-dimensional disturbance is governed by the same equations as a certain two-dimensional disturbance in a similar flow at lower Reynolds number. This means that two-dimensional waves have a greater tendency to instability than three-dimensional ones; and it follows that a two-dimensional analysis is completely adequate if only the stability of a flow is in question. The suitability of a two-dimensional analysis is further demonstrated by Binnie's experiments, noted immediately below, which showed that waves at fairly small Reynolds numbers are very approximately uniform along the horizontal line of their crests.

The experimental results reported by Binnie (1957) have been found to provide confirmation of the theory in several important respects. These results were kindly made known to me during the course of my theoretical work, and I was encouraged by them to explore the long-wave approximation described in §5. The experiments were made with vertical water films, and their results bear out the theoretical predictions on the following three counts: (i) the Reynolds number at which large amplifications of unstable disturbances first occur, so that observable waves develop; (ii) the velocity of the wave of maximum instability; (iii) the corresponding wavelength. The theoretical argument also accounts for the irregularity of the observed waves.

2. Properties of the primary flow

The laminar flow whose stability is to be examined is a uniform two-dimensional stream bounded on one side by a fixed wall and on the other by a free surface; the fluid has constant density and viscosity. The velocity U is everywhere parallel to x (see figure 1), and the graph of U *vs* y is a parabola which has its vertex in the free surface since, as the fluid is viscous, the rate of shearing dU/dy must vanish there. In this paper the coordinates (x, y) are made non-dimensional by taking the stream depth h as the unit of length, so that $y = 0$ and $y = 1$ define the free surface and the fixed boundary respectively. Also, velocities are made non-dimensional by taking the undisturbed velocity at $y = 0$, denoted by u_0, as the unit of velocity.

Thus we have
$$U = 1 - y^2. \tag{2.1}$$

By integration this immediately shows that the dimensionless mean velocity is $u_m = \frac{2}{3}$ (i.e. in dimensional units $u_m = Q/h = \frac{2}{3}u_0$). The motion is steady, so that the shear force $-(\mu u_0/h)\,dU/dy$ on the wall is balanced by the total gravity force on the stream in the direction of flow; thus

$$2\mu u_0/h = \rho h g \sin\theta,$$

where θ is the slope (figure 1). This gives directly

$$u_0 = \tfrac{1}{2}h^2 g \sin\theta/\nu, \tag{2.2}$$

$$R = Q/\nu = \tfrac{2}{3}u_0 h/\nu = \tfrac{1}{3}h^3 g \sin\theta/\nu^2. \tag{2.3}$$

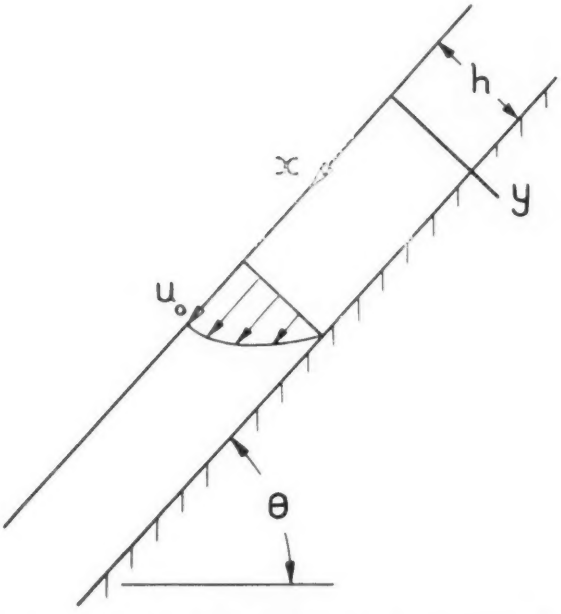

Figure 1. Diagram of the undisturbed flow, showing the velocity profile.

The existence of an explicit relation (2.3) between flow rate and depth suggests that any gradual or 'long-wave' disturbance from the uniform state would be propagated downstream with a (dimensional) velocity $C = dQ/dh$ (cf. the account of 'kinematic waves' given by Lighthill & Whitham (1955)). In fact (2.3) leads to

$$C = h^2 g \sin\theta/\nu = 2u_0. \tag{2.4}$$

This simple result provides an interesting check on the subsequent analysis, which shows by a totally different method that very long periodic waves are indeed propagated with a phase velocity equal to $2u_0$.

3. The stability problem

Suppose that the free surface is given a perturbation represented by the equation

$$y = \eta(x,t) = \delta e^{i\alpha(x-ct)}, \tag{3.1}$$

where α is the dimensionless wave number ($= 2\pi h/\text{wavelength}$), and t is time made non-dimensional by taking h/u_0 as the unit. Either the real or the imaginary part of (3.1) may, of course, be taken to describe a wave on the physical surface. In the usual manner of stability analyses, the wave amplitude δ is taken to be a small quantity whose square is negligible. The corresponding perturbation of the stream function may be written as

$$-\delta f(y)e^{i\alpha(x-ct)},$$

which implies that the velocity components satisfying the continuity condition for incompressible flow are

$$\left.\begin{aligned} u &= \delta f'(y)e^{i\alpha(x-ct)} + U, \\ v &= -i\alpha\delta f(y)e^{i\alpha(x-ct)}. \end{aligned}\right\} \tag{3.2}$$

The elimination of the pressure from the linearized equations of motion leads to an equation for $f(y)$:

$$(U-c)(f''-\alpha^2 f) - U''f = \frac{\nu}{i\alpha u_0 h}(f^{\mathrm{iv}} - 2\alpha^2 f'' + \alpha^4 f), \tag{3.3}$$

which is commonly known as the Orr–Sommerfeld equation (Lin 1955, § 1.3). After substituting for U from (2.1), it is convenient for our purpose to rearrange (3.3) in the form

$$f^{\mathrm{iv}} = (n - cn + 2\alpha^2 - ny^2)f'' + (2n - \alpha^2 n + c\alpha^2 n - \alpha^4 + \alpha^2 n y^2)f, \tag{3.4}$$

and then

$$f^{\mathrm{iv}} = (p + qy^2)f'' + (r + s^2 y^2)f, \tag{3.5}$$

where we have first put $n = i\alpha u_0 h/\nu = 3i\alpha R/2$, and then

$$\left.\begin{aligned} p &= n - cn + 2\alpha^2; & q &= -n; \\ r &= 2n - \alpha^2 n + c\alpha^2 n - \alpha^4; & s^2 &= \alpha^2 n. \end{aligned}\right\} \tag{3.6}$$

This greatly simplifies the writing-out of the subsequent heavy algebra.

The problem entails five boundary conditions as follows. First, the kinematical surface condition is

$$\frac{\partial \eta}{\partial t} + U_0 \frac{\partial \eta}{\partial x} = v_0,$$

where U_0 and v_0 are the values of U and v at $y = 0$; hence, because of (2.1), (3.1) and (3.2),

$$f(0) = c - 1. \tag{3.7}$$

This equation simply shows the connection between the assumed perturbation of the free surface and the corresponding perturbation of the stream function; it bears out the intuitively reasonable expectation that, provided c is not excessively large, the two perturbations are of the same order of magnitude. Since both velocity components must vanish at the fixed boundary, we also have

$$f(1) = 0, \tag{3.8}$$

$$f'(1) = 0. \tag{3.9}$$

The remaining boundary conditions relate to the continuity of stresses across the free surface. It is assumed that the only stress acting on the outside of this surface is a uniform pressure p_0; therefore, since the fluid is viscous, the rate of shearing in the stream $\partial u/\partial y + \partial v/\partial x$ must vanish at $y = \eta$, which requires that

$$f''(0) = 2 - \alpha^2(c-1). \tag{3.10}$$

The equation expressing the continuity of normal stress across the free surface may be written, after division by the density ρ,

$$\frac{p_1}{\rho} - \frac{2\nu u_0}{h}\left(\frac{\partial v}{\partial y}\right)_{y=\eta} = \frac{p_0}{\rho} + \sigma\Gamma - g\cos\theta\,\eta, \tag{3.11}$$

where p_1 is the (dimensional) pressure just inside the stream, σ is the principal curvature of the surface, and Γ, which may be called the 'kinematic surface tension', is equal to the usual surface tension coefficient divided by density. To the first order in δ, the curvature is

$$\sigma = \frac{1}{h}\frac{\partial^2\eta}{\partial x^2} = -\frac{\alpha^2\delta}{h}\,e^{i\alpha(x-ct)}. \tag{3.12}$$

Also, the pressure p satisfies the Navier–Stokes equation

$$\frac{\partial u}{\partial t} + u\frac{\partial u}{\partial x} + v\frac{\partial u}{\partial y} = -\frac{1}{\rho u_0^2}\frac{\partial p}{\partial x} + \frac{\nu}{hu_0}\left\{\frac{\partial^2 u}{\partial x^2} + \frac{\partial^2 u}{\partial y^2}\right\} + hg\sin\theta/u_0^2. \tag{3.13}$$

Hence, with the use of (3.11) and (3.12), separation of the variable part of (3.13) (i.e. the part with δ as a common factor) at $y = \eta$ leads to

$$(n - cn + 3\alpha^2)f'(0) = f'''(0) + \frac{i}{\nu u_0}(\alpha^3\Gamma + \alpha h^2 g\cos\theta). \tag{3.14}$$

The first four of the boundary conditions, (3.7) to (3.10), will be used to determine the four constants arising in the solution of the fourth-order equation (3.4). The boundary condition (3.14) will then be used to find c as a function of α and the parameters of the mean flow. This procedure resembles the usual one in stability problems (cf. Lin 1955). Instability is revealed for a particular wave mode when the respective c turns out to have a positive imaginary part, for then the mode has an exponentially-increasing time factor. As usual it is convenient to express the results of the calculations by setting down the conditions which make c wholly real; c is then simply the phase velocity of a neutral disturbance. These conditions represent a division between stability and instability.

The present problem is somewhat unusual in that two stress conditions, (3.10) and (3.14), replace the two additional kinematic conditions, like (3.8) and (3.9), which arise in problems concerning flow between fixed boundaries. It may, incidentally, be asked why five boundary conditions have been written down whereas most treatments of stability problems (cf. Lin 1955) make do with four? However, the limited meaning of the first boundary condition (3.7) has already been noted above; it contributes nothing to the essential characteristic-value problem, since an assumed perturbation of either the free surface or the stream function may equally well be taken as a starting point, and one simply follows from the other according to (3.7).

The only important difference between this and the better-known problems of hydrodynamic stability lies in the method of solution of the Orr–Sommerfeld equation set out in the next section. In view of existing experimental evidence, attention may confidently be restricted to the case of fairly small Reynolds numbers and wave numbers, and indeed the end results of the calculation confirm the adequacy of this approach.

4. Power-series approximation to the stream function

It was Kelvin (1887) who first noted that in linearized problems like the present one where the function $f(y)$ satisfies the fourth-order differential equation (3.4), the solution may be expressed as an ascending power series in y. He demonstrated that this series is convergent for all physically realizable conditions, but observed that the rate of convergence is very slow when R is not small. The approach suggested by Kelvin is of little use at fairly large Reynolds numbers, with which the greater part of the existing work on hydrodynamic stability is concerned. For the present problem, however, the method is definitely useful, since the values of R and of α are expected to be fairly small in the range of physical interest.

If one formally puts

$$f(y) = \sum_{N=0}^{\infty} A_N y^N, \tag{4.1}$$

then this series is seen to constitute a solution of (3.5) when the coefficients A_N are made to satisfy the recurrence relation

$$N(N-1)(N-2)(N-3)A_N = (N-2)(N-3)pA_{N-2} + \\ + \{r + (N-4)(N-5)q\}A_{N-4} + s^2 A_{N-6} \tag{4.2}$$

for $N > 3$. This relation follows directly from the differential equation. The first four coefficients A_0 to A_3 are simply the four constants arising essentially in the solution of a fourth-order equation, and (4.2) gives every other A_N in terms of these four and the parameters p, q, r, s. If these parameters are now regarded as small quantities of the same order of magnitude, the four coefficients A_4 to A_7 may be said to be $O(p)$, and each successive set of four coefficients is of decreasing order of magnitude with reference to powers of p. From (3.4), (3.5) and (3.6) it is seen that provided α is small, then p, q, r, s are of the order of n: that is, the order

of αR. Thus, a limited number of terms of the series would amount to an approximate solution in terms of ascending powers of αR (and, incidentally, of α^2); this may be contrasted to the commonly-used asymptotic solutions in descending powers of αR, suitable when R is large (see, for instance, Lin 1955, chapter 3).

We choose to approximate $f(y)$ in this way as far as $O(p^3) = O(n^3)$, which requires sixteen terms of the expansion (4.1). In this procedure there is an implicit assumption that c is not large, which is confirmed by the final results. In order simply to keep symmetry in the approximation, terms which are $O(\alpha^2)$, for instance, are given equal status with terms which are $O(n)$, although it may be anticipated that $\alpha^2 \ll |n|$ (i.e. $\alpha \ll R$) for the physically interesting cases discussed later.

Although the various manipulations made with the approximate solution for $f(y)$ are very laborious, they are quite straightforward. Accordingly, only an outline of the method of calculation need be given, together with the results of the more important stages.

The third-order approximation to the series solution (4.1), as calculated by means of (4.2), is most conveniently arranged as follows:

$$\begin{aligned}
f(y) = A_0[&1 + (1/4!)ry^4 + (1/6!)(pr + s^2)y^6 + (1/8!)(12qr + r^2 + p^2r + 2ps^2)y^8 + \\
&+ (1/10!)(2pr^2 + 42pqr + 60qs^2 + 32rs^2)y^{10} + \\
&+ (1/12!)(672q^2r + 68qr^2 + r^3)y^{12}] + \\
+ A_1[&y + (1/5!)ry^5 + (1/7!)(pr + 6s^2)y^7 + \\
&+ (1/9!)(20qr + r^3 + p^2r + 6ps^2)y^9 + \\
&+ (1/11!)(62pqr + 2pr^2 + 252qs^2 + 48rs^2)y^{11} + \\
&+ (1/13!)(1440q^2r + 92qr^2 + r^3)y^{13}] + \\
+ A_2[&y^2 + (2/4!)py^4 + (2/6!)(2q + r + p^2)y^6 + \\
&+ (2/8!)(14pq + 2pr + 12s^2 + p^3)y^8 + \\
&+ (2/10!)(60q^2 + 32qr + r^2 + 44p^2q + 3p^2r + 42ps^2)y^{10} + \\
&+ (2/12!)(560pq^2 + 10pqr + 672qs^2 + 12rs^2)y^{12}] + \\
+ A_3[&y^3 + (6/5!)py^5 + (6/7!)(6q + r + p^2)y^7 + \\
&+ (6/9!)(26pq + 2pr + 20s^2 + p^3)y^9 + \\
&+ (6/11!)(252q^2 + 48qr + r^2 + 68p^2q + 3p^2r + 62ps^2)y^{11} + \\
&+ (6/13!)(2124pq^2 + 218pqr + 3pr^2 + 1872qs^2 + 92rs^2)y^{13} + \\
&+ (6/15!)(27720q^3 + 5532q^2r + 158qr^2 + r^3)y^{15}]. \qquad (4.3)
\end{aligned}$$

To use this result, the boundary conditions (3.7), (3.10) and (3.14) are first expressed in terms of the coefficients A_N; these equations give respectively

$$A_0 = c - 1, \qquad (4.4)$$

$$2A_2 = 2 - \alpha^2(c - 1), \qquad (4.5)$$

$$(n - cn + 3\alpha^2)A_1 = 6A_3 + \frac{i}{\nu u_0}(\alpha^3\Gamma + \alpha h^2 g \cos\theta). \qquad (4.6)$$

Thus, A_0 and A_2 are related very simply to the main parameters of the problem. To find A_1 and A_3 for use in (4.6), the boundary conditions (3.8) and (3.9) are employed. By setting equal to zero $f(y)$ and $f'(y)$ as given by (4.3), we have a pair of simultaneous equations for A_1 and A_3 in terms of A_0 and A_2. The solutions of these equations are then expressed in ascending powers of p, q, r, s by a straightforward, though rather lengthy, inversion process. By this stage of the calculation, some of the numerical coefficients would become very cumbersome if left as fractions, and so all but the simple coefficients of the leading terms are expressed as decimals. Note that to satisfy (4.6) as far as $O(n^3)$, A_3 is required to $O(n^3)$, but A_1 is required *only to* $O(n^2)$. Accordingly, although A_1 was calculated to $O(n^3)$ to provide certain checks on the result for A_3, the third-order terms in A_1 need not be reproduced here.

After some condensation made possible by the fact that $r = -2q$ in the third-order terms, the results may be expressed as follows:

$$\begin{aligned} A_1 = A_0\Big[&-\frac{3}{2} + \Big(\frac{1}{40}p + \frac{1}{140}q + \frac{1}{105}r\Big) + (-0{\cdot}0013\,095p^2 - \\ &- 0{\cdot}0006\,052pq - 0{\cdot}0003\,373pr - 0{\cdot}0000\,773q^2 - \\ &- 0{\cdot}0000\,167qr + 0{\cdot}0000\,357r^2 + 0{\cdot}0010\,913s^2)\Big] + \\ + A_2\Big[&-\frac{1}{2} + \Big(\frac{1}{60}p + \frac{1}{840}q - \frac{1}{840}r\Big) + (-0{\cdot}0007\,738p^2 - \\ &- 0{\cdot}0001\,389pq + 0{\cdot}0001\,190pr - 0{\cdot}0000\,054q^2 + \\ &+ 0{\cdot}0000\,123qr - 0{\cdot}0000\,049r^2 - 0{\cdot}0001\,984s^2)\Big], \end{aligned} \tag{4.7}$$

$$\begin{aligned} A_3 = A_0\Big[&\frac{1}{2} + \Big(-\frac{1}{20}p - \frac{3}{280}q - \frac{11}{280}r\Big) + (0{\cdot}0032\,143p^2 + \\ &+ 0{\cdot}0012\,831pq + 0{\cdot}0010\,450pr + 0{\cdot}0001\,349q^2 + \\ &+ 0{\cdot}0000\,320qr - 0{\cdot}0000\,891r^2 - 0{\cdot}0022\,487s^2) + \\ &+ (-0{\cdot}0001\,759p^3 - 0{\cdot}0000\,315p^2r + 0{\cdot}0000\,130pr^2 + \\ &+ 0{\cdot}0000\,030r^3 + 0{\cdot}0001\,040ps^2 + 0{\cdot}0000\,507rs^2)\Big] + \\ + A_2\Big[&-\frac{1}{2} + \Big(-\frac{3}{40}p - \frac{1}{315}q + \frac{1}{315}r\Big) + (0{\cdot}0023\,413p^2 + \\ &+ 0{\cdot}0003\,538pq - 0{\cdot}0003\,108pr + 0{\cdot}0000\,139q^2 - \\ &- 0{\cdot}0000\,276qr + 0{\cdot}0000\,119r^2 + 0{\cdot}0003\,638s^2) + \\ &+ (-0{\cdot}0001\,068p^3 - 0{\cdot}0000\,758p^2r - 0{\cdot}0000\,192pr^2 - \\ &- 0{\cdot}0000\,020r^3 - 0{\cdot}0000\,445ps^2 - 0{\cdot}0000\,122rs^2)\Big]. \end{aligned} \tag{4.8}$$

When p, q, r, s are expressed in terms of n and α^2 by means of (3.6), these results lead to

$$A_1 = A_0\Big[-\frac{3}{2}+\Big(-\frac{1}{40}cn+\frac{31}{840}n+\frac{1}{20}\alpha^2\Big)+ \\ +(-0{\cdot}0013\,095c^2n^2+0{\cdot}0026\,885cn^2-0{\cdot}0012\,798n^2+ \\ +0{\cdot}0147\,619c\alpha^2n-0{\cdot}0138\,095\alpha^2n-0{\cdot}0147\,619\alpha^4)\Big]+ \\ +A_2\Big[-\frac{1}{2}+\Big(-\frac{1}{60}cn+\frac{11}{840}n+\frac{1}{30}\alpha^2\Big)+ \\ +(-0{\cdot}0007\,738c^2n^2+0{\cdot}0011\,706cn^2-0{\cdot}0004\,463n^2+ \\ +0{\cdot}0019\,048c\alpha^2n-0{\cdot}0013\,492\alpha^2n-0{\cdot}0019\,048\alpha^4)\Big], \quad (4.9)$$

$$A_3 = A_0\Big[\frac{1}{2}+\Big(\frac{1}{20}cn-\frac{33}{280}n-\frac{1}{10}\alpha^2\Big)+(0{\cdot}0032\,143c^2n^2-0{\cdot}0072\,354cn^2+ \\ +0{\cdot}0037\,357n^2-0{\cdot}0521\,429c\alpha^2n+0{\cdot}0515\,079\alpha^2n+ \\ +0{\cdot}0521\,429\alpha^4)+(0{\cdot}0001\,759c^3n^3-0{\cdot}0004\,963c^2n^3+ \\ +0{\cdot}0004\,519cn^3-0{\cdot}0001\,345n^3-0{\cdot}0032\,712c^2\alpha^2n^2+ \\ +0{\cdot}0054\,363c\alpha^2n^2-0{\cdot}0022\,483\alpha^2n^2+0{\cdot}0083\,413c\alpha^4n- \\ -0{\cdot}0068\,254\alpha^4n-0{\cdot}0065\,926\alpha^6)\Big]+ \\ +A_2\Big[-\frac{1}{2}+\Big(\frac{3}{40}cn-\frac{11}{168}n-\frac{3}{20}\alpha^2\Big)+(0{\cdot}0023\,413c^2n^2- \\ -0{\cdot}0037\,070cn^2+0{\cdot}0014\,826n^2-0{\cdot}0061\,905c\alpha^2n+ \\ +0{\cdot}0046\,032\alpha^2n+0{\cdot}0061\,905\alpha^4)+(0{\cdot}0001\,068c^3n^3- \\ -0{\cdot}0002\,447c^2n^3+0{\cdot}0001\,881cn^3-0{\cdot}0000\,485n^3- \\ -0{\cdot}0003\,300c^2\alpha^2n^2+0{\cdot}0004\,767c\alpha^2n^2-0{\cdot}0001\,729\alpha^2n^2+ \\ +0{\cdot}0003\,492c\alpha^4n-0{\cdot}0002\,103\alpha^4n-0{\cdot}0002\,328\alpha^6)\Big]. \quad (4.10)$$

When these expressions are substituted into (4.6) and as much condensation as possible is made, the result is

$$\frac{i}{\nu u_0}(\alpha^3\Gamma+\alpha h^2g\cos\theta)+3c-6+n\Big(-\frac{6}{5}c^2+\frac{68}{35}c-\frac{24}{35}\Big)+\alpha^2(5{\cdot}4c-4{\cdot}8)+ \\ +n^2(-0{\cdot}0057\,143c^3+0{\cdot}0215\,873c^2-0{\cdot}0254\,628c+0{\cdot}0102\,907)+ \\ +\alpha^2n(-0{\cdot}1628\,571c^2+0{\cdot}3029\,095c-0{\cdot}1397\,619)+ \\ +\alpha^4(-0{\cdot}1371\,429c+0{\cdot}0742\,857)+ \\ +n^3(-0{\cdot}0002\,540c^4+0{\cdot}0011\,412c^3-0{\cdot}0018\,007c^2+ \\ +0{\cdot}0012\,414c-0{\cdot}0003\,178)+ \\ +\alpha^2n^2(0{\cdot}0073\,968c^3-0{\cdot}0240\,506c^2+0{\cdot}0257\,008c-0{\cdot}0090\,556)+ \\ +\alpha^4n(-0{\cdot}0506\,667c^2+0{\cdot}0966\,906c-0{\cdot}0468\,574)+ \\ +\alpha^6(0{\cdot}0547\,302c-0{\cdot}0504\,127)=0. \quad (4.11)$$

This result can be regarded as an equation for c in terms of n and α, hence of R and α, and of the 'restoring force' due to gravity and surface tension as expressed by the first group of terms in the equation. In particular, the equation can be used to find the relation between R and α which makes c wholly real, i.e. which gives the case of neutral stability. To do this, we first separate the real part of (4.11), noting that n is purely imaginary, and hence quite easily obtain an explicit expression for c by a process of successive approximation in terms of α^2 and $n^2 = -9\alpha^2R^2/4$. We finally get, for c real,

$$c = 2(1 - \alpha^2 + 11\alpha^4/6 + 0{\cdot}0077\,581\alpha^2R^2 - 3{\cdot}3555\,556\alpha^6), \qquad (4.12)$$

where the values of R and α must be consistent with the imaginary part of (4.11) being satisfied. The error in (4.12) is known to be considerably less, due to numerical factors, than $O(\alpha^4R^4)$. Note that there is no term in $(\alpha R)^1$ in (4.12); this result occurs by the cancellation of terms with fairly complicated numerical factors. (This may seem perhaps to suggest some special significance; but I can see no other way of arriving at such a result beyond a direct calculation like the present one.)

The imaginary part of (4.11) is now considered. On eliminating c by means of (4.12), and using the following relations found easily from (2.2) and (2.3):

$$u_0^2h = (3^{5/3}/4)(g\sin\theta)^{1/3}\nu^{4/3}R^{5/3},$$
$$u_0^2/h = \tfrac{3}{4}g\sin\theta R,$$

we finally obtain the approximation

$$\frac{4\zeta}{3^{5/3}}\frac{\alpha^2}{R^{5/3}} + \frac{4\cot\theta}{3R} - \frac{8}{5} + 5{\cdot}5289\,142\alpha^2 - \\ - 0{\cdot}0000\,639\alpha^2R^2 - 14{\cdot}6352\,952\alpha^4 = 0, \qquad (4.13)$$

where ζ is defined by

$$\zeta = \Gamma(g\sin\theta)^{-1/3}\nu^{-4/3}. \qquad (4.14)$$

Equation (4.13) expresses the required approximate relation between R and α for neutral stability. The equation is easily solved, since for a specified value of R it becomes a quadratic in α^2.

In passing it may be noted that the formula for real values of c, i.e. (4.12) subject to (4.11), appears to differ from the result obtained by Yih (1954), which was presented only in graphical form. The discrepancy is not understood. For $\alpha \to 0$ (i.e. for very long waves), equation (4.12) gives simply $c = 2$, which agrees with the result (2.4) obtained by a very simple argument. This also agrees with the result found by Kapitza (1948), who used a different form of argument applicable only to very long waves.

Let us now consider, for example, the case of a vertical wall ($\theta = 90°$). The term involving $\cot\theta$ in (4.13) now vanishes, and we have $\zeta = \Gamma g^{-1/3}\nu^{-4/3}$. (The parameter ζ is about 3300 for water at 19° C.) Figure 2 shows the relation between R and α according to (4.13) for various values of ζ and a range of R up to 20. The curves shown in the figure are curves of neutral stability; and it can be inferred that, for a particular ζ, the region lying

above the respective curve represents stability, while that below it represents instability. The following features of figure 2 may be specially noted.

(i) Every curve for $\zeta > 0$ passes through the origin, and has infinite slope there. (The case $\zeta = 0$ is discussed below.) Thus, for all finite values of R there is a finite range of unstable α, and therefore the flow is never completely stable. On the other hand, equation (4.13) shows that stability occurs for sufficiently small R when $0 < \theta < 90°$.

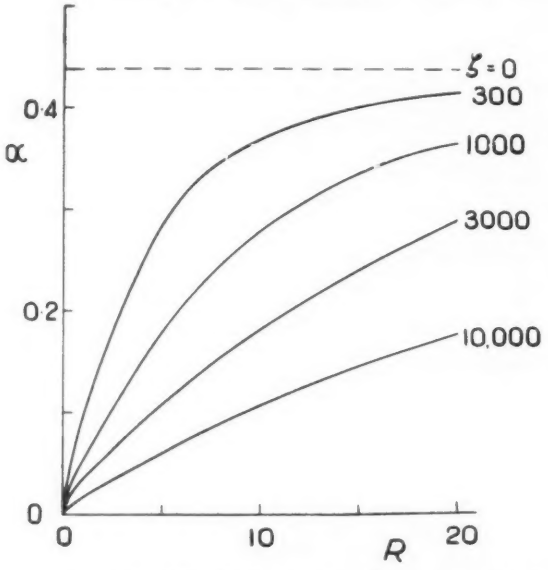

Figure 2. Curves of neutral stability for laminar flow down a vertical wall with various values of the parameter $\zeta = \Gamma g^{-1/3} \nu^{-4/3}$.

(ii) The stabilizing tendency of surface tension is demonstrated by the fact that the curves bend nearer the R-axis for increasing ζ. Thus, as might be expected intuitively, the range of unstable α for a given R is reduced as Γ, and hence ζ, is increased. Note that surface tension cannot induce complete stability, although it may stabilize waves whose length is less than a certain limit.

(iii) The curve according to (4.13) for $\zeta = 0$ is included in the figure, being shown as a broken line, although the values of α in this case are rather too large for confidence in the accuracy of the result. (We recall that the theory has been developed on the assumption that α is fairly small.) However, the trend of the other curves in the figure shows definitely that the unstable region of the (R, α)-chart is largest when $\zeta = 0$. This fact is useful, since it seems to rule out the possibility that the neglect of surface tension in Yih's treatment of the problem may be responsible for the discrepancy between his and the present general conclusions regarding stability.

In connection with the general role of surface tension in the mathematical problem, the following matter is worth noting. Equation (4.13) shows that $\alpha \to O(R^{5/6}/\zeta^{1/2})$ for $R \to 0$ with $\theta = 90°$. Thus, for small R the curve α *vs* $R^{5/3}$ is a parabola whose vertex touches the α-axis at the origin. The curvature at the vertex is directly proportional to ζ, and so in the limit $\zeta \to 0$ the curvature is zero and the curve coincides with the α-axis. It may hence be inferred that the curve α *vs* R also coincides with the α-axis for $\zeta \to 0$, although **for** this curve the curvature at the origin is infinite for for all finite values of ζ. Clearly, the same result should occur if surface tension were ignored (i.e. $\zeta = 0$) from the outset of the analysis, and so one might question why no such result is forthcoming if we put directly $\zeta = 0$ and $\theta = 90°$ in (4.13). However, in proceeding from the dimensional form of the dynamical equation (3.13) to as far as (4.13), a division of all the terms by $u_0^2 h$, which is proportional to $R^{5/3}$, has been entailed. Hence, to preserve the appropriate 'physical' status of surface tension with respect to the limiting process $R \to 0$, equation (4.13) should be multiplied by $R^{5/3}$; when this is done there is no ambiguity about the fact that $R = 0$ is a solution regardless of α when $\zeta = 0$. This result that the flow is unstable, or at least neutral, for all finite R and α seems correct intuitively, since for a vertical wall and zero surface tension there is no restoring force to act on the disturbed flow.

(iv) Owing to the particular method of approximation used for the theory, the most accurate part of the figure is the vicinity of the origin. The upper half, at least, of the figure is somewhat uncertain; but the figure as a whole is quite adequate as a qualitative picture of the neutral-stability conditions. Moreover, the line of argument to be developed in § 5 shows that it is sufficient to consider a range of R and α very near the origin to account satisfactorily for the relevant experimental facts.

5. Simplified theory for long waves

In this section some formulae are derived which are suitable for a straightforward check with experiment. In contrast with the results of the last section, they are compact and easily manipulated; and although these advantages are gained by sacrificing the higher-order terms calculated in § 4, the loss of precision entailed is found not to be serious. Let us therefore proceed on the assumption, to be justified later, that α is quite small. Our knowledge of the second- and third-order terms in (4.11) shows conclusively that a valid first approximation to this equation is simply

$$\frac{i}{\nu u_0}\{\alpha^3\Gamma + \alpha h^2 g\cos\theta\} + 3c - 6 + \frac{3}{2}i\alpha R\left\{-\frac{6}{5}c^2 + \frac{68}{35}c - \frac{24}{35}\right\} = 0. \quad (5.1)$$

Suppose now that $c = c_r + ic_i$, where c_r and c_i are wholly real, and that $c_r \gg c_i$. The latter assumption will also be justified later. On separation of real and imaginary parts, equation (5.1) gives, as a first approximation,

$$c_r = 2, \quad (5.2)$$

and hence

$$c_i = \frac{1}{2} R \left\{ \frac{8}{5} \alpha - \frac{\alpha^3 \Gamma}{h u_0^2} - \frac{\alpha h g \cos\theta}{u_0^2} \right\}. \tag{5.3}$$

Therefore, since unstable waves have $c_i > 0$, the condition for instability is

$$\frac{8}{5} > \frac{\alpha^2 \Gamma}{h u_0^2} + \frac{hg \cos\theta}{u_0^2}. \tag{5.4}$$

Some special cases following from (5.4) deserve to be noted. If one puts $\alpha \to 0$ in (5.4) and substitutes (2.2) and (2.3) in the second term on the right-hand side, this instability condition becomes

$$R > \frac{5}{6} \cot\theta. \tag{5.5}$$

Thus, when (5.5) is just satisfied, very long waves ($\alpha \to 0$) become unstable. Moreover, if surface tension is zero, all fairly long waves are unstable when (5.5) is satisfied, which rather suggests that in practice a bore (in other words, a discontinuous 'roll wave') would be formed. It is notable, though not at all unexpected, that except for the numerical factor the instability condition (5.5) is identical with the condition found by Jeffreys (1925) for the formation of roll waves on a turbulent stream, assumed to be subject to the Chézy law of friction. Indeed, the present result can be deduced directly, with only a very small discrepancy in the numerical factor, from the roll-wave theory developed by Dressler (1952) for a generalized law of friction. The details of this comparison need not be given here; it is sufficient to note that the result follows in a straightforward way when the primary-flow relationships for laminar flow (as in § 2) are introduced into Dressler's generalized instability condition.

The action of gravity may be expected to encourage instability if $\theta > 90°$, that is, if the fixed wall slopes backwards and the stream runs down its under side. The ability of liquid streams to adhere beneath solid surfaces is popularly known as the 'tea-pot effect', and will be familiar to any one who has poured liquid from a vessel with an ill-designed spout. The destabilizing influence of gravity in this case is properly expressed by the gravitational term in (5.4), which becomes negative when $\theta > 90°$. As an extreme case, let $\theta = 180°$ and hence $u_0 = 0$ in accordance with (2.2). The liquid now forms a stationary film on the under side of a horizontal plane, and the instability condition (5.4) becomes

$$gh^2 > \alpha^2 \Gamma,$$

or

$$\lambda > 2\pi(\Gamma/g)^{1/2}, \tag{5.6}$$

if the wavelength $\lambda = 2\pi h/\alpha$ is introduced. This is seen to check with the result obtained by Bellman & Pennington (1954, equation (3.7)), who calculated the effect of surface tension on the Taylor instability of the boundary between two fluids accelerated perpendicularly to its plane

(Taylor 1950). (It should be noted that the effect of gravity is here equivalent to an upward acceleration.)

The final special case which we shall discuss arises when $\theta = 90°$, that is, when the fixed boundary is vertical. This is the case for which a comparison between theory and experiment will be made in § 6, and also the one in which there is marked disagreement between the present work and that of Yih (1954). The rest of this section will be devoted to it.

For $\theta = 90°$, (5.4) becomes

$$\frac{8}{5} > \frac{\alpha^2 \Gamma}{h u_0^2}. \tag{5.7}$$

Hence, the flow is always unstable, since sufficiently small values of α can always be found to satisfy this instability condition; indeed, this fact is already clear from the discussion at the end of § 4 and also from (5.5), which becomes simply $R > 0$ when $\theta = 90°$. As pointed out in an early part of this paper, this result is remarkable in view of existing experimental work on vertical liquid films, much of which seems to indicate an absence of waves at sufficiently low Reynolds numbers. However, the following straightforward argument appears to bring the present theory into a completely satisfactory agreement with experiment, in particular the work mentioned in § 6.

It is reasonable to suppose that the wave most prominent in an experimental observation will be the one whose rate of growth according to linearized theory is largest. The use of such an assumption has many precedents; for instance, Rayleigh (1894, § 87) discussed its theoretical basis, and used it in several of his investigations. There is various experimental evidence to suggest that often the growth of a 'wave of maximum instability' eventually, through non-linear effects, tends to suppress other waves which are unstable according to linearized theory but have smaller rates of growth; thus, the well-defined pattern of the particular wave mode of greatest rate of amplification may be observed (see Benjamin & Ursell 1954 for a discussion of this point in a rather similar context). In the present problem unstable waves grow in amplitude according to a time factor $\exp(\alpha c_i t)$. To find α for the most unstable wave, we have therefore only to maximize αc_i, which, by virtue of (5.3), amounts to maximizing the function

$$\frac{8}{5}\alpha^2 - \frac{\alpha^4 \Gamma}{h u_0^2}.$$

Hence, the optimum value of α (say α_m) is given by

$$\alpha_m^2 = \frac{4 h u_0^2}{5\Gamma}. \tag{5.8}$$

When the formulae of § 2 for the primary flow are used (with $\theta = 90°$) to eliminate u_0 and h from this expression, it leads directly to

$$\alpha_m = 1{\cdot}12\{\nu^{2/3} g^{1/6} \Gamma^{-1/2}\} R^{5/6}, \tag{5.9}$$

where the numerical factor is an approximation to $(3/5)^{1\cdot2}3^{1/3}$. This together with (5.3) shows that the maximum value of c_i is

$$(c_i)_m = 0{\cdot}224\{\nu^{2\cdot3}g^{1\cdot6}\Gamma^{-1\cdot2}\}R^{11\cdot6}. \tag{5.10}$$

The quantity within the braces in (5.9) and (5.10) depends only on the particular liquid considered. For example, taking the values appropriate to water at 19° C: $\nu = 0{\cdot}0103$ cm^2/sec and $\Gamma = 72{\cdot}9$ cm^3/sec^2, and also $g = 981$ cm/sec^2, we get from (5.9) and (5.10)

$$\alpha_m = 0{\cdot}0195R^{5\cdot6}, \tag{5.11}$$

$$(c_i)_m = 0{\cdot}00391R^{11\cdot6}. \tag{5.12}$$

Provided R is not much greater than unity, these results justify the initial assumptions that α and c_i are small.

Now, to illustrate the likelihood of waves being observed experimentally, we shall calculate the amplification experienced by the wave of maximum instability on a vertical water film as it travels a distance of 10 cm. Since the wave velocity is approximately $2u_0$, the amplification factor is approximately $\mathscr{A} = \exp\{10\alpha_m(c_i)_m/2h\}$, where h is in cm. Hence, using (5.11) and (5.12), and eliminating h by means of the primary-flow relations of § 2, we finally get

$$\mathscr{A} = \exp\{0{\cdot}0543R^{8\cdot3}\}. \tag{5.13}$$

Values of $\mathscr{A}$ given by (5.13) are plotted as a function of R in figure 3. The figure shows the amplification to be large only for values of R greater than about 4; above this the rate of increase of $\mathscr{A}$ is enormous. Thus, one might expect observable waves to develop reasonably near the beginning of the stream as soon as the Reynolds number is brought up to a value near 4. Of course, the linearized theory ceases to apply when large amplifications occur; but the present result does seem to offer a convincing explanation of why, in experiments where the Reynolds number is gradually increased from small values, waves should suddenly appear on a previously untroubled stream. However, it has been shown here that a critical Reynolds number in the usual sense does not exist for a vertical stream; for, even when the Reynolds number is extremely small, there are unstable waves which, presumably, would grow to appreciable size if the stream were long enough. The present result suggests that experimental measurements of the 'quasi-critical' Reynolds number (R_{qc} say, which seems from the theory to be about 4 for water) may depend to a large extent on the method and precision of the observations (even perhaps on the eyesight of the observer); this may explain the wide scatter among existing estimates. Note that the value of R_{qc} depends in a fairly complicated way on the kinematic surface tension and viscosity; according to the present theory, it is definitely not the same for different liquids.

In conclusion a formula for the dimensional wavelength λ_m corresponding to the most unstable wave number α_m is worth noting, being more convenient than (5.9) for comparison with experiment. Putting $\lambda_m = 2\pi h/\alpha_m$ and using (2.3) and (5.9), we find that

$$\lambda_m = 8{\cdot}11\{\Gamma^{1/2}g^{-1\cdot2}\}R^{-1\cdot2}. \tag{5.14}$$

For water at 19° C, this gives

$$\lambda_m = 2{\cdot}21R^{-1/2}\text{ cm} = 0{\cdot}871R^{-1/2}\text{ in.} \tag{5.15}$$

This is suggested as the most likely wavelength of observed disturbances, at least when instability first becomes noticeable, and a wave structure can be distinguished.

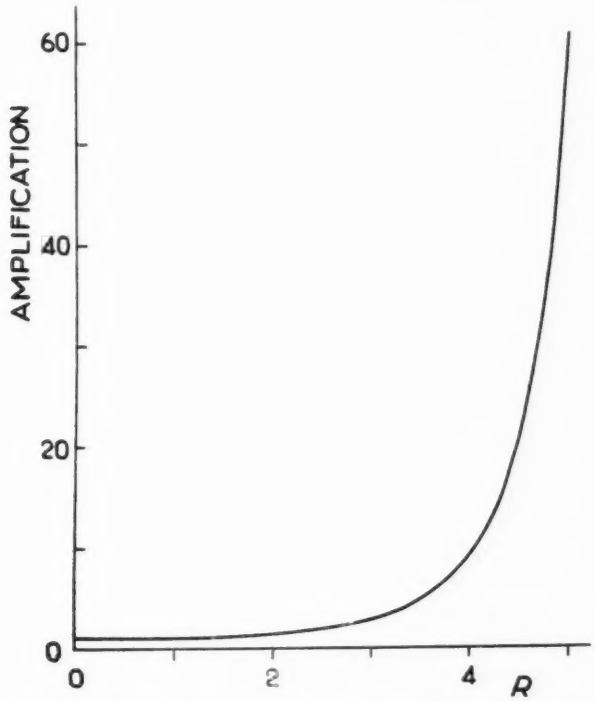

Figure 3. The amplification experienced by the most unstable wave on a vertical water film as the wave travels 10 cm.

Nevertheless, one can scarcely expect waves to appear with a strictly uniform and distinct periodicity; because under all conditions infinitesimal waves with a wide range of wavelengths are unstable, and the wave with length λ_m comes into prominence only through a rather uncritical selection process depending on differences in the rates of amplification at different wavelengths. The ultimate state of the amplified waves is, of course, determined largely by non-linear effects which remain unknown.

6. Comparison with the experiments by Binnie

The reader may refer to the paper by Binnie (1957) for an account of these experiments, which were carried out with water at 19° C. The waves

described by him were somewhat irregular in length even when the flow was delicately adjusted until the waves were just perceptible (see the photograph in his paper). This feature is understandable from the considerations made in the final paragraph of § 5, and suggests the unlikelihood of a very precise agreement between experiment and any linearized theory.

The three main points of comparison are as follows:

(i) The Reynolds number at which observable waves first occur was estimated experimentally as 4·4. Although the theory does not provide a correspondingly precise estimate, this value appears quite reasonable in the light of equation (5.13) and figure 3.

(ii) The records of wave velocity and length were taken when the measured value of Q was $6{\cdot}9 \times 10^{-3}$ in.^{3}/sec per inch span. On the substitution of this value and the value of ν quoted in § 5 for water at 19° C, equations (2.2) and (2.3) (with $\theta = 90°$) lead to $h = 4{\cdot}4 \times 10^{-3}$ in. and hence $2u_0 = 4{\cdot}7$ in./sec. According to (5.2) the latter figure is the first approximation to the wave velocity. The mean experimental value for the wave velocity was 5·5 in./sec, i.e. 17% in excess of the theoretical estimate. The order of magnitude of the extra terms involved in an approximation to c_r better than (5.2) is found to be too small to account for this discrepancy, which seems more likely to be due to the finite size of the measured waves. (The velocities of other kinds of surface wave are known to increase with the wave amplitude; e.g. irrotational waves in an inviscid fluid (Lamb 1932, § 250).) However, the comparison seems quite good in view of the obvious limitations of linearized theory in this type of investigation; in any case, it appears definitely to support the present theoretical results in favour of those found by Yih (1954) which indicate that the wave velocity should be many times greater than the experimental values.

(iii) With $R = 4{\cdot}4$ as measured, equation (5.15) gives $\lambda_m = 0{\cdot}42$ in. for the most unstable wavelength. This is in surprisingly close agreement with the value 0·45 in. obtained as the mean of the experimental observations.

The above three items seem in large measure to confirm the usefulness of the simplified method developed in § 5. However, further experiments would be necessary for a complete check; for instance, measurements of R_{ie} for different liquids would provide a particularly severe test. Suitable experiments on films with a finite slope would be more difficult than those on vertical films, since the convenience of a cylindrical wall is lost and difficulties with edge effects are bound to arise, but such experiments would be very desirable.

I wish to acknowledge the encouragement given throughout this work by Mr A. M. Binnie, and his invaluable help in checking the lengthy algebraic calculations of § 4. I should like also to express my thanks to Professor T. R. C. Fox, who first stimulated my interest in this problem, and to Dr G. K. Batchelor, who noticed that a powerful criticism based on energy considerations could be brought against my results for a vertical stream; this proved indecisive in the end, but led to a helpful clarification of some aspects of the problem.

References

Bellman, R. & Pennington, R. H. 1954 *Quart. Appl. Math.* **12,** 151.

Benjamin, T. B. & Ursell, F. 1954 *Proc. Roy. Soc.* A, **225,** 505.

Binnie, A. M. 1957 *J. Fluid Mech.* **2,** 551.

Dressler, R. F. 1952 Gravity Waves, *Nat. Bur. Stan., Wash., Circular* no. 521, p. 237.

Dukler, A. E. & Bergelin, O. P. 1952 *Chem. Engng Progress* **48,** 557.

Friedman, S. J. & Miller, C. O. 1941 *Industr. Engng Chem.* **33,** 885.

Grimley, S. S. 1945 *Trans. Inst. Chem. Engrs* **23,** 228.

Jeffreys, H. 1925 *Phil. Mag.* (6), **49,** 793.

Kapitza, P. L. 1948 *J. Exp. Theor. Phys., U.S.S.R.*, **18,** 3.

Kelvin, Lord 1887 *Mathematical and Physical Papers*, Vol. **4,** 321. Cambridge University Press.

Kirkbride, C. G. 1934 *Industr. Engng Chem.* **26,** 425. *Trans. Amer. Inst. Chem. Engrs* **30,** 170.

Lamb, H. 1932 *Hydrodynamics*, 6th Ed. Cambridge University Press.

Lighthill, M. J. & Whitham, G. B. 1955 *Proc. Roy. Soc.* A, **229,** 281.

Lin, C. C. 1955 *The Theory of Hydrodynamic Stability*. Cambridge University Press.

Nusselt, W. 1916 *Z. ver. Dtsch. Ing.* **60,** 541.

Rayleigh, Lord 1894 *The Theory of Sound*, 2nd Ed., Vol. **1**. London : Macmillan.

Squire, H. B. 1933 *Proc. Roy. Soc.* A, **142,** 621.

Taylor, G. I. 1950 *Proc. Roy. Soc.* A, **201,** 192.

Yih, C.-S. 1954 *Proc.* 2nd *U.S. Congr. Appl. Mech., Amer. Soc. Mech. Engrs*, 623.

Note added at proof stage

In the course of a recent correspondence with Prof. C.-S. Yih, light has been thrown on the possible reasons for the discrepancy between the present results and those published by him in 1954, to which frequent reference has been made in the text above. He has also kindly communicated some valuable comments on general aspects of the stability problem. It seems desirable that the main points to have emerged from the correspondence should be put on record here, particularly since this may obviate the confusing position which the differences between our two papers may otherwise have created. The points listed for convenience as follows are all due essentially to Prof. Yih, although the wording is chiefly mine.

(1) The direct numerical method used by Yih (1954) in calculating the neutral stability conditions for a vertical film was based on only two terms of a certain series expansion, and was rather sensitive to small computational errors. Thus, although his results were an effective demonstration of the low Reynolds numbers at which instability can be expected, they cannot be relied upon as more than a rough indication of the range of

unstable conditions ; in particular, they cannot be held to confute the present precise results concerning instability near the origin of the (R, α)-diagram.

(2) In unpublished work, Yih has obtained a proof that, for a vertical film, disturbances with sufficiently large wave number are stable irrespectively of surface tension or Reynolds number. This conclusion is perfectly in accord with the present work, although beyond its scope since the nature of the approximations introduced here preclude an accurate account of very short waves.

(3) The case of zero wave number (i.e. indefinitely long waves) is somewhat ambiguous from the mathematical point of view. For the long-wave approximation used in this paper, the wave number is taken to be small enough for its square to be negligible but remains a finite quantity throughout the calculations. This approach, which seems the most reasonable physically, reveals instability in a vertical film even for vanishingly small wave numbers. On the other hand, the long-wave case might be approached by setting the wave number equal to zero from the start. This step corresponds to a strictly uni-directional disturbance, with the free surface entirely undisturbed and undisplaced. In fact, the disturbance need not be infinitesimal, since the Navier–Stokes equations can be exactly solved. Yih has observed that the latter approach leads to a result indicating stability. This result appears to indicate that there is a higher mode which is always damped at zero wave number.

(4) The distinctive features of this problem, notably the instability of a vertical film at all Reynolds numbers, all stem from the fact that the energy supply to the flow is from gravity potential—in contrast to, say, the energy supply from the free stream in the case of boundary layers. If gravity were absent, any motion of the film would eventually be damped out ; in this sense the film would be stable, although, of course, any form of *static* disturbance is neutral when surface tension is also absent.

(5) From the mathematical point of view, a distinctive feature of the problem is that the complex wave velocity c appears not only in the differential equations but also in the boundary conditions. This fact, in addition to those presented in the last three items, points to the possibility that for each pair of values of R and α there may be two values of c—one for the primary mode and one for the higher mode. There are no numerical results for this possible higher mode, which in any case is not as significant physically as the primary mode.

A note on the application of the supersonic area rule to the determination of the wave drag of rectangular wings

By R. C. LOCK
Aerodynamics Division, National Physical Laboratory, Teddington

(*Received* 12 *April* 1957)

SUMMARY

A proof is given that, in spite of certain singularities in the oblique area distributions, the supersonic area rule can be used to determine correctly the wave drag, according to linearized theory, of thin symmetrical rectangular wings at zero incidence. The proof could be extended to cover the case of swept wings with supersonic edges, for which similar singularities also exist.

1. INTRODUCTION

It has recently been suggested that the 'supersonic area rule' (Jones 1953), when used to determine the wave drag at zero lift of wings with straight supersonic edges, gives results which disagree with those of conventional thin wing theory, due to certain singularities which appear in the oblique area distributions. It is the purpose of the present note to show that this is not the case, provided that these singularities are handled with care. A proof is given of the equivalence of the wave drag as calculated by the two methods for unswept wings of rectangular planform; the proof could easily be extended to cover the case of untapered swept wings with supersonic leading and trailing edges.

2. THE SUPERSONIC AREA RULE

We consider a rectangular wing of unit chord and span $b = 2s$, and use standard rectangular axes with origin O at the centre of the leading edge, Ox in the direction of the free stream, Oy along the leading edge and Oz vertically upward; we shall also use cylindrical coordinates $r = \sqrt{(y^2+z^2)}$ and $\theta = \tan^{-1}z/y$. The wing section, which must be symmetrical with sharp leading and trailing edges, is taken to be

$$z = \pm f(x) \qquad (0 \leqslant x \leqslant 1), \tag{1}$$

and we define $f(x)$ to be zero outside this range.

The area rule for calculating the wave drag, according to the linearized theory of supersonic flow, of any body which can be represented solely by a distribution of sources, may be deduced from considerations of momentum flux across the large cylinder $r = R$; use is made of Hayes's theorem on

equivalent source positions (see, for example, Heaslet, Lomax & Spreiter 1952), which states that, for closed source distributions at large values of r and for a given value of θ, the flow due to a unit source is independent of its position on the plane

$$x = x_0 + \beta(y\cos\theta + z\sin\theta), \tag{2}$$

where x_0 is constant and $\beta = \sqrt{(M^2-1)}$. When applied to plane wings, for which the source strength is proportional to the local slope of the surface in the x-direction, the theorem shows that the planar source distribution may be concentrated onto the x-axis so that, again for a given value of θ, the effect at large distances is the same as that of an 'equivalent body of revolution' whose cross-sectional area at $x = \xi$ is $S(\xi, \theta)$, defined as the area of the projection on a plane normal to the axis Ox of the section of the wing by the plane.

$$x = \xi + \beta y\cos\theta. \tag{3}$$

In this way the following well-known formula for the wave drag D may be obtained:

$$\frac{D}{\frac{1}{2}\rho_0 U^2} = -\frac{1}{4\pi^2}\int_0^{2\pi} d\theta \iint d\xi d\eta \log|\xi-\eta| S''(\xi,\theta)S''(\eta,\theta), \tag{4}$$

where ρ_0 and U are the density and velocity of the free stream, $S(\xi, \theta)$ is defined above, and primes denote differentiation with respect to ξ (or η). For symmetrical unyawed wings this reduces to

$$\frac{D}{\frac{1}{2}\rho_0 U^2} = -\frac{1}{\pi^2}\int_0^{\frac{1}{2}\pi} d\theta \iint d\xi d\eta \log|\xi-\eta| S''(\xi,\theta)S''(\eta,\theta). \tag{5}$$

In order that equations (4) and (5) shall be valid, it is necessary that $S'(\xi, \theta)$ shall be a continuous function of ξ, though $S''(\xi, \theta)$ may have a finite number of discontinuities. But it is evident that, in the case of a rectangular wing, this requirement is not satisfied when $\theta = \frac{1}{2}\pi$; $S'(\xi, \frac{1}{2}\pi)$ is in fact proportional to $f'(\xi)$, with discontinuities at $\xi = 0$ and 1. To put this in another way, we see that when the source distribution representing the wing is concentrated onto the axis along lines $x = \xi$ (cf. (3) with $\theta = \frac{1}{2}\pi$) *parallel to the leading edge*, the resulting axial distribution is of finite strength at the leading and trailing edges; and such a distribution is inadmissible since it leads to infinite velocities on the Mach cones from these points. Physically, the situation is due to the fact that (according to unmodified linearized theory), the flow in the plane $\theta = \frac{1}{2}\pi$ is always partly two-dimensional in character, with leading and trailing edge shocks of first order strength, however large R may be; and such a flow can never be represented by a continuous distribution of purely axial sources. The effect is however concentrated, so far as the control surface $r = R$ is concerned, in the immediate neighbourhood of the points $(\beta R, 0, \pm R)$ and $(\beta R + 1, 0, \pm R)$ (when R is sufficiently large); and such isolated singularities do not invalidate the use of equations (4) and (5) for the overall wave drag, provided that care is taken near $\theta = \pm\frac{1}{2}\pi$.

3. Determination of oblique area distributions

It is convenient to write

$$\sigma(\theta) = \beta s \cos\theta.$$

There are two principal cases to be considered, according as $\sigma \gtrless \frac{1}{2}$.

(*a*) $\sigma \geqslant \frac{1}{2}$ or $|\sec\theta| \leqslant 2\beta s$ (see figure 1 *a*). Since the sections in question are simply oblique sections of a cylinder, it is easily seen that

$$S(\xi,\theta) = \frac{2\sec\theta}{\beta}\int_0^{\xi+\sigma} f(x)\,dx \qquad (-\sigma \leqslant \xi \leqslant 1-\sigma) \tag{6a}$$

$$= \frac{2\sec\theta}{\beta}\int_0^{1} f(x)\,dx \qquad (1-\sigma \leqslant \xi \leqslant \sigma) \tag{7a}$$

$$= \frac{2\sec\theta}{\beta}\int_{\xi-\sigma}^{1} f(x)\,dx \qquad (\sigma \leqslant \xi \leqslant 1+\sigma). \tag{8a}$$

(*b*) $0 < \sigma \leqslant \frac{1}{2}$ or $|\sec\theta| \geqslant 2\beta s$ (see figure 1 *b*). In this case the sections for $\sigma \leqslant \xi \leqslant 1-\sigma$ cut both wing tips, and the results have to be modified as follows:

$$S(\xi,\theta) = \frac{2\sec\theta}{\beta}\int_0^{\xi+\sigma} f(x)\,dx \qquad (-\sigma \leqslant \xi \leqslant \sigma) \tag{6b}$$

$$= \frac{2\sec\theta}{\beta}\int_{\xi-\sigma}^{\xi+\sigma} f(x)\,dx \qquad (\sigma \leqslant \xi \leqslant 1-\sigma) \tag{7b}$$

$$= \frac{2\sec\theta}{\beta}\int_{\xi-\sigma}^{1} f(x)\,dx \qquad (1-\sigma \leqslant \xi \leqslant 1+\sigma). \tag{8b}$$

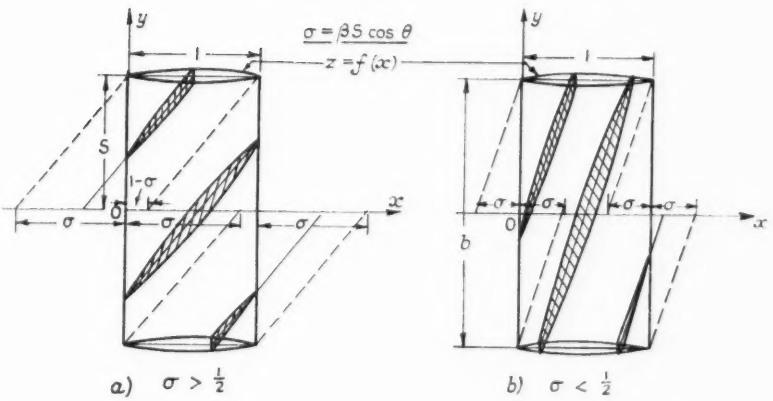

Figure 1. Determination of oblique area distributions. S is the projection of the shaded area on a plane perpendicular to Ox.

Differentiating (6) to (8) with respect to ξ, we find that in both cases

$$\left.\begin{aligned} S'(\xi,\theta) &= 2\beta^{-1}\sec\theta\{f(\xi+\sigma)-f(\xi-\sigma)\} \qquad (9)\\ S''(\xi,\theta) &= 2\beta^{-1}\sec\theta\{f'(\xi+\sigma)-f'(\xi-\sigma)\} \qquad (10)\end{aligned}\right\} \quad 0 \leqslant \theta < \tfrac{1}{2}\pi,$$

remembering that $f(x) = f'(x) = 0$ for $x < 0$ and $x > 1$. When $\theta = \frac{1}{2}\pi$, it is evident that

$$S'(\xi, \tfrac{1}{2}\pi) = 2sf'(\xi). \tag{11}$$

The function $S'(\xi, \theta)$ is sketched for some typical cases of a biconvex section in figure 2. It is clear that, except when $\theta = \frac{1}{2}\pi$, $S'(\xi, \theta)$ is everywhere continuous as required in (5), though $S''(\xi, \theta)$ has four discontinuities.

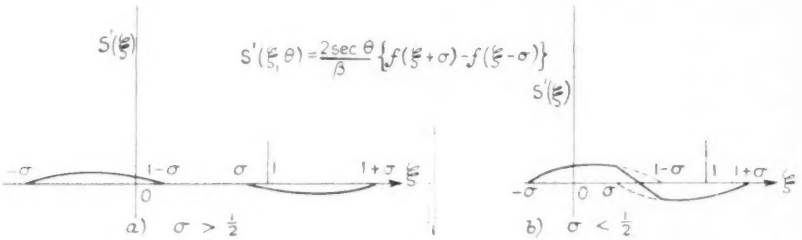

Figure 2. The function $S'(\xi, \theta)$.

4. Evaluation of the wave drag

Substituting from (10) in (5), we obtain

$$\frac{D}{\frac{1}{2}\rho_0 U^2} = -\frac{4}{\pi^2\beta^2}\int_0^{\frac{1}{2}\pi} \sec^2\theta\, d\theta \iint d\xi d\eta \log|\xi - \eta| \{f'(\xi+\sigma)f'(\eta+\sigma) + f'(\xi-\sigma)f'(\eta-\sigma) - f'(\xi+\sigma)f'(\eta-\sigma) - f'(\xi-\sigma)f'(\eta+\sigma)\}. \tag{12}$$

Each of the four double integrals with respect to ξ and η may be simplified by linear transformations of the type

$$\xi \pm \sigma = x,$$
$$\eta \pm \sigma = y,$$

leading to the result

$$\frac{D}{\frac{1}{2}\rho_0 U^2} = \frac{4}{\pi^2\beta^2}\int_0^{\frac{1}{2}\pi} \sec^2\theta\, d\theta \int_0^1\int_0^1 dx dy\, f'(x)f'(y)\log\left|1 - \frac{\beta^2 b^2\cos^2\theta}{(x-y)^2}\right|. \tag{13}$$

When the function $f(x)$ is given, the double integral with respect to x and y can be evaluated directly, and it is found that the resulting function of θ is integrable over the range 0 to $\frac{1}{2}\pi$ and yields the correct result for the wave drag D. But in order to obtain a general result it is clearly necessary to perform the integration with respect to θ first; this must however be done with care, since the function

$$F(\theta, x, y) = \sec^2\theta \log\left|1 - \frac{\beta^2 b^2\cos^2\theta}{(x-y)^2}\right|,$$

although regular as $\theta \to \frac{1}{2}\pi$ if $x \neq y$ and having only logarithmic singularities if $\theta \neq \frac{1}{2}\pi$, has an essential singularity when $\theta = \frac{1}{2}\pi$, $x = y$. The triple integral (13) for D cannot therefore be expressed as a volume integral,

and the order of integration cannot be inverted in the usual way; but this difficulty may be overcome as follows.

An alternative expression for D is

$$\frac{D}{\frac{1}{2}\rho_0 U^2} = \frac{8}{\pi^2\beta^2}\int_0^{\frac{1}{2}\pi}\sec^2\theta\,d\theta\int_0^1 f'(x)\,dx\int_0^x f'(y)\log\left|1-\frac{\beta^2b^2\cos^2\theta}{(x-y)^2}\right|dy, \quad (14)$$

and this may be written in the form

$$\frac{D}{\frac{1}{2}\rho_0 U^2} = \lim_{\epsilon\to 0}\frac{8}{\pi^2\beta^2}\{I_1(\epsilon)+I_2(\epsilon)\}, \quad (15)$$

where

$$I_1(\epsilon) = \int_0^{\frac{1}{2}\pi}\sec^2\theta\,d\theta\int_0^1 f'(x)\,dx\int_0^{x-\epsilon} f'(y)\log\left|1-\frac{\beta^2b^2\cos^2\theta}{(x-y)^2}\right|dy, \quad (16)$$

and

$$I_2(\epsilon) = \int_0^{\frac{1}{2}\pi}\sec^2\theta\,d\theta\int_0^1 f'(x)\,dx\int_{x-\epsilon}^{x} f'(y)\log\left|1-\frac{\beta^2b^2\cos^2\theta}{(x-y)^2}\right|dy. \quad (17)$$

The singularity at $\theta = \frac{1}{2}\pi$, $x = y$, has been isolated from the region of integration in I_1, so that the integration with respect to θ may be performed first.

Using the result (see Appendix)

$$\left.\begin{aligned}\int_0^{\frac{1}{2}\pi}F(\theta,x,y)\,d\theta &= -\pi \qquad (\epsilon < |x-y| \leqslant \beta b),\\ &= -\pi\left\{1-\sqrt{\left[1-\frac{\beta^2b^2}{(x-y)^2}\right]}\right\}(|x-y| \geqslant \beta b),\end{aligned}\right\} \quad (18)$$

we obtain

$$I_1(\epsilon) = -\pi\int_0^1 f'(x)\,dx\int_0^{x-\epsilon} f'(y)\,dy + \\ +\pi\int_{\beta b}^1 f'(x)\,dx\int_0^{x-\beta b} f'(y)\sqrt{\left\{1-\frac{\beta^2b^2}{(x-y)^2}\right\}}\,dy;$$

the second integral occurs only if $\beta b < 1$.

Now

$$\int_0^1 f'(x)\,dx\int_0^{x-\epsilon} f'(y)\,dy = \int_0^1 f'(x)f(x-\epsilon)\,dx = O(\epsilon),$$

since

$$\int_0^1 f'(x)f(x)\,dx = 0.$$

Hence

$$I_1(\epsilon) = \pi\int_{\beta b}^1 f'(x)\,dx\int_0^{x-\beta b} f'(y)\sqrt{\left\{1-\frac{\beta^2b^2}{(x-y)^2}\right\}}\,dy + O(\epsilon). \quad (19)$$

In evaluating I_2 we must retain the original order of integration. Now

$$\int_{x-\epsilon}^{x} f'(y)\log\left|1-\frac{\beta^2b^2\cos^2\theta}{(x-y)^2}\right|dy = f'(x)\{1+O(\epsilon)\}\int_{x-\epsilon}^{x}\log\left|1-\frac{\beta^2b^2\cos^2\theta}{(x-y)^2}\right|dy$$

$$= f'(x)\{1+O(\epsilon)\}\left\{\epsilon\log\left|1-\frac{\beta^2b^2}{\epsilon^2}\cos^2\theta\right| + \beta b\cos\theta\log\left|\frac{1+(\beta b/\epsilon)\cos\theta}{1-(\beta b/\epsilon)\cos\theta}\right|\right\}.$$

Thus

$$I_2(\epsilon) = \{1+O(\epsilon)\}\int_0^{\frac{1}{2}\pi}\sec^2\theta\,d\theta\int_0^1\{f'(x)\}^2\times$$
$$\times\left\{\epsilon\log\left|1-\frac{\beta^2b^2}{\epsilon^2}\cos^2\theta\right|+\beta b\cos\theta\log\left|\frac{1+(\beta b/\epsilon)\cos\theta}{1-(\beta b/\epsilon)\cos\theta}\right|\right\}dx$$
$$= \{1+O(\epsilon)\}\int_0^1\{f'(x)\}^2\,dx\times$$
$$\times\int_0^{\frac{1}{2}\pi}\sec^2\theta\left\{\epsilon\log\left|1-\frac{\beta^2b^2}{\epsilon^2}\cos^2\theta\right|+\beta b\cos\theta\log\left|\frac{1+(\beta b/\epsilon)\cos\theta}{1-(\beta b/\epsilon)\cos\theta}\right|\right\}d\theta.$$

Using the results proved in the Appendix

$$\int_0^{\frac{1}{2}\pi}\sec^2\theta\log\left|1-\frac{\beta^2b^2}{\epsilon^2}\cos^2\theta\right|d\theta = -\pi \quad (\epsilon < \beta b),$$
$$\int_0^{\frac{1}{2}\pi}\sec\theta\log\left|\frac{1+(\beta b/\epsilon)\cos\theta}{1-(\beta b/\epsilon)\cos\theta}\right|d\theta = \tfrac{1}{2}\pi^2 \quad (\epsilon < \beta b),$$

we find that
$$I_2(\epsilon) = \tfrac{1}{2}\pi^2\beta b\int_0^1\{f'(x)\}^2\,dx\,\{1+O(\epsilon)\}. \tag{20}$$

Substituting from equations (19) and (20) in (15), and taking the limit as $\epsilon\to 0$, we obtain finally

$$C_D = \frac{D}{\frac{1}{2}\rho_0U^2b} = \frac{4}{\beta}\int_0^1\{f'(x)\}^2\,dx \qquad (\beta b \geqslant 1), \tag{21 a}$$
$$= \frac{4}{\beta}\int_0^1\{f'(x)\}^2\,dx +$$
$$+\frac{8}{\pi\beta^2b}\int_{\beta b}^1 f'(x)\,dx\int_0^{x-\beta b}f'(y)\sqrt{\left\{1-\frac{\beta^2b^2}{(x-y)^2}\right\}}\,dy \quad (\beta b < 1). \tag{21 b}$$

Equation (21 a) is simply the well-known result that the drag coefficient of a rectangular wing is equal to the corresponding two-dimensional value, being unaffected by the presence of the wing tips, provided that the aspect ratio is greater than β^{-1}; equation (21 b) contains the additional term that has to be added when the aspect ratio is less than β^{-1}, and it has been verified that for a biconvex section this gives results in agreement with those of Harmon (1947).

5. Conclusions

The argument given above shows that the area rule can be applied successfully to determine the wave drag of a rectangular wing, in spite of the singular area distribution which occurs when $\theta = \frac{1}{2}\pi$, the meaning of which has been discussed in § 2. In fact the complications introduced by this singularity in the anlysis of § 4 are due to the necessity of inverting the order of integration in (13) in order to obtain a general proof; if the integrations with respect to x and y had been performed first no such difficulty would have been experienced, though it should be mentioned

that, in view of the simplicity of the final result, the labour involved is quite considerable, even for a simple biconvex section.

It is evident that the method of proof given in the present note could easily be extended to cover the case of untapered swept wings. Again singular area distribution would occur when $\theta = \cos^{-1}(\beta^{-1}\tan\Lambda)$, where Λ is the angle of sweep, but again they would not lead to serious difficulties.

Appendix. Evaluation of two definite integrals

(i) $$\mathcal{I}(a) = \int_0^{\frac{1}{2}\pi} \sec^2\theta \log|1 - a\cos^2\theta|\, d\theta \quad (a > 0).$$

Write $\tan\theta = t$; then

$$\mathcal{I} = \int_0^\infty \log\left|\frac{t^2+1-a}{t^2+1}\right| dt.$$

(*a*) If $a < 1$, write $1-a = c^2$; then

$$\begin{aligned}\mathcal{I} &= \int_0^\infty \log\left(\frac{t^2+c^2}{t^2+1}\right) dt \\ &= \left[t\log\left(\frac{t^2+c^2}{t^2+1}\right) + 2c\tan^{-1}\frac{t}{c} - 2\tan^{-1}t\right]_{t=0}^{\infty} \\ &= (c-1)\pi = -\pi\{1-\sqrt{(1-a)}\}.\end{aligned}$$

(*b*) If $a > 1$, write $a-1 = d^2$; then

$$\begin{aligned}\mathcal{I} &= \int_0^\infty \log\left|\frac{t^2-d^2}{t^2+1}\right| dt \\ &= \left[t\log\frac{|t^2-d^2|}{(t^2+1)} + d\log\left|\frac{t+d}{t-d}\right| - 2\tan^{-1}t\right]_{t=0}^{\infty} \\ &= -\pi.\end{aligned}$$

(ii) $$\mathcal{J}(a) = \int_0^{\frac{1}{2}\pi} \sec\theta \log\left|\frac{1+a\cos\theta}{1-a\cos\theta}\right| d\theta \quad (a > 1)$$

$$= \int_0^{\pi} \sec\theta \log|1+a\cos\theta|\, d\theta.$$

We shall first show that $\mathcal{J}(a)$ is independent of a, if $a \geqslant 1$. For

$$\frac{d}{da}\mathcal{J}(a) = \int_0^{\pi} \frac{d\theta}{(a\cos\theta - 1)},$$

where the Cauchy principal value must be taken. Writing $\tan\frac{1}{2}\theta = \tau$, we find that

$$\begin{aligned}\frac{d}{da}\mathcal{J}(a) &= \frac{2}{(1+a)}\int_0^\infty \frac{d\tau}{\alpha^2-\tau^2}, \quad \text{where } \alpha = \sqrt{\left(\frac{a-1}{a+1}\right)}, \\ &= \frac{1}{\alpha(1+a)}\left[\log\left|\frac{\alpha+\tau}{\alpha-\tau}\right|\right]_{\tau=0}^{\infty} = 0.\end{aligned}$$

Hence
$$\begin{aligned}
\mathcal{J}(a) = \mathcal{J}(1) &= \int_0^{\frac{1}{2}\pi} \sec\theta \log\left(\frac{1-\cos\theta}{1+\cos\theta}\right) d\theta \\
&= -4\int_0^1 \frac{\log\tau}{(1-\tau^2)}\, d\tau, \qquad \text{where } \tau = \tan\tfrac{1}{2}\theta, \\
&= 2\int_0^1 \frac{1}{\tau}\log\left(\frac{1+\tau}{1-\tau}\right) d\tau \\
&= 4\lim_{x\to 1}\int_0^x \left(1+\frac{\tau^2}{3}+\frac{\tau^4}{5}+\ldots\right) d\tau \\
&= 4\lim_{x\to 1}\left(x+\frac{x^3}{3^2}+\frac{x^5}{5^2}+\ldots\right) \\
&= \tfrac{1}{2}\pi^2.
\end{aligned}$$

The work described above was carried out in the Aerodynamics Division of the National Physical Laboratory and is published by permission of the Director of the Laboratory.

References

Harmon, S. M. 1947 Theoretical supersonic wave drag of untapered sweptback and rectangular wings at zero lift, *Nat. Adv. Comm. Aero., Wash., Tech. Note* no. 1449.

Heaslet, M. A., Lomax, H. & Spreiter, J. R. 1952 Linearised compressible flow theory for sonic flight speeds, *Nat. Adv. Comm. Aero., Wash., Rep.* no. 956.

Jones, R. T. 1953 Theory of wing-body drag at supersonic speeds, *Nat. Adv. Comm. Aero., Wash., Res. Mem.* no. A53H18a. (Also as *Aero. Res. Counc., Lond., unpub. rep.* no. 16603.)

Experiments on convection of isolated masses of buoyant fluid

By R. S. SCORER
Department of Meteorology, Imperial College, London

(*Received* 15 *February* 1957)

SUMMARY

Isolated masses of buoyant fluid were released in a water tank. Their width, $2r$, and the distance travelled, z, were measured as functions of time and were found to follow roughly the laws

$$r = nz, \qquad w = C(g\overline{B}r)^{1/2},$$

where w is the vertical velocity, $\overline{B}$ the mean buoyancy, and n and C are constants. These equations are predicted by dimensional analysis, assuming viscosity to be negligible, and the constants appear to be independent of the Reynolds number. It is found that $C \doteqdot 1{\cdot}2$, and n is in the neighbourhood of 4.

Since the Froude number relating the buoyancy and inertia forces is the same as for isolated masses of buoyant air in the atmosphere, it is concluded that the constants will have the same value in this latter case. This is confirmed roughly by observation of cumulus cloud towers.

Some of the characteristics of the motion observed in the experiments are described and comparison is made with vortex rings.

1. THE NATURE OF THE PROBLEM

It was desired to study motion produced in a fluid by buoyancy forces alone far from solid boundaries, in order to simulate buoyant convection in the atmosphere. From the behaviour of cumulus clouds and the experience of glider pilots over many years, it appears that convection, by which in this paper we mean convection produced by buoyancy forces, consists largely of more or less isolated masses of buoyant air rising into and mixing with their surroundings from intermittent sources on the ground or within clouds (see, for example, Ludlam & Scorer 1953; Welch, Welch & Irving 1955).

For simplicity in the experiments, masses of heavy solutions were released from rest at the top of a water tank, and their growth downwards was observed photographically. If the volume at release is sufficiently small compared with its subsequent volume and no impulse is applied, the subsequent growth can be expected to be largely independent of the initial configuration of the substance released. In such case the factors determining the motion are so few that a very simple dimensional analysis

can be applied. The method has been discussed by Batchelor (1954), and experiments of this kind have been carried out by Morton, Taylor & Turner (1956), and Scorer & Ronne (1956). The motion is so complicated that no way was seen whereby the simplest dimensional analysis could be improved upon, and so the numerical coefficients relating a bulk dimension of the cloud of buoyant fluid to its buoyancy and vertical velocity were measured, with a view to applying them to the atmosphere.

2. The characteristics of 'thermals'

Following the usage of glider pilots, the buoyant masses of fluid are called 'thermals' herein. Over the advancing front of the thermal, mixing with the fluid ahead takes place. Inside and at the rear the fluid circulates rather as in a vortex ring, the motion being relatively smooth. As a result of the mixing the volume continuously grows, and, although the vertical

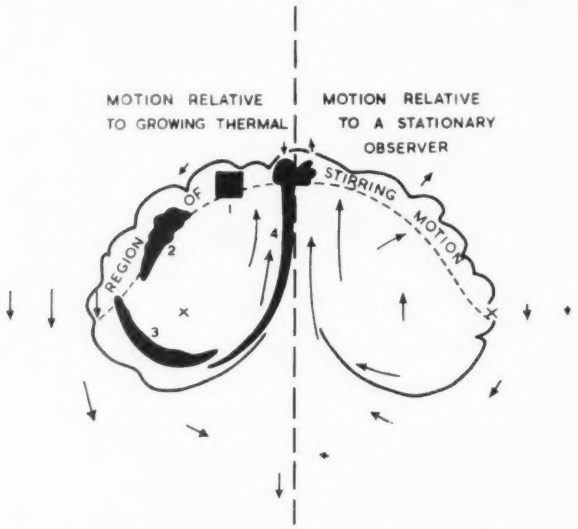

Figure 4. Approximate distribution of velocity in a typical thermal. The black area illustrates successive positions of a portion of the thermal, into which mixing has just occurred, beginning with the square.

momentum steadily increases through action of the buoyancy force, the velocity decreases on account of the incorporation of exterior fluid. Examples are seen in figures 1, 2 and 3 (plates 1 and 2). The pattern of motion is represented in figure 4. An idea of the exterior motion is gained from figure 3 (plate 2).

The thermals were released from a thin hemispherical copper cup (seen in figure 3, plate 2) pivoted about a horizontal axis, the level of the fluid inside being made the same as outside before release so as to avoid any

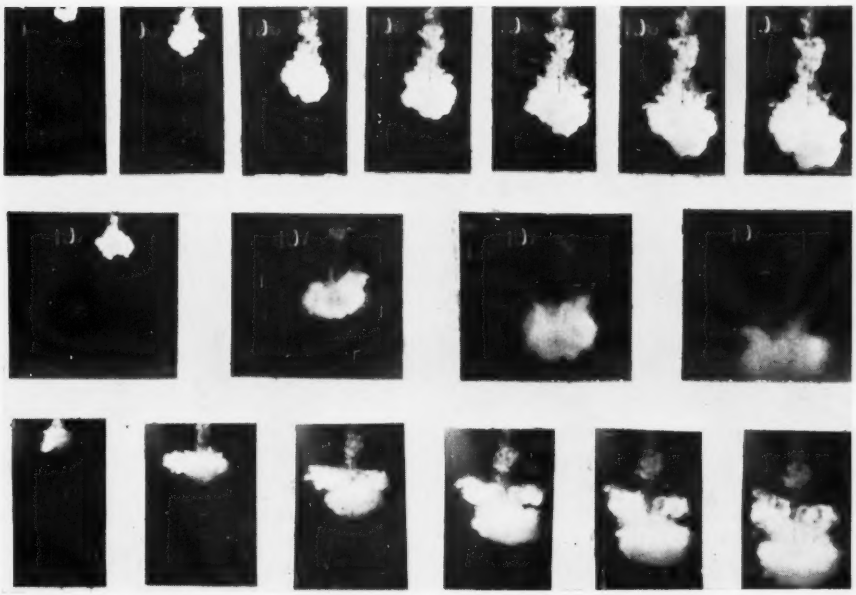

Figure 1. Series of pictures taken from cine film showing the growth of thermals in a water tank, made visible by white precipitate. (Experimental numbers 106, 107, 111). No. 107 is unusually well formed.

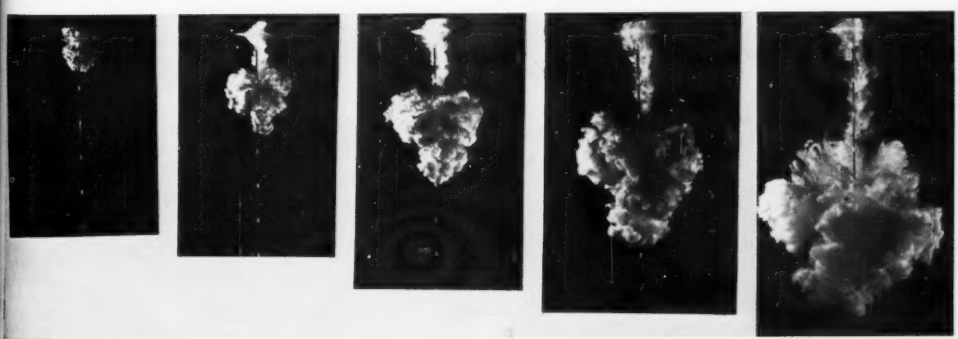

Figure 2. Pictures illustrating how a shape assumed early in the life of a thermal may persist while the volume increases several times. This may be contrasted with no. 111 of figure 1 in which the protuberances are shed. Note the 'cauliflower' nature of the surface. No shearing motion is visible in these protuberances.

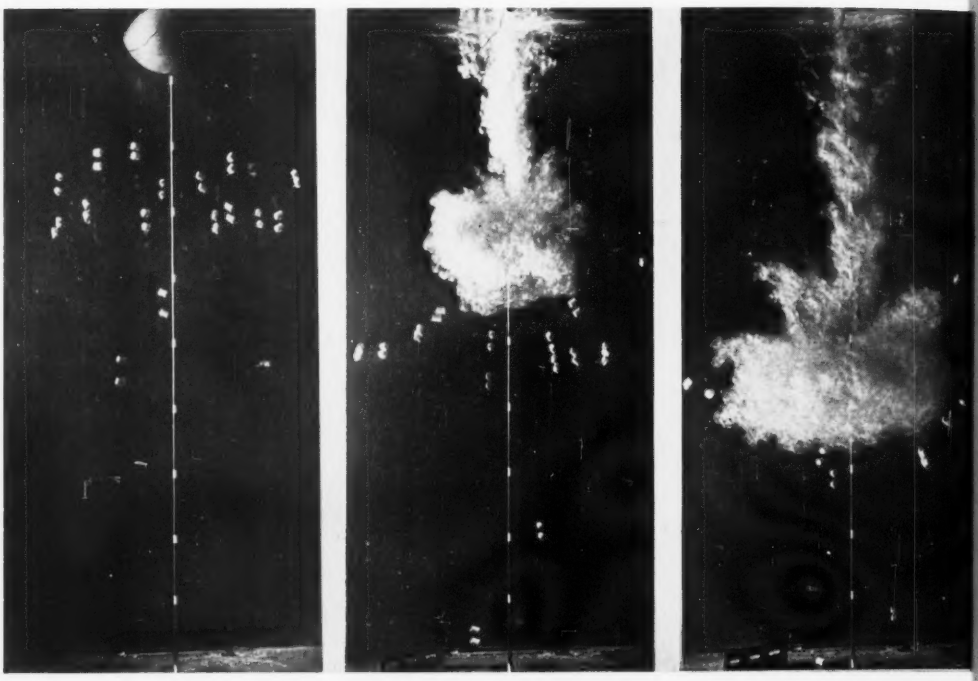

Figure 3. In each picture there are two exposures about $\frac{1}{2}$ sec apart. The first picture shows the free rate of sink of some slowly sinking particles. In the second and third pictures an idea of the velocity field outside the thermal can be gained. The particles immediately in front of the thermal are displaced downwards as much as the faster sinking ones lower down, while those at the side are in an upcurrent. Those that have disappeared have entered the advancing 'front' of the thermal, not the rear. The markings on the vertical rod are at 10 cm intervals.

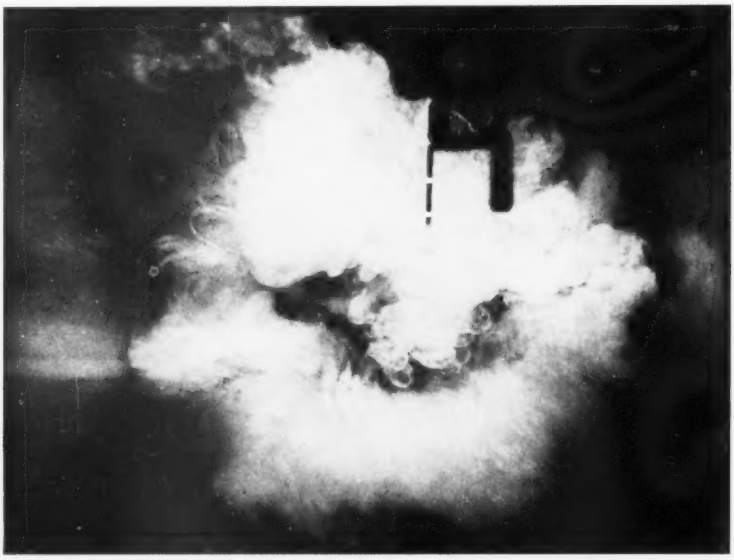

Figure 9. View of a thermal from above showing the hollowed-out rear.

he free
of the
hermal
ide are
ermal,

initial impulse. The cup was turned over quickly by hand, and a negligible amount of motion was produced thereby. A dense white precipitate was used to make the buoyant fluid visible. Immediately after release the front surface of the thermal became covered with protuberances and the volume began to increase. After the main mass escaped from the surface there was often a stem left behind. But this was very dilute and had negligible velocity in it, and was therefore assumed to contain a negligible fraction of the original material. This stem is thought to be a kind of 'splash' produced as the original material becomes rearranged into the configuration which it ultimately assumes.

The motion consists initially of an acceleration. After the thermal has travelled about 1·5 diameters deceleration begins, and the measurements were concerned with the subsequent motion.

In order that simple dimensional analysis should be applicable it is necessary to suppose that the thermal behaves as it if originated at a virtual point origin. Therefore, in order to allow location of this origin as closely as possible, the same cup (radius 3 in.) was used in nearly all the experiments and was filled to approximately the same depth each time. Thus at least the geometry of the initial conditions was approximately the same, and the origin was assumed to be in the same position in all these cases. Some other cases were included when they were susceptible of easy measurement, that is, when the thermals grew with reasonable symmetry.

The density differences were kept small, and were initially less than 15%. If this is not done two difficulties arise. First, the motion may be different according to whether the heavier fluid is inside or outside (downward or upward motion), and, second, it may vary according to the magnitude of the density differences. During the measured part of the thermals' lives the density differences were mostly much less than 5%, and were reduced to around 0·1% towards the end of each experiment.

Some thermals grew in a grossly asymmetrical manner. This is thought to be due to internal motions of the thermal, or occasionally in the tank, at the moment of release. These cases were rejected.

Occasionally odd characteristics of shape seen in the early stages were retained almost throughout the observed life of a thermal (see figure 2, plate 1). In particular the angle subtended at the point of origin tended to remain the same, though it varied somewhat from thermal to thermal.

3. Simple dimensional analysis

The only factors which can determine the velocities are the buoyancy forces and the size. The local buoyancy force on unit mass of fluid is

$$g\frac{\rho_0-\rho_i}{\rho_0}=gB, \tag{1}$$

ρ_i and ρ_0 being the interior and exterior densities. The density ratio B varies within the thermal because the dilution varies, and so the mean value $\bar{B}$ will be used, the distribution of B being at present unknown. If r is

the radius of the largest horizontal section, the vertical velocity of the front of the thermal must then be of the form

$$w^2 = C^2 g\overline{B} r \tag{2}$$

from dimensional considerations. C^2 is a Froude number, being a ratio between inertia forces and buoyancy forces.

The same formula can likewise be derived for the rise of a bubble of buoyant fluid which will not mix the surroundings. One example of this is the formula for the rise of bubbles of air through water, derived by Davies & Taylor (1950). There are some interesting differences. The buoyancy B in that case is virtually unity, but it is also constant, and for this reason it is not necessary to assume that B is small in the case of immiscible fluids. The drag is here due to the formation of a wake, so that the buoyant energy is converted into energy of turbulent motion of the surroundings; in our case there is no wake, but the 'drag' is due to the continuous incorporation of outside fluid.

If z is the height of the foremost part of the thermal the two velocities dz/dt and dr/dt are proportional to all other velocities, and so

$$z = nr \tag{3}$$

if the origin of z is suitably chosen. This, the virtual origin, is at the apex of the cone swept out by the largest horizontal section. n has to be determined by experiment, and, like C, must be the same for all thermals, according to the assumptions made. Since only one representative velocity exists (which is equivalent to saying that there is no Froude number other than C^2), the motion is similar at all stages in the life of a thermal and all thermals are similar.

The volume V of the thermal, which is seen in the experiments to possess a clearly defined outline, is given by

$$V = mr^3, \tag{4}$$

where m is another number to be determined by experiment. The total buoyancy of the thermal is constant, so that if suffix 0 denotes the values at the moment of release, when ρ_i is uniform,

$$g\overline{B} m r^3 = g B_0 V_0. \tag{5}$$

In the experiments B_0 and V_0 were measured before the release of the thermal.

Writing $w = dz/dt$ and integrating (2), we obtain

$$kz^2 = t, \tag{6}$$

where

$$k = m^{1/2}/2nC(gB_0 V_0)^{1/2}, \tag{7}$$

the origin of t being suitably chosen.

The objective in the experiments was first to confirm the relation (6) for each thermal separately, and then (7) for a variety of values of $gB_0 V_0$, the total weight (deficiency or excess) of the thermal.

4. The effect of viscosity

In previous work on experiments and analysis of this kind (Batchelor 1954; Morton, Taylor & Turner 1956), the motion has been described as 'fully turbulent', and it has been assumed that the viscous forces are negligible in comparison with the inertia forces (including the eddy stresses) and the buoyancy forces. In the case of a conical plume from a maintained source of buoyancy, the fact that the plume is conical confirms the correctness of this assumption because the Reynolds number varies up the plume. Furthermore, the motion is quite evidently turbulent throughout the volume of the plume. However, when small drops of coloured fluid are let fall in clear fluid they do not develop turbulent motion but retain a smooth outline. In an individual thermal from a source which is not maintained, the Reynolds number wr/ν is equal to $1/2k\nu$, which is the same throughout the life of a thermal; so that it would in any case be expected to grow along a cone and retain a constant shape even if viscous forces were important. But the Reynolds number varies from one thermal to another, and so if (7) is confirmed we can assume that variations in Reynolds number make no difference and that viscous forces are negligible.

In the case of thermals in cumulus clouds (see § 7 below) the Reynolds number is about one thousand times greater than in these experiments. The constant C is roughly the same, and so the assumption that viscosity can be neglected is further justified.

5. Experimental results

The thermals were released into a tank with horizontal section 2 ft. × 4 ft. The thermals traversed the depth of $3\frac{1}{2}$ ft. in between 5 and 30 seconds according to the weight excess.

The virtual origin was determined roughly by plotting r against z, extrapolating backwards, and taking $z = 0$ where $r = 0$. Variations in the position of the virtual origin by 3–4 cm had a negligible effect on the value of k obtained when z^2 was plotted against t, and so the origin was taken to have the same position relative to the bottom point of the cup in all cases in which V_0 was nearly the same. In a few cases V_0 was substantially different and for those the origin was determined individually.

The crudeness with which the measurements have to be made must be mentioned. Successive outlines of four typical thermals are shown in figure 5. With them are the plots of z^2 against t and the straight lines drawn to determine k. As expected, the points deviate from the line in the early part of the life while the thermal grows into its ultimate shape. Some of the thermals grew somewhat asymmetrically or irregularly but nevertheless yielded fairly definite values of k. The results are given in table 1.

No qualitative difference in the motion was evident when the motion was upwards. A fluorescent dye was used to make the thermal of methyl alcohol visible, but the outline was less sharp than with the white precipitate. Only one upward moving case (no. 201) was measured, and this agrees closely with the others.

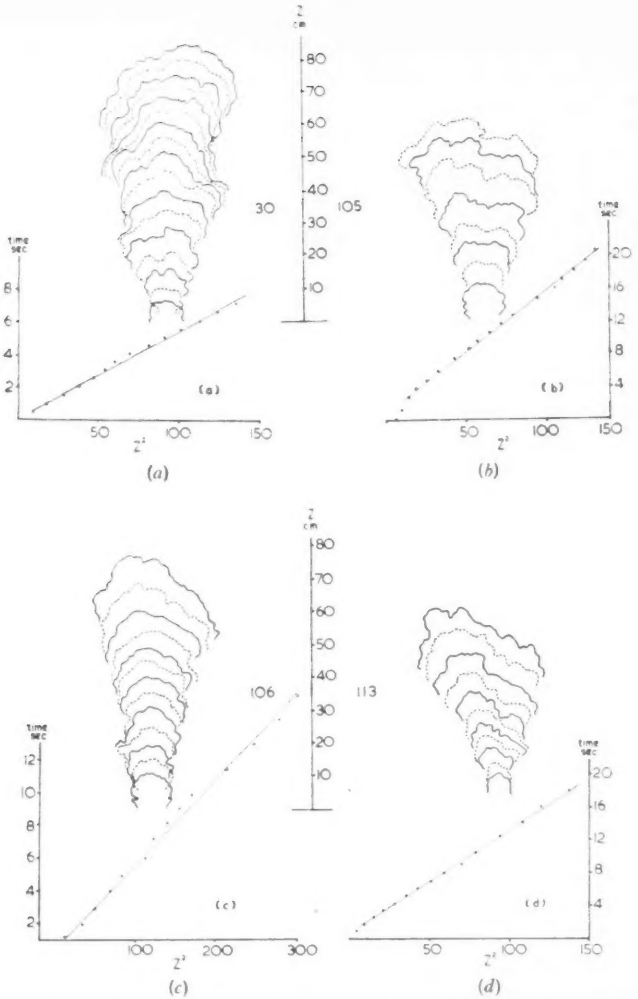

Figure 5. Successive outlines of thermals traced from photographs. Beneath each is a graph of z^2 against t. (*a*) and (*b*) show fairly typical thermals; 106 (*c*) is an example of a very large value of n; 113 (*d*) shows a very asymmetrical thermal.

In figure 6 we have plotted $(V_0 B_0)^{1/2}$ against k^{-1}, and the straight line was drawn by eye through the origin to fit the points. There is no evident systematic deviation from this line and so viscosity can reasonably be assumed to be negligible. The straight line represents the relation $k^{-1} = 180(V_0 B_0)^{1/2}$, i.e. (see (7))

$$2nC/m^{1/2} = 180g^{1/2} = 5{\cdot}7. \tag{8}$$

It was observed that n and m were not the same in all thermals, rough mean values being

$$m = 3, \qquad n = 4. \tag{9}$$

The variations in m did not appear to be related to other properties of the thermals, but some systematic variation in n was detected (see below). With these values we find

$$C \doteqdot 1{\cdot}2. \tag{10}$$

Experiment no.	$(V_0 B_0)^{1/2}$ cm$^{3/2}$	k^{-1} cm^2 sec^{-1}	$(V_0 B_0)^{-1/2} k^{-1}$	n	$(V_0 B_0)^{-1/2} k^{-1} n^{-1/2}$
25	6·63	1140	170	3·8	87
110	6·53	1390	210	4·8	96
107	6·31	1090	170	3·7	89
112	5·81	1320	220	4·8	100
104	5·49	1010	200	4·1	99
102	4·97	1000	200	4·1	99
109	4·54	880	190	4·2	93
24	4·45	850	190	3·6	100
72	3·86	625	160	3·1	91
111	3·45	568	160	3·0	93
30	2·82	490	170	3·3	93
106	—	477	—	5·0	—
108	2·44	406	170	3·5	91
118	1·94	357	190	3·6	100
201	1·47	250	170	4·8	78
117	1·37	250	180	4·0	90
113	1·26	200	150	2·9	88
105	1·01	172	170	2·9	100

Table 1. Measurements of total mass (deficiency or excess), k (giving the velocity as a function of height), and rate of widening n.

6. Variations in the angle of the enveloping cone

We may attempt to take account of the variations of n in the following way. If the volume is expressed in terms of $r^2 z$, and suffix 1 is used to denote values at a given time, then

$$\overline{B} r^2 z = \overline{B}_1 r_1^2 z_1. \tag{11}$$

In the place of (2), we have

$$w = Cn^{-1/2}(g\overline{B}z)^{1/2} = Cn^{1/2}(g\overline{B}_1 r_1^2 z_1)^{1/2} z^{-1}. \tag{12}$$

Accordingly instead of having C as a constant we might have $Cn^{1/2}$ as a constant, for now $g\overline{B}_1 r_1^2 z_1$ represents the weight (deficiency or excess) of the thermal. In that case

$$\tfrac{1}{2} m^{1/2}(gB_0 V_0)^{-1/2} k^{-1} n^{-1/2} = Cn^{1/2} = \text{const.} \tag{13}$$

To test this we have plotted $(V_0 B_0)^{-1/2} k^{-1}$ against n in figure 7, and the curve drawn is part of the parabola represented by

$$n = 0{\cdot}00012(V_0 B_0)^{-1} k^{-2}. \tag{14}$$

If the points lay on this curve it would imply that $Cn^{1/2}$ was in fact constant. This appears to take some account of the variations in n, because over this series of experiments $Cn^{1/2}$ varies by only half as much as C itself (see table 1); we have no indication of the mechanism, except that if the thermal grows along a wider cone it travels more slowly at a given distance from the virtual origin, presumably because it has been more diluted. If $m = 3$, equations (13) and (14) give

$$Cn^{1/2} = 2{\cdot}5. \tag{15}$$

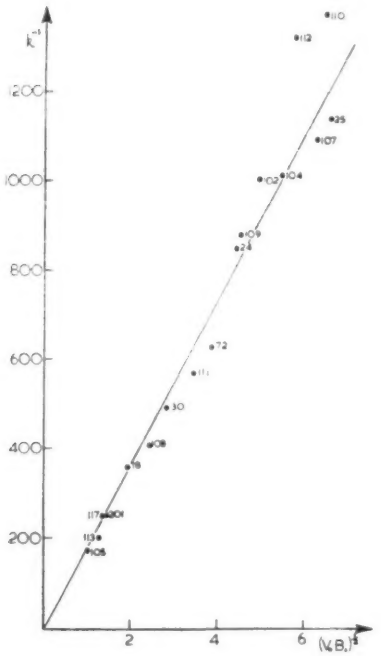

Figure 6.

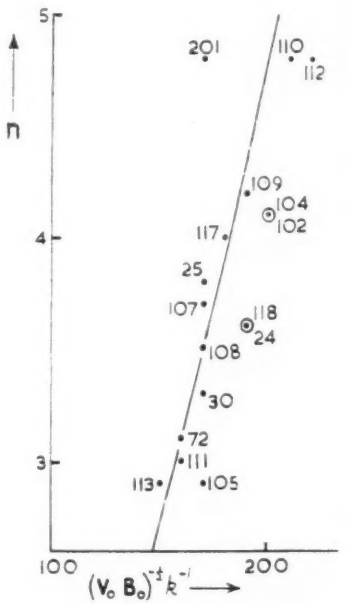

Figure 7.

Figure 6. $(V_0 B_0)^{1/2}$ plotted against k^{-1} for the thermals enumerated in table 1. The straight line represents $k^{-1} = 180\ (V_0 B_0)^{1/2}$.

Figure 7. The relationship $n = 0{\cdot}00012/V_0 B_0 k^2$, indicated by the curve drawn, is an improvement upon the crude assumption that n is the same for all experiments.

The tendency of a thermal to keep the same value of n throughout its life may be compared with the behaviour of the air bubbles of Davies and Taylor whose angular 'aperture' varied from one bubble to another.

In general, the wider thermals (smaller n) tended to leave more 'debris' behind and this may possibly account for their slower motion. The unusually slow one (113, shown in figure 5 (*d*)) developed very asymmetrically and only part of it was in effect measured, which would imply that its

total buoyancy was overestimated. The point derived from it lies below the line in figure 6.

7. Comparison with atmospheric thermals

The only published measurements of thermals in the atmosphere available for comparison are those given by Malkus & Scorer (1955). They measured the rate of rise of isolated cumulus towers, and found that early in their life on emerging from the parent cloud the relationship

$$w^2 = \tfrac{8}{9}g\overline{B}r \tag{16}$$

was fairly well obeyed. The cloud towers ceased to rise after ascending about 1·5 diameters, mainly because the buoyancy decreased to zero, or even changed sign, as the cloud droplets evaporated when the thermal was mixed with the surrounding dry air. In 1·5 diameters the whole of the interior of the thermal would have been exposed to mixing. Inside the parent cloud there is no such evaporation, so that soon after emerging the motion would have been little affected by evaporation in the exterior shell of the thermal.

In the light of the present experiments and the nature of the mixing process it is probable that their estimates of buoyancy were too high; hence the value $C = 8/9$ obtained for clouds by comparing (2) and (16) would be expected to be a little below the true value. This agrees satisfactorily with the value of 1·2 obtained from the present experiments, and is certainly within experimental error. Of course not all differences should be attributed to such errors. It should be pointed out that the cloud thermals were ascending into stably stratified surroundings and were not increasing in size as they ascended, so that the terminal velocity may have differed on this account; but the difference cannot have been very great because the thermals were decelerating. The measurement of r in the case of the clouds was made soon after emergence from the parent cloud.

Recently Ludlam & Saunders (1956) have made measurements of the vertical velocity of cumulus towers just as they began to emerge as thermals from the parent cloud. They did not attempt to measure the diameter but, having (12) in mind, expressed the size simply as distance above the ground. It cannot be much in error to assume that the virtual source is at the ground. Consequently it was possible to make an estimate of the 'constant' $Cn^{-1/2}$ in (12), and the mean value they obtained was roughly 0·5. This was based on the behaviour of the most rapidly rising thermals at any moment and not on the motion of many slower ones which could have originated at higher levels with unknown z. The closeness of agreement with the value of 0·6 obtained in our experiments is certainly fortuitous in view of the roughness of the various estimates that are necessary, but it encourages the belief that no new dynamical process is involved even though the linear scale is much greater. Their calculations are not given in the paper referred to, other aspects of the observations being discussed there, but they will be submitted for publication in due course.

An attempt was made during the summer of 1956 by Miss Betsy Woodward to make the appropriate measurements in clear air thermals below cloud base in a Skylark II glider. The humidity and temperature inside and outside of a thermal were measured using a wet and dry thermistor out-of-balance resistance thermometer, the readings being spoken into a wire recorder during flight. Spot readings had to be used to determine mean buoyancy of the thermal. The size of the thermal was estimated very roughly from the size of the turning circle which she could use during the ascent. The vertical velocity is not easily measured because it varies from one part of the thermal to another. It can be properly measured only if the glider has risen through the thermal to near the top, where, because of the decrease of vertical velocity and the outward radial component (which is equivalent to a downward velocity for a circling glider) the glider can rise only as fast as the whole thermal.

Using the observed buoyancies, etc. (Woodward 1956), a vertical velocity of 2 m/sec was deduced using a value of 1·2 for C and $r = 160$ m, $\overline{B} = \frac{1}{540}$, but since the uncertainties are so many it is neither surprising nor gratifying that the observed rate of rise of the glider when near the top of the thermal was only 1 m/sec. It is not considered profitable to attempt to explain away this discrepancy because there are too many different ways in which to do it easily. The observation is quoted because it shows that the model experiments again lead to an estimate of w of the correct order of magnitude.

8. The interior motion of a thermal

Miss Woodward has made the interior motion visible by releasing a transparent thermal containing white pellets about 5 mm in diameter balanced with pieces of fine wire attached to them so that they had a very small terminal velocity in water. The thermal was then illuminated by a flat beam of light about 3 cm thick, and the motion in the central vertical section of the thermal was photographed on 16 mm cine film.

The positions of particles within the thermal in successive pictures were drawn by steadily reducing the picture of the thermal to a constant size on a screen as the motion proceeded. The motion during the whole life of the thermal was thus concentrated into one picture, on the assumption that the motion was similar at all stages. Isopleths of horizontal and vertical component of velocity obtained in this way are shown in figure 8. Speeds are expressed as multiples of the forward velocity of the front of the thermal. This figure is based on observation of only one thermal.

It is seen that the velocity is a maximum in the centre, whereas in a vortex in which the vorticity is concentrated in a ring the velocity is a maximum at the inner surface of the ring and decreases towards the axis.

9. Comparison with buoyant vortex rings

In a recent paper Turner (1957) has discussed the behaviour of buoyant fluid ejected in the form of a ring vortex. Several years ago some glider

pilots were accustomed to think of the thermals in which they soared as possessing a configuration like a ring vortex. We now see that there is much justification for this. One important difference is that a thermal is not possessed of any circulation, kinetic energy, or forward momentum at the moment of release. The circulation is generated gradually in the early stages of its existence. As Dr Batchelor noted to me in correspondence, the circulation round a thermal when it has achieved the final configuration is proportional to wz and is therefore constant (see (2), (3) and (5)). In

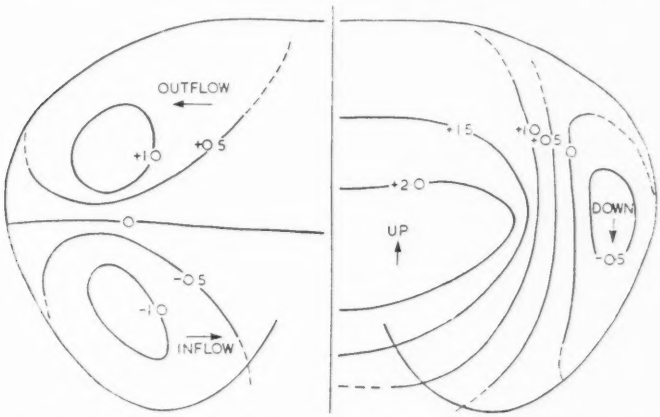

Figure 8. The distribution of velocity obtained by observing the motion of particles inside a liquid thermal. The values of the horizontal (left hand diagram) and vertical (right) velocities are expressed as multiples of the vertical velocity of the front of the thermal.

the early stages there is a hydrostatic buoyancy force acting on a column of buoyant fluid up the centre and increasing the circulation. Later on much of this column is replaced by exterior fluid, as is seen in figure 9 (plate 2). If the rate of change of circulation is zero, then

$$\oint \frac{dp'}{\rho} = 0 \tag{17}$$

for a circuit passing through the centre of the thermal and round the outside, p' being the departure of the pressure from the hydrostatic value in the exterior fluid. If the fluid is buoyant along any part of the axis of the thermal the tendency to produce circulation must be counteracted by departure from the hydrostatic pressure due to the motion. Since the motion has been produced by the buoyancy forces we should expect the configuration of buoyancy to change to a distribution which does not continue to produce circulation; this means reducing the depth of buoyant fluid up the axis of the thermal.

In Turner's vortex rings the circulation remained constant because the buoyant fluid did not extend to the centre. The initial impulse was of the

order of 1500 gm cm sec^{-1}. The buoyancy force was of the order of 300 dynes and the impulse of a ring was increased by a factor of between 2 and 10 during the period of observation. One would suspect that ultimately its motion would tend towards that of an isolated thermal as the initial impulse tended towards a small fraction of the total, but the rings did not reach this stage in his experiments.

The only constant characteristics of a thermal are its total weight (deficiency or excess), $g\bar{B}V$, and the fluid density ρ. Dimensional considerations show that its circulation K must therefore be given by

$$K = \text{const}(g\bar{B}V/\rho)^{1/2}. \tag{18}$$

It seems that if the circulation is less than this value the buoyancy forces create circulation. But if the circulation is much in excess of this value mixing towards the axis must be inhibited. The vortex ring could only become a thermal if the circulation is reduced to the value appropriate to its total buoyancy according to (18). This might happen ultimately on account of viscosity, but then the viscous forces would interfere with the motion of the thermal. In Turner's case the total buoyancy of the rings was about 0·3 gm wt., which is much less than in the present experiments, in which it ranged from 1 to 40 gm wt., so that they are not immediately comparable.

Among those who have participated in this work Miss Betsy Woodward deserves special thanks for her assistance in performing the experiments and measuring the photographs. She has also done much pioneer work in the investigation of thermals in gliders. Her work is at present supported by the Munitalp Foundation.

References

Batchelor, G. K. 1954 Heat convection and buoyancy effects in fluids, *Quart. J. Roy. Met. Soc.* **80,** 339.

Davies, R. M. & Taylor, G. I. 1950 The mechanics of large bubbles rising through extended liquids and through liquids in tubes, *Proc. Roy. Soc.* A, **200,** 375.

Ludlam, F. H. & Saunders, P. M. 1956 Shower formation in large cumulus, *Tellus* **8,** 424.

Ludlam F. H. & Scorer, R. S. 1953 Convection in the atmosphere, *Quart. J. Roy. Met. Soc.* **79,** 317.

Malkus, J. S. & Scorer, R. S. 1955 The erosion of cumulus towers, *J. Met.* **12,** 43.

Morton, B. R., Taylor, G. I. & Turner, J. S. 1956 Turbulent gravitational convection from maintained and instantaneous sources, *Proc. Roy. Soc.* A, **234,** 1.

Scorer, R. S. & Ronne, C. 1956 Experiments with convection bubbles, *Weather* **11,** 151.

Turner, J. S. 1957 Buoyant vortex rings, *Proc. Roy. Soc.* A, **239,** 61.

Welch, A., Welch, L., & Irving, F. G. 1955 *The Soaring Pilot.* London: John Murray.

Woodward, B. 1956 Exploration by sailplanes of the structure of thermals, *O.S.T.I.V. News*; Supplement to *Swiss Aero. Revue*, Sept., 1956.

Erratum

The first equation in the Summary should read as $z = nr$.

The vorticity jump across a gasdynamic discontinuity

By WALLACE D. HAYES

Department of Aeronautical Engineering, Princeton University, and the Ramo-Wooldridge Corporation

(*Received* 21 *May* 1957)

SUMMARY

An expression is obtained for the jump in the vorticity across a gasdynamic discontinuity in an inviscid flow. This result generalizes results of Truesdell (1952) and Lighthill (1957) for the vorticity behind a steady curved shock in a uniform flow and that of Emmons (1957) for the vorticity jump across a steady flame. The derivation is a dynamical one, and no assumptions on the composition or thermodynamic properties of the fluid are made. The jump in vorticity in the steady flow case is found to depend upon the jump in density and upon gradients along the discontinuity surface of the tangential velocity component and of the normal mass flow. An analogous result is found with unsteady flow.

INTRODUCTION

It is a well-known fact that the vorticity in a steady compressible flow is generally discontinuous across a shock wave. Truesdell (1952) first obtained a general expression for the vorticity behind a curved two-dimensional steady shock in a uniform flow. Truesdell states his result thus: *the magnitude of the vorticity generated by a shock of given strength and curvature depends only on the magnitude of the tangential component of velocity and is independent of the form of the equation of state.* Here the strength of a shock is defined as the density jump across the shock divided by the density in front. Other investigators, including this writer and Lighthill, unaware of Truesdell's work, later rederived the result. However, Lighthill (1957, pp. 14, 15) also provided a significant generalization in showing that the result was valid, when expressed in terms of the axes of principal curvature, for a steady shock wave of general shape in a uniform flow. Lighthill specified the density ratio across the shock to be the limiting value for a very strong shock, but this restriction is not used in his analysis and is unnecessary.

The vorticity relations just discussed depend upon a number of assumptions, of which the most restrictive is that the flow in front of the shock is uniform. The methods used all require the application of Crocco's vorticity law relating the vorticity with the entropy gradient, and the assumptions which underlie this law must be made. These assumptions are that the flow is steady, is isocompositional, and is isoenergetic (i.e. has constant total enthalpy).

A similar question arises in the theory of the propagation of a laminar flame in a combustible gas mixture, as to the magnitude of the vorticity engendered by the flame. In this case the disturbance caused by the flame is felt in the fluid region in front of the flame, and the assumption of uniform flow in this region cannot be made. Emmons (1957) has obtained an expression for the change in vorticity across a flame in terms of the density ratio across the discontinuity and the jump in tangential entropy gradient. Emmons uses a modified form of Crocco's vorticity law in his derivation, and his results are also restricted to steady and isocompositional flows. Emmons's results and the results of this paper were obtained independently and are not directly comparable.

The simplicity of Truesdell's relation and its independence of the thermodynamic state of the fluid suggests that the relation is a purely dynamical one. A purely dynamical relation must be derivable without recourse to a thermodynamic law such as Crocco's vorticity law. In presenting a dynamical derivation for the vorticity jump we shall consider first the case of steady flow, in which the principal features of the derivation are not obscured by the complexity of an arbitrarily moving discontinuity. Our method involves a vector decomposition normal to and tangential to the discontinuity surface. The discontinuities considered are gasdynamic ones, including shock waves, deflagrations, and detonations, but excluding contact discontinuities or slip streams.

The vorticity jump in steady flow

The discontinuity surface is assumed to be sufficiently smooth and continuous, without discontinuities in slope. The orientation of the surface is specified at any point by the unit normal vector $\mathbf{n}$, which is assumed to be differentiable along the surface. A natural local coordinate system is imagined, based on any intrinsic two-dimensional coordinate system on the surface. The additional coordinate n is distance along a straight normal from the discontinuity surface, with the corresponding coordinate surfaces geodesic parallels to the discontinuity surface.

The unit vector $\mathbf{n}$ is the gradient of this normal coordinate, and we obtain immediately

$$\nabla \times \mathbf{n} = 0. \tag{1}$$

The negative of the gradient of $\mathbf{n}$ is the two-dimensional curvature tensor in the discontinuity surface

$$\mathfrak{K} = -\nabla \mathbf{n}, \tag{2}$$

which from (1) must be symmetric. Because $\mathbf{n}$ is a unit vector $\nabla \mathbf{n}$ can have no component normal to the surface. The curvature is defined so as to be positive if the surface is concave on the side from which $\mathbf{n}$ is directed.

In general, all vectors will be considered in a form decomposed, with respect to the surface, into a normal component and a tangential

two-dimensional vector. Thus, with the velocity vector $\mathbf{q}$ for the flow field, we have

$$\mathbf{q} = \mathbf{n}q_n + \mathbf{q}_t, \tag{3}$$

where
$$q_n = \mathbf{n} \cdot \mathbf{q}, \qquad \mathbf{q}_t = \mathbf{n} \times (\mathbf{q} \times \mathbf{n}). \tag{4}$$

The vorticity is the curl of $\mathbf{q}$, and is expressed as

$$\begin{aligned} \boldsymbol{\zeta} &= \nabla \times (\mathbf{n}q_n) + \nabla \times \mathbf{q}_t \\ &= \mathbf{n}(\nabla \times \mathbf{q}_t)_n + (\nabla \times \mathbf{q}_t)_t - \mathbf{n} \times \nabla q_n ; \end{aligned} \tag{5}$$

we note that
$$\zeta_n = (\nabla \times \mathbf{q}_t)_n. \tag{6}$$

Vector expansion of the identity $\nabla(\mathbf{n} \cdot \mathbf{q}_t) = 0$ gives us the result

$$(\nabla \times q_t) \times \mathbf{n} = \mathbf{n} \cdot \nabla \mathbf{q}_t + \mathbf{q}_t \cdot \nabla \mathbf{n}, \tag{7}$$

and from (5) we obtain an expression for $\boldsymbol{\zeta}_t$

$$\boldsymbol{\zeta}_t = \mathbf{n} \times \left(\frac{\partial \mathbf{q}_t}{\partial n} - \mathbf{q}_t \cdot \mathfrak{K} - \nabla_t q_n \right), \tag{8}$$

in which the subscript t on the nabla operator ∇ indicates that only the tangential part of the derivative is included.

We need also an expression for the tangential part of the directional derivative of the velocity, $\mathbf{q} \cdot \nabla \mathbf{q}$. A straightforward analysis starting with (3) gives

$$(\mathbf{q} \cdot \nabla \mathbf{q})_t = q_n \left(\frac{\partial \mathbf{q}_t}{\partial n} - \mathbf{q}_t \cdot \mathfrak{K} \right) + \mathbf{q}_t \cdot \nabla_t \mathbf{q}_t. \tag{9}$$

We now turn to the steady discontinuity relations, with the symbol δ indicating the jump of a quantity across the discontinuity. The continuity condition is

$$\delta(\rho q_n) = 0, \tag{10}$$

while the tangential momentum condition is

$$\delta \mathbf{q}_t = 0. \tag{11}$$

It is at this point, in establishing (11), that we assume non-zero mass flow through the discontinuity and exclude contact discontinuities from our consideration. The normal momentum condition is

$$-\delta p = \rho q_n \delta q_n. \tag{12}$$

The energy condition across the discontinuity is not used. Since relations (10), (11) and (12) hold everywhere on the discontinuity surface we may differentiate them along the surface. Also, the operators δ and ∇_t are commutable. The increment in the vorticity is

$$\delta \zeta_n = 0, \tag{13}$$

$$\delta \boldsymbol{\zeta}_t = \mathbf{n} \times \delta \left(\frac{\partial \mathbf{q}_t}{\partial n} - \nabla_t q_n \right), \tag{14}$$

from (6) and (8). Equation (13) is a statement of the obvious fact that the normal component of the vorticity is continuous across a discontinuity.

We next write the tangential part of the momentum equation for the fluid flow. Since the flow is assumed steady, we obtain immediately with the aid of (9)

$$-\nabla_t p = \rho q_n \left(\frac{\partial \mathbf{q}_t}{\partial n} - \mathbf{q}_t \cdot \mathfrak{K} \right) + \rho \mathbf{q}_t \cdot \nabla_t \mathbf{q}_t. \tag{15}$$

Our method now is to equate the tangential gradient of (12) with the jump in (15);

$$\begin{aligned} -\delta \nabla_t p &= (\rho q_n) \delta \nabla_t q_n + \nabla_t (\rho q_n) \delta q_n \\ &= \rho q_n \, \delta \left(\frac{\partial \mathbf{q}_t}{\partial n} \right) + \mathbf{q}_t \cdot \nabla_t \, \mathbf{q}_t \delta \rho. \end{aligned} \tag{16}$$

Combining (10), (14) and (16) gives us our desired expression for $\delta \boldsymbol{\zeta}_t$;

$$\delta \boldsymbol{\zeta}_t = \mathbf{n} \times [\nabla_t (\rho q_n) \delta(\rho^{-1}) - (\rho q_n)^{-1} \mathbf{q}_t \cdot \nabla_t \mathbf{q}_t \delta(\rho)]. \tag{17}$$

In this expression the only jumps which appear are jumps in the density, and these are multiplied by quantities which are continuous across the discontinuity. Because of (13), the subscript t on $\boldsymbol{\zeta}$ in (17) is not needed.

Finally, we obtain Truesdell's expression with Lighthill's generalization, taking the flow in front of the discontinuity to be uniform with density ρ_0 and velocity $\mathbf{U}$. We evaluate the quantities appearing in (17),

$$\rho q_n = \rho_0 U_n, \tag{18a}$$

$$\nabla_t (\rho q_n) = \rho_0 \mathbf{U} \cdot \nabla \mathbf{n} = -\rho_0 \mathbf{U}_t \cdot \mathfrak{K}, \tag{18b}$$

$$\mathbf{q}_t \cdot \nabla_t \mathbf{q}_t = \mathbf{n} \times (\mathbf{U} \times \mathbf{U}_t \cdot \nabla \mathbf{n}) = U_n \, \mathbf{U}_t \cdot \mathfrak{K}, \tag{18c}$$

and obtain

$$\delta \boldsymbol{\zeta}_t = \mathbf{n} \times \mathbf{U}_t \cdot \mathfrak{K} (\rho_1^{-1} - \rho_0^{-1}) \delta \rho, \tag{19}$$

or, since the flow in front of the discontinuity is irrotational,

$$\boldsymbol{\zeta}_1 = -\frac{(1-\epsilon)^2}{\epsilon} \mathbf{n} \times \mathbf{U}_t \cdot \mathfrak{K}. \tag{20}$$

Here ρ_1 is the density behind the discontinuity, and

$$\epsilon = \rho_0 / \rho_1 \tag{21}$$

is the density ratio across the discontinuity. It should be noted that this result is not limited to shock waves, but would hold also for a condensation shock or detonation.

The vorticity jump in unsteady flow

In dealing with the unsteady flow case we must take into account not only the unsteady nature of the flow field but also an arbitrary motion of the discontinuity surface. Many of the relations obtained for the steady flow case are still valid, principally the kinematic relations (6), (8) and (9), and the jump relations for the tangential velocity and the vorticity (11), (13) and (14). The primary modification which must be made is to the relations (10) and (12) involving the normal mass flow across the discontinuity.

Of the available ways in which the shock motion may be specified, the most convenient is in terms of its normal velocity $\mathbf{n} q_s$. We use the notation d/dt to denote the time derivative taken at a point which always lies on the

discontinuity and which moves in a direction normal to the discontinuity when the discontinuity moves. If $\boldsymbol{\omega}_s$ is the angular velocity of the surface measured at such a point and is defined as a tangential vector, we may show that

$$\frac{d\mathbf{n}}{dt} = \boldsymbol{\omega}_s \times \mathbf{n} = -\nabla_t q_s. \tag{22}$$

We designate the relative normal velocity component q_r as

$$q_r = q_n - q_s, \tag{23}$$

and obtain the discontinuity relations

$$\delta(\rho q_r) = 0 \tag{24}$$

in place of (10), and

$$-\delta p = (\rho q_r)\delta q_r = (\rho q_r)\delta q_n \tag{25}$$

in place of (12). We use the symbol D to designate the classical total or material derivative with respect to time; and we introduce the symbol D_t to designate a tangential total time derivative, the time derivative with respect to an observer who moves along the shock with a total velocity $\mathbf{n}q_s + \mathbf{q}_t$. If such a derivative is a vector, we shall include only its tangential part. Note that for such an observer the discontinuity is a normal one. The distinction between the derivatives D and D_t is immaterial when they are applied to the vector $\mathbf{n}$, because the space derivative of $\mathbf{n}$ in the normal direction is zero. Thus we have

$$D\mathbf{n} = D_t\,\mathbf{n} = \frac{d\mathbf{n}}{dt} + \mathbf{q}_t \cdot \nabla\mathbf{n}. \tag{26}$$

For the tangential velocity $\mathbf{q}_t$ we have

$$\frac{d\mathbf{q}_t}{dt} = \frac{\partial \mathbf{q}_t}{\partial t} + q_s \frac{\partial \mathbf{q}_t}{\partial n}, \tag{27}$$

and

$$D_t\,\mathbf{q}_t = (D\mathbf{q}_t)_t - q_r \frac{\partial \mathbf{q}_t}{\partial n} = \left(\frac{d\mathbf{q}_t}{dt}\right)_t + \mathbf{q}_t \cdot \nabla_t \mathbf{q}_t. \tag{28}$$

In place of (15) we may now write

$$\begin{aligned} -\nabla_t p &= \rho(D\mathbf{n}q_n)_t + \rho(D\mathbf{q}_t)_t \\ &= \rho(q_r + q_s)D_t\,\mathbf{n} + \rho q_r \frac{\partial \mathbf{q}_t}{\partial n} + \rho D_t\,\mathbf{q}_t. \end{aligned} \tag{29}$$

Applying the same procedure as was used in the case of steady flow, we obtain the desired expression for the vorticity jump as

$$\delta\boldsymbol{\zeta}_t = \mathbf{n} \times [\nabla_t(\rho q_r)\delta(\rho^{-1}) - (\rho q_r)^{-1}(D_t\,\mathbf{q}_t + q_s D_t\,\mathbf{n})\delta(\rho)] \tag{30}$$

in place of (17). The quantity $D_t\mathbf{n}$ is given in (26), or, with (2) and (22), may be re-expressed as

$$D_t\mathbf{n} = -\nabla_t q_s - \mathbf{q}_t \cdot \mathfrak{K}. \tag{31}$$

The quantity $D_t\mathbf{q}_t$ is given by (28) with (27). It may be checked that (30) is invariant under a velocity transformation to another unaccelerated frame of reference. Again, the subscript t on $\boldsymbol{\zeta}$ in (30) is not needed.

As an example of our result (30) for unsteady flow we apply it to the case in which the flow in front of the discontinuity is at a uniform density ρ_0 and uniform velocity $\mathbf{U}$. We evaluate the quantities appearing in (30) to obtain, in analogy with (18),

$$\rho q_r = \rho_0(U_n - q_s), \tag{32a}$$

$$\nabla_t(\rho q_r) = \rho_0 D_t \mathbf{n}, \tag{32b}$$

$$D_t \mathbf{q}_t = \mathbf{n} \times (\mathbf{U} \times D_t \mathbf{n}) = -U_n D_t \mathbf{n}. \tag{32c}$$

The vorticity jump is then obtained from (30),

$$\delta \boldsymbol{\zeta}_s = \mathbf{n} \times (\mathbf{U}_t \cdot \mathbf{k} + \nabla_t q_s)(\rho_1^{-1} - \rho_0^{-1})\delta\rho, \tag{33}$$

in place of (19), or

$$\boldsymbol{\zeta}_1 = -\frac{(1-\epsilon)^2}{\epsilon} \mathbf{n} \times (\mathbf{U}_t \cdot \mathbf{k} + \nabla_t q_s) \tag{34}$$

in place of (20), with ϵ given as before by (21). This result is the generalization to unsteady flow of the Truesdell–Lighthill vorticity expression. It may be noted that the fundamental quantity appearing in (20) or (34) is the angular velocity of the discontinuity surface with respect to the observer for whom a derivative is D_t. We may rewrite (20) or (34) in the form

$$\boldsymbol{\zeta}_1 = \frac{(1-\epsilon)^2}{\epsilon} \boldsymbol{\omega}, \tag{35}$$

where the angular velocity $\boldsymbol{\omega}$ is

$$\boldsymbol{\omega} = \mathbf{n} \times D_t \mathbf{n} \tag{36a}$$

$$= \boldsymbol{\omega}_s + \mathbf{U}_t \cdot \mathbf{k} \times \mathbf{n}, \tag{36b}$$

with $\boldsymbol{\omega}_s$ defined in (22).

References

Emmons, H. W. 1957 Article in *Fundamentals of Gas Dynamics* (Ed. H. W. Emmons), Vol. III of *High Speed Aerodynamics and Jet Propulsion*. Princeton University Press.

Lighthill, M. J. 1957 *J. Fluid Mech.* **2**, 1–32.

Truesdell, C. 1952 *J. Aero. Sci.* **19**, 826–828.

The collision of two ionized streams

By F. D. KAHN

Department of Astronomy, Physical Laboratories, University of Manchester

(*Received* 15 *April* 1957)

SUMMARY

It is shown that the interpenetration of two ionized streams is arrested, as a rule, not because of individual collisions between particles belonging to opposite streams, but because the whole system of charged particles is unstable. The smallest wavelength of an unstable oscillation is $\lambda_{\min}$, where

$$\lambda_{\min} = \sqrt{\left(\frac{\pi m_0 U^2}{2N\epsilon^2}\right)\left(1 - \frac{U^2}{c^2}\right)^{-3/4}}.$$

Here $\pm U$ are the velocities of the undisturbed streams, and N is the density of electrons in each.

A further calculation for the non-relativistic case deals with the amplification of the plasma oscillations present in two colliding streams. It is shown that these grow rapidly and that $\tau_{\text{crit}}\sqrt{(m_0 U^2/\pi N\epsilon^2)}$ is the distance of interpenetration achieved before the counterstreaming of the electrons is brought to a halt. The value of τ_{crit} depends only insensitively on the ratio of the internal plasma energy densities T_{pl} to the kinetic energy densities T_{kin} in the streams. For example, $\tau_{\text{crit}} = 9{\cdot}0$ when $T_{\text{pl}} : T_{\text{kin}} = 1 : 10$, and $\tau_{\text{crit}} = 19{\cdot}0$ when $T_{\text{pl}} : T_{\text{kin}} = 1 : 10^5$.

1. INTRODUCTION

The interpenetration of two fully ionized streams of gas is considered in this paper. It is shown that, as a rule, the counterstreaming is stopped because of a collective instability among the electrons present, and that close encounters between charged particles belonging to the two streams are relatively unimportant in destroying the systematic motion.

Advance information of some of the results in this paper was given by the author in an earlier paper (Kahn 1955) where it was suggested that this instability effect leads to the conversion of the kinetic energy of the two streams into the energy of irregular plasma oscillations. A particular example of this might be found in the collision of two galaxies—as in the radio source Cygnus A. One would therefore expect random electric fields to be present in the plasma left after a collision. A fast charged particle passing through such a medium would then be expected to radiate electromagnetic waves.

The instability effect may also be important in the laboratory. It may, for instance, explain the smallness of the distance to which two counterstreaming masses of plasma can interpenetrate. That the distance is small is shown, for instance, by Bostick's (1956) experiments.

In the following two sections we derive the condition that an oscillation of a particular wavelength may be amplified. The treatment given is non-relativistic in § 2, and relativistic in § 3. In § 4 we consider the amplification of the oscillations which are present in the two streams before they have collided, and find a closer estimate of the time that elapses before the counterstreaming is stopped.

Some calculations concerning this effect have been given by Lampert (1956), who uses the dispersion relations for a plasma.

2. A NON-RELATIVISTIC TREATMENT

Consider two interpenetrating streams, each of infinite extent, and each consisting of N protons and N electrons per cm^3. Let stream 1 have a velocity U in the direction of increasing x, and stream 2 a velocity U in the direction of decreasing x. Let ϵ be the charge on the electron and m_0 its rest mass. Let the temperature T in each stream be such that $kT \ll m_0 U^2$. The thermal motion among the particles may then be neglected.

An electron passing within a distance r of a charged particle from the other stream experiences a change ϵ^2/r in potential energy. Its kinetic energy relative to this particle is $\frac{1}{2}m_0(2U)^2 = 2m_0 U^2$. An appreciable deflection in the direction of the electron's motion occurs if

$$\epsilon^2/r = O(2m_0 U^2),$$

that is,

$$r = O(\epsilon^2/2m_0 U^2). \tag{1}$$

The effective cross-sectional area for such a close collision is thus of the order of $S = \pi\epsilon^4/4m_0^2 U^4$. These encounters would eventually destroy the systematic motion. The distance of interpenetration will at most be of the order of

$$\frac{1}{2N^2S} = \frac{2m_0^2 U^4}{\pi N\epsilon^4}. \tag{2}$$

But there is a collective instability among the electrons which will stop the counterstreaming very much sooner. Assume, for the moment, that the protons, because of their much greater mass, continue their uniform motion, and provide a uniform background of positive charge. Let the densities in the electron streams be $N(1+s_1)$ and $N(1+s_2)$, respectively, and let the velocities be $U+u_1$ and $-U+u_2$; s_1, s_2, u_1 and u_2 are here regarded as functions of position and time. We shall confine ourselves to one-dimensional disturbances, so that the position enters through the x-coordinate only. The resulting electrostatic field will be parallel to Ox; let E be its magnitude.

Poisson's equation then gives

$$\frac{\partial E}{\partial x} = 4\pi N\epsilon(s_1+s_2), \tag{3}$$

and the linearized equations of motion for the two electron streams are

$$\frac{\partial u_1}{\partial t} + U\frac{\partial u_1}{\partial x} = \frac{\epsilon}{m}E, \tag{4}$$

$$\frac{\partial u_2}{\partial t} - U\frac{\partial u_2}{\partial x} = \frac{\epsilon}{m}E. \tag{5}$$

The equations of continuity for the two electron streams are

$$\left[\frac{\partial}{\partial t} + (U+u_1)\frac{\partial}{\partial x}\right]N(1+s_1) + N(1+s_1)\frac{\partial u_1}{\partial x} = 0,$$

$$\left[\frac{\partial}{\partial t} - (U-u_2)\frac{\partial}{\partial x}\right]N(1+s_2) + N(1+s_2)\frac{\partial u_2}{\partial x} = 0,$$

or, in linearized form,

$$\frac{\partial s_1}{\partial t} + U\frac{\partial s_1}{\partial x} + \frac{\partial u_1}{\partial x} = 0, \tag{6}$$

$$\frac{\partial s_2}{\partial t} - U\frac{\partial s_2}{\partial x} + \frac{\partial u_2}{\partial x} = 0. \tag{7}$$

The combination of (3) and (4) leads to

$$\left(\frac{\partial}{\partial t} + U\frac{\partial}{\partial x}\right)\frac{\partial u_1}{\partial x} = \Omega^2(s_1+s_2), \tag{8}$$

where $\Omega^2 = 4\pi N\epsilon^2/m_0$. With the aid of (6),

$$\left(\frac{\partial}{\partial t} + U\frac{\partial}{\partial x}\right)^2 s_1 = -\Omega^2(s_1+s_2). \tag{9}$$

Similarly,

$$\left(\frac{\partial}{\partial t} - U\frac{\partial}{\partial x}\right)^2 s_2 = -\Omega^2(s_1+s_2). \tag{10}$$

Now look for solutions of (9) and (10) in the form

$$s_1 = a_1 e^{i(kx-\omega t)}, \qquad s_2 = a_2 e^{i(kx-\omega t)}. \tag{11}$$

If a solution can be found, with a given real k, for which $\omega = \mu + i\sigma$, where μ and σ are real, and $\sigma > 0$, then the counterstreaming is unstable, for the amplitude of the corresponding oscillation can grow indefinitely. The maximum value $k_{\max}$ for which this is possible gives the minimum value $\lambda_{\min}$ of the wavelengths at which there is instability, through the relation $\lambda_{\min} = 2\pi/k_{\max}$. If such counterstreaming were ever to occur it would be stopped within a distance of the order of $\lambda_{\min}$.

The evaluation of $k_{\max}$ is straightforward. Substitution from (11) into (9) leads to

$$(\omega+kU)^2 a_1 = \Omega^2(a_1+a_2),$$

or

$$[(\omega+kU)^2 - \Omega^2]a_1 - \Omega^2 a_2 = 0. \tag{12}$$

Similarly, from (10),

$$-\Omega^2 a_1 + [(\omega-kU)^2 - \Omega^2]a_2 = 0. \tag{13}$$

Elimination of a_1 and a_2 from (12) and (13) gives

$$[(\omega+kU)^2 - \Omega^2][(\omega-kU)^2 - \Omega^2] - \Omega^4 = 0,$$

or

$$\omega^4 - 2\omega^2(k^2U^2+\Omega^2) + k^2U^2(k^2U^2-2\Omega^2) = 0. \tag{14}$$

Since $$(k^2U^2+\Omega^2)^2 \geqslant k^2U^2(k^2U^2-2\Omega^2)$$
for all real values of k, U and Ω, it follows that (14) always has real roots for ω^2. However, if $k^2U^2-2\Omega^2$ is negative, one possible value of ω^2 is negative, say $-\sigma^2$, and this leads to

$$\omega = \pm i\sigma,$$

with instability as a consequence.

The critical wave-number is given by $k^2U^2-2\Omega^2=0$, so that

$$k_{\max} = \sqrt{2}\Omega/U.$$

The corresponding critical wavelength is

$$\lambda_{\min} = 2\pi/k_{\max} = \sqrt{2}\pi U/\Omega.$$

Any disturbance with a wavelength exceeding $\lambda_{\min}$ will be amplified. The counterstreaming thus becomes unstable within a distance of the order of $\lambda_{\min}$. In terms of N, ϵ, m_0 and U,

$$\lambda_{\min} = \sqrt{\left(\frac{\pi m_0 U^2}{2N\epsilon^2}\right)}. \tag{15}$$

This is much shorter than the limit set to the counterstreaming by close collisions if

$$\frac{2m_0^2 U^4}{\pi N\epsilon^4} \ll \sqrt{\left(\frac{\pi m_0 U^2}{2N\epsilon^2}\right)},$$

that is, if

$$N \ll \frac{8m_0^3 U^6}{\pi^3\epsilon^6}. \tag{16}$$

To give a numerical value, when $U = 10^8$ cm/s the condition states that N need only be much smaller than 2×10^{22} particles per cm^3. This critical density is very large. The instability effect is therefore usually the one that arrests the counterstreaming of the electrons.

It is harder to say exactly what happens to the protons. They have a larger value of $\lambda_{\min}$, but in their case the greater effectiveness of the instability, as opposed to that of close collisions, is even more marked (as is shown by substitution of a larger value for m_0 in (15)). However the presence of the oscillating electron gas cannot be left out of account in any calculation, and the theory is rather harder. It seems nonetheless clear that the protons also contribute their kinetic energy to the collective oscillation, rather than to thermal motion.

3. The extension to the relativistic case

Let $U+u_1$ be the velocity of an electron in the first stream. Its momentum is

$$p_1 = \frac{m_0(U+u_1)}{\{1-(U+u_1)^2/c^2\}^{1/2}} = \frac{m_0 U}{(1-U^2/c^2)^{1/2}} + \frac{m_0 u_1}{(1-U^2/c^2)^{1/2}}\left(1+\frac{U^2/c^2}{1-U^2/c^2}\right)+\ldots$$

$$= \frac{m_0 U}{(1-U^2/c^2)^{1/2}} + \frac{m_0 u_1}{(1-U^2/c^2)^{3/2}}+\ldots$$

to the first order. The linearized equation of motion is

$$\left(\frac{\partial}{\partial t}+U\frac{\partial}{\partial x}\right)p_1=\epsilon E,$$

or

$$\left(\frac{\partial}{\partial t}+U\frac{\partial}{\partial x}\right)u_1=\epsilon E/M,$$

where $M=m_0(1-U^2/c^2)^{-3/2}$. There is a similar change in the equation for the second stream. Thus, the only alteration is that the rest mass m_0 is replaced by a virtual mass $M=m_0(1-U^2/c^2)^{-3/2}$.

The linearized equations of continuity do not change.

Finally there is no change in the equation relating s_1 and s_2 to E, unless $\omega/k=c$. To see this we note that the vector potential is parallel to Ox. Let A be its magnitude. Then

$$\frac{\partial^2 A}{\partial x^2}-\frac{1}{c^2}\frac{\partial^2 A}{\partial t^2}=-\frac{1}{c}\{4\pi N\epsilon(1+s_1)(U+u_1)+4\pi N\epsilon(1+s_2)(-U+u_2)\}. \quad (17)$$

For the scalar potential ϕ,

$$\frac{\partial^2\phi}{\partial x^2}-\frac{1}{c^2}\frac{\partial^2\phi}{\partial t^2}=-4\pi N\epsilon(s_1+s_2). \quad (18)$$

We operate on (17) with $-\partial/c\,\partial t$ and on (18) with $-\partial/\partial x$. Then since,

$$E=-\frac{1}{c}\frac{\partial A}{\partial t}-\frac{\partial\phi}{\partial x}$$

we find, on adding and linearizing, that

$$\frac{\partial^2 E}{\partial x^2}-\frac{1}{c^2}\frac{\partial^2 E}{\partial t^2}=4\pi N\epsilon\left[\frac{1}{c^2}\frac{\partial}{\partial t}(u_1+Us_1)+\frac{\partial s_1}{\partial x}+\frac{1}{c^2}\frac{\partial}{\partial t}(u_2-Us_2)+\frac{\partial s_2}{\partial x}\right]. \quad (19)$$

But, according to the linearized equations of continuity (6) and (7),

$$\frac{\partial}{\partial x}(u_1+Us_1)=-\frac{\partial s_1}{\partial t},\qquad \frac{\partial}{\partial x}(u_2-Us_2)=-\frac{\partial s_2}{\partial t},$$

and it follows that

$$\left(\frac{\partial^2}{\partial x^2}-\frac{1}{c^2}\frac{\partial^2}{\partial t^2}\right)E=4\pi N\epsilon\left(\frac{\partial^2}{\partial x^2}-\frac{1}{c^2}\frac{\partial^2}{\partial t^2}\right)\int^x(s_1+s_2)\,dx. \quad (20)$$

Equation (20) is equivalent to equation (3), unless the wave motion is such that

$$\left(\frac{\partial^2}{\partial x^2}-\frac{1}{c^2}\frac{\partial^2}{\partial t^2}\right)E=0$$

and

$$\left(\frac{\partial^2}{\partial x^2}-\frac{1}{c^2}\frac{\partial^2}{\partial t^2}\right)(s_1+s_2)=0,$$

that is, unless the disturbance propagates with the speed of light.

Since the only change made in the relativistic treatment is to replace m_0 by $m_0(1-U^2/c^2)^{-3/2}$ we find that the critical wavelength now becomes

$$\lambda_{\min}=\sqrt{\left(\frac{\pi m_0 U^2}{2N\epsilon^2}\right)}\left(1-\frac{U^2}{c^2}\right)^{-3/4}. \quad (21)$$

4. The amplification of oscillations

We now return to the non-relativistic case. Suppose that two uniform, ionized, semi-infinite streams collide with one another. Once again let there be N protons and N electrons per unit volume, and let $+U$ and $-U$ be the undisturbed velocities in the two streams. Let the first impact occur at $x = 0$ at time $t = 0$.

We assume further that the temperature in each stream is initially zero, but that there are present in it random electrostatic oscillations, whose energy per unit mass is small compared with $\frac{1}{2}U^2$. We shall try to find out how long it is likely to be before these oscillations are amplified sufficiently to make the linear approximation break down. When this happens the electrostatic energy will be comparable with the energy of counterstreaming, and the latter may then be expected to be brought to a halt. The calculation should give a closer estimate of the possible distance of interpenetration of the electrons in the two streams.

The neglect of the initial temperature T_0 is justified provided $U^2 \gg kT_0/m_0$. For, as Bohm and Gross have shown (see, for instance, Spitzer (1956)), the thermal motions do not appreciably affect plasma oscillations whose wavelengths are much in excess of $\sqrt{(kT_0/N\epsilon^2)}$, whereas the oscillations that are amplified most readily in the present case are those with wavelengths of the order of $\sqrt{(m_0 U^2/N\epsilon^2)}$.

The introduction of dimensionless variables will simplify the further working. We set

$$\tau = \Omega t, \qquad X = \Omega x/U, \qquad \mathscr{E} = \epsilon E/m_0 \Omega U, \qquad v_1 = u_1/U, \qquad v_2 = u_2/U.$$

(The meanings of E, Ω, ϵ, m_0, u_1 and u_2 are the same as in § 2.) The equations of § 2 become

$$\left.\begin{aligned} \left(\frac{\partial}{\partial\tau} + \frac{\partial}{\partial X}\right)v_1 &= \mathscr{E}, & \left(\frac{\partial}{\partial\tau} - \frac{\partial}{\partial X}\right)v_2 &= \mathscr{E}, \\ \left(\frac{\partial}{\partial\tau} + \frac{\partial}{\partial X}\right)s_1 + \frac{\partial v_1}{\partial X} &= 0, & \left(\frac{\partial}{\partial\tau} - \frac{\partial}{\partial X}\right)s_2 + \frac{\partial v_2}{\partial X} &= 0, \\ \frac{\partial\mathscr{E}}{\partial X} &= s_1 + s_2, \end{aligned}\right\} \tag{22}$$

where s_1 and s_2 also have the same meaning as in § 2. The equations (22) combine to give

$$\left.\begin{aligned} \left(\frac{\partial}{\partial\tau} + \frac{\partial}{\partial X}\right)^2 s_1 + s_1 &= -s_2, \\ \left(\frac{\partial}{\partial\tau} - \frac{\partial}{\partial X}\right)^2 s_2 + s_2 &= -s_1, \end{aligned}\right\} \tag{23}$$

or

$$\left(\frac{\partial}{\partial\tau} + \frac{\partial}{\partial X}\right)^2\left(\frac{\partial}{\partial\tau} - \frac{\partial}{\partial X}\right)^2 s_{1,2} + \left(\frac{\partial}{\partial\tau} + \frac{\partial}{\partial X}\right)^2 s_{1,2} + \left(\frac{\partial}{\partial\tau} - \frac{\partial}{\partial X}\right)^2 s_{1,2} = 0 \tag{24}$$

(the symbol $s_{1,2}$ stands for either s_1 or s_2).

A set of coordinates alternative to X and τ is given by

$$\xi = \tau - X, \qquad \eta = \tau + X,$$

and leads to

$$\frac{\partial}{\partial \tau} - \frac{\partial}{\partial X} = 2\frac{\partial}{\partial \xi}, \qquad \frac{\partial}{\partial \tau} + \frac{\partial}{\partial X} = 2\frac{\partial}{\partial \eta}.$$

Equations (23) then become

$$4\frac{\partial^2 s_1}{\partial \eta^2} + s_1 = -s_2, \tag{25}$$

$$4\frac{\partial^2 s_2}{\partial \xi^2} + s_2 = -s_1, \tag{26}$$

and (24) becomes

$$4\frac{\partial^4 s_{1,2}}{\partial \xi^2 \partial \eta^2} + \frac{\partial^2 s_{1,2}}{\partial \xi^2} + \frac{\partial^2 s_{1,2}}{\partial \eta^2} = 0. \tag{27}$$

Now the first stream is moving in the direction of increasing X; at time τ its front surface is at $X = \tau$, while the front surface of the second stream is at $X = -\tau$. Counterstreaming therefore occurs only in the part of the half-plane $\tau > 0$ which lies between the lines $X = \tau$ and $X = -\tau$, or, alternatively, between $\xi = 0$ and $\eta = 0$ (region A in figure 1).

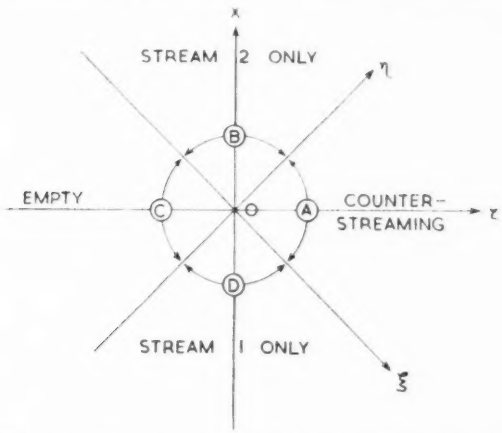

Figure 1. The nature of the motion in various regions.

Regions B and D in figure 1 are occupied only by streams 2 and 1, respectively. Region C is empty. Our equations therefore apply only in region A; to find the appropriate solutions adequate boundary conditions must be known on the positive parts of $O\xi$ and $O\eta$. These boundary conditions are determined by the oscillations present in the single streams occupying regions B and D.

In figure 2 the diagram is re-drawn with the ξ-axis horizontal and the η-axis vertical. Suppose we seek the solution of the equations within a

region to the right of and above a curve PQ whose gradient never takes a finite positive value. The solution of equation (25) may be written

$$s_1(\xi,\eta) = s_1(\xi,\eta_0)\cos\tfrac{1}{2}\eta + 2\frac{\partial s_1}{\partial\eta}(\xi,\eta_0)\sin\tfrac{1}{2}\eta - 2\int_{\eta_0}^{\eta} s_2(\xi,u)\sin\tfrac{1}{2}(\eta-u)\,du, \quad (28)$$

and this shows that the value of s_1 at a typical point R is determined solely by the values of s_1 and $\partial s_1/\partial\eta$ at the point S_0, directly below R on PQ, and by the value of s_2 at all points of RS_0.

Repetition of the argument shows that the value of s_2 at R', say, depends only on the values of s_2 and $\partial s_2/\partial\xi$ at T_0', which lies on PQ to the left of R', and on all the values taken by s_1 on $T_0'R'$. Continuing in this way we find that the values of s_1 and s_2 at R are determined completely by the values of s_1 and $\partial s_1/\partial\eta$, s_2 and $\partial s_2/\partial\xi$ on the stretch T_0S_0 of PQ, where T_0 lies to the left of R and on PQ. In fact these values define the function within the area RS_0T_0. It follows that the solution within the region $0 \leqslant \xi \leqslant \xi_0$, $0 \leqslant \eta \leqslant \eta_0$ is fully determined when s_1 and $\partial s_1/\partial\eta$ are known on the stretch of the ξ-axis from 0 to ξ_0, and when s_2 and $\partial s_2/\partial\xi$ are known on the η-axis, from 0 to η_0.

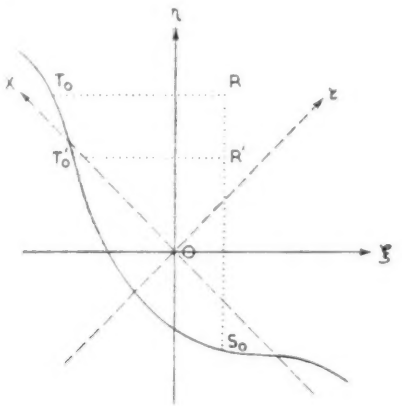

Figure 2. The domain of dependence for a point R.

But the η-axis has the equation $X = \tau$ in the other set of coordinates. Its positive part therefore represents the front surface of stream 1 from time $\tau = 0$ onwards. The required boundary conditions are therefore equivalent to a knowledge of s_2 and $\partial s_2/\partial\xi$ at this front surface, and of s_1 and $\partial s_1/\partial\eta$ at the other front surface, that is, to a knowledge of the conditions at various times in the part of stream 2 which is just about to collide with stream 1, and vice versa.

The equations are linear and so a general solution may be built up by the addition of various basic solutions corresponding to simple boundary conditions. Finally the solution for the first quadrant of the (ξ,η)-plane due to two semi-infinite streams will be the same as that due to two infinite

streams of the same density provided only the same boundary values on the positive halves of the ξ- and η-axes apply in the two cases.

We shall now find the solution that corresponds to the following simple boundary conditions:

$$s_1 = \delta(\xi - \xi_0), \qquad \partial s_1/\partial\eta = 0,$$

on the positive half of the ξ-axis;

$$s_2 = 0, \qquad \partial s_2/\partial\xi = 0$$

on the positive half of the η-axis. Here $\delta(\xi)$ stands for the Dirac delta function.

Let P be the point $(\xi_0, 0)$. The solutions we shall find will be valid only to the right of and above P (see figure 3). In this region, the solution with the above boundary conditions is the same as that given by the boundary conditions $s_1 = \delta(\xi - \xi_0)$, $\partial s_1/\partial\eta = 0$, $s_2 = 0$, $\partial s_2/\partial\xi = 0$, *on the line* AB through P, provided the slope of this line is negative, say -1. This alternative set of conditions leads to the same values on $P\xi$ and $P\eta'$, since the values of s_2 and $\partial s_2/\partial\xi$ are zero at all points to the right of AP and to the left of $P\eta'$, and therefore by continuity on $P\eta'$. Similarly the values of s_1 and $\partial s_1/\partial\eta$ are zero at all points above PB and below $P\xi$, with the exception of the point P.

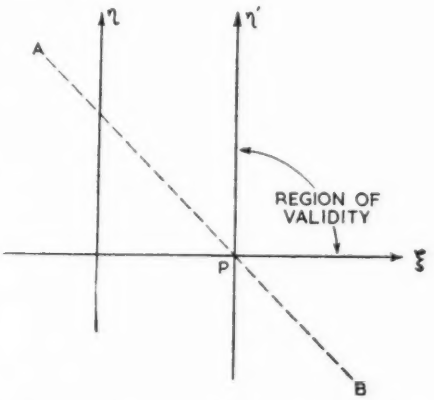

Figure 3. Region of validity of the basic solution.

The nature of the solution corresponding to these boundary conditions is not affected by the exact value of ξ_0; the solutions for the points ξ_0 and ξ_0' are identical except for a relative displacement $\xi_0 - \xi_0'$ parallel to $O\xi$. We therefore choose $\xi_0 = 0$ for the sake of simplicity. The line AB then has the equation $\xi + \eta = 0$, or $\tau = 0$ in (X, τ) coordinates.

The equivalent boundary conditions are now

$$\left.\begin{aligned} s_1 &= \delta(\tau - X), & \frac{\partial s_1}{\partial\eta} &= \frac{1}{2}\left(\frac{\partial s_1}{\partial\tau} + \frac{\partial s_1}{\partial X}\right) = 0, \\ s_2 &= 0, & \frac{\partial s_2}{\partial\xi} &= \frac{1}{2}\left(\frac{\partial s_2}{\partial\tau} - \frac{\partial s_2}{\partial X}\right) = 0, \end{aligned}\right\} \text{ on } \tau = 0, \qquad (29)$$

or

$$\left.\begin{aligned} s_1 &= \delta(X), & \frac{\partial s_1}{\partial \tau} &= -\frac{\partial s_1}{\partial X} \\ s_2 &= 0, & \frac{\partial s_2}{\partial \tau} &= 0, \end{aligned}\right\} \text{ on } \tau = 0. \tag{29}$$

With the aid of the first of the equations (23) the third and fourth conditions (29) may be written

$$\left.\begin{aligned} \left(\frac{\partial}{\partial \tau} + \frac{\partial}{\partial X}\right)^2 s_1 &= -s_1 = -\delta(X), \\ \frac{\partial}{\partial \tau}\left(\frac{\partial}{\partial \tau} + \frac{\partial}{\partial X}\right)^2 s_1 &= -\frac{\partial s_1}{\partial \tau} = \frac{\partial s_1}{\partial X}, \end{aligned}\right\} \text{ on } \tau = 0. \tag{29a}$$

A possible solution of the differential equation (27) for s_1 is

$$s_1 = e^{i[KX + \mu(K)\tau]}$$

provided $\mu(K)$ satisfies

$$(\mu^2 - K^2)^2 - 2(\mu^2 + K^2) = 0,$$

that is,

$$\mu^4 - 2\mu^2(K^2 + 1) + (K^4 - 2K^2) = 0. \tag{30}$$

(This equation is the dimensionless equivalent of (14).) Corresponding to any given positive value of K there are four values of μ, of which two may be imaginary. The most general solution of (27) is, in the complex notation,

$$s_1 = \sum_{r=1}^{4} \int_{K=0}^{\infty} \alpha_r(K) e^{i[KX + \mu_r(K)\tau]}\, dK. \tag{31}$$

The four α_r coefficients for each K have now to be determined from the boundary conditions for $\tau = 0$. In the complex notation,

$$\delta(X) = \frac{1}{\pi}\int_0^\infty e^{iKX}\, dK = s_1(X, 0)$$

so that

$$\frac{\partial}{\partial X} s_1(X, 0) = \frac{1}{\pi}\int_0^\infty K e^{iKX}\, dK.$$

Hence, from (29) and (31),

$$\sum_{r=1}^{4} \int_0^\infty \alpha_r(K) e^{iKX}\, dK = \frac{1}{\pi}\int_0^\infty e^{iKX}\, dK.$$

Comparison of coefficients then shows that

$$\sum_{r=1}^{4} \alpha_r(K) = \frac{1}{\pi}.$$

Setting

$$\beta_r = \pi \alpha_r, \tag{32}$$

we have

$$\sum_{r=1}^{4} \beta_r = 1. \tag{33}$$

The other conditions give that

$$\sum_{r=1}^{4} \beta_r \mu_r = -K, \tag{34}$$

$$\sum_{r=1}^{4} \beta_r[K+\mu_r]^2 = 1, \tag{35}$$

$$\sum_{r=1}^{4} \mu_r \beta_r[K+\mu_r]^2 = -K. \tag{36}$$

Now the operation $(35)-2K\times(34)-K^2\times(33)$ gives

$$\sum_{r=1}^{4} \beta_r \mu_r^2 = K^2+1, \tag{35 a}$$

and the operation $(36)-2K\times(35\,\text{a})-K^2\times(34)$ gives

$$\sum_{r=1}^{4} \beta_r \mu_r^3 = -K^3-3K. \tag{36 a}$$

But the roots of (30) occur in pairs, such that

$$\mu_1 = -\mu_2, \qquad \mu_3 = -\mu_4, \qquad \mu_1^2+\mu_3^2 = 2(K^2+1).$$

After some manipulation the solution for β_1 is found to be

$$\beta_1 = \frac{1}{4} - \frac{K}{4\mu_1}\left\{\frac{\mu_1^2-K^2+1}{\mu_1^2-K^2-1}\right\}. \tag{37}$$

We are especially interested in the disturbances that are amplified most rapidly, that is, in those for which μ_1 takes its numerically largest imaginary value, which is readily seen to be $\pm\frac{1}{2}i$, and occurs when $K = \frac{1}{2}\sqrt{3}$. In this case $\beta_1 = \frac{1}{4}$. It is seen that $\mu_1 = -\frac{1}{2}i$ is the appropriate coefficient for an amplified wave.

In general, when μ_1 is imaginary, the second term on the right-hand side of (37) gives the imaginary part of β_1. This is of the first order in $\kappa \equiv K-\frac{1}{2}\sqrt{3}$, and so $|\beta| = \frac{1}{4}$, to the second order in κ

The solution of (30) in terms of κ is

$$\begin{aligned}\mu_1^2 &= (\tfrac{1}{2}\sqrt{3}+\kappa)^2+1-\sqrt{\{4(\tfrac{1}{2}\sqrt{3}+\kappa)^2+1\}}\\ &= -\tfrac{1}{4}(1-3\kappa^2+\ldots)\end{aligned}$$

to the second order in κ, and so

$$\mu_1 = -\tfrac{1}{2}i(1-\tfrac{3}{2}\kappa^2+\ldots) \tag{38}$$

also to the second order.

Finally, the imaginary part of β_1 is given by

$$\begin{aligned}\mathscr{I}(\beta_1) &= \frac{\frac{1}{2}\sqrt{3}+\kappa}{4(-\frac{1}{2})}\left\{\frac{-\frac{1}{4}-(\frac{1}{2}\sqrt{3}+\kappa)^2+1}{-\frac{1}{4}-(\frac{1}{2}\sqrt{3}+\kappa)^2-1}\right\}\\ &= -\tfrac{3}{8}\kappa\end{aligned}$$

to the first order in κ, so that

$$\beta_1 = \tfrac{1}{4}-\tfrac{3}{8}i\kappa$$

and

$$\alpha_1 = \frac{1}{4\pi}\left(1-\frac{3i\kappa}{2}\right). \tag{39}$$

For large values of τ the solution therefore asymptotically tends to

$$\begin{aligned} s_1 &= \int_K \alpha_1(K) e^{i(KX - \mu_1 \tau)}\, dK \\ &\sim \frac{1}{4\pi} e^{i\sqrt{3}X/2} \int_\kappa \left(1 - \frac{3i\kappa}{2}\right) e^{\frac{1}{2}(1-3\kappa^2/2)\tau} e^{i\kappa X}\, d\kappa \\ &\sim \frac{1}{4\pi} e^{i\sqrt{3}X/2} e^{\tau/2} \int_\kappa e^{-3\kappa^2\tau/4}\, e^{i\kappa X} d\kappa \\ &\sim \frac{1}{\sqrt{(12\pi\tau)}} e^{i\sqrt{3}X/2}\, e^{\tau/2} e^{-X^2/3\tau}. \end{aligned} \tag{40}$$

The solution is valid only at points where $|X| < \tau$, that is at all points where there is double streaming.

If the condensation $s_1(X, \tau)$ is produced by an input function $\delta(\xi - 2u)$ on the line $\eta = 0$, the corresponding point P in figure 3 has the coordinates $\xi = 2u$, $\eta = 0$, or $X = -u$, $\tau = u$. The expression for the condensation is now

$$s_1(X, \tau) = \frac{1}{\sqrt{(12\pi\tau)}} \exp\left[\frac{i\sqrt{3}}{2}(X+u) + \frac{\tau - u}{2} - \frac{(X+u)^2}{3\tau}\right]. \tag{41}$$

In general, let the input function be $e^{iq\tau_b}$ at the point $X = -\tau_b$ at time $\tau = \tau_b$, for $\tau_b > 0$; this instant is on the line $X + \tau = \eta = 0$. The corresponding condensation will be

$$s_1(X, \tau) = \int_{\tau_b=0}^{\infty} \frac{e^{iq\tau_b}}{\sqrt{[12\pi(\tau - \tau_b)]}} \exp\left[\frac{i\sqrt{3}}{2}(X+\tau_b) + \frac{\tau - \tau_b}{2} - \frac{(X+\tau_b)^2}{3(\tau - \tau_b)}\right] d\tau_b. \tag{42}$$

The integrand in (42) has the form $R(\tau_b)\exp[P(\tau_b) + iQ(\tau_b)]$, where P, Q and R are real, and $P(\tau_b)$ is a decreasing function of τ_b. The integral may therefore be approximated by

$$R(0)\exp[P(0) + iQ(0)] \int_0^\infty \exp[P'(0) + iQ'(0)]\tau_b\, d\tau_b$$

and so

$$s_1(X, \tau) \doteq \frac{1}{\sqrt{(12\pi\tau)}} \frac{\exp\left\{i\dfrac{\sqrt{3}X}{2}\right\} \exp\left\{\tau\left(\dfrac{1}{2} - \dfrac{X^2}{3\tau^2}\right)\right.}{i\left(\dfrac{\sqrt{3}}{2} + q\right) - \dfrac{1}{2} - \left(\dfrac{2X}{3\tau} + \dfrac{X^2}{3\tau^2}\right)}.$$

This is large only when $\tau \gg 1$, and in that case the greatest values of s_1 occur where $|X| \ll \tau$, giving, at such points,

$$s_1(X, \tau) \doteq \frac{1}{\sqrt{(12\pi\tau)}} \frac{\exp\left\{i\dfrac{\sqrt{3}X}{2}\right\} \exp\left\{\tau\left(\dfrac{1}{2} - \dfrac{X^2}{3\tau^2}\right)\right\}}{i\left(\frac{1}{2}\sqrt{3} + q\right) - \frac{1}{2}}. \tag{43}$$

When the input function is given by

$$f(\tau_b) = \int_{-\infty}^{\infty} g(q) e^{iq\tau_b}\, dq \tag{44}$$

we find

$$s_1(X,\tau) \doteq -\frac{\exp\left\{i\frac{\sqrt{3}X}{2}+\frac{\tau}{2}-\frac{X^2}{3\tau}\right\}}{\sqrt{(12\pi\tau)}}\int_{-\infty}^{\infty}\frac{g(q)\,dq}{\frac{1}{2}-i(q+\frac{1}{2}\sqrt{3})}. \tag{45}$$

As we shall show, the plasma oscillation in stream 1 before the collision generates an input function which may be described in the form of a Fourier integral, as in (44). The function $g(q)$ is such that

$$\langle g(q)g^*(q')\rangle = [w(q)w(q')]^{1/2}\delta(q-q') \tag{46}$$

where $\delta(q)$ is once again the Dirac delta function, and the diamond-shaped brackets $\langle\ldots\rangle$ stand for "expectation value of ...". There is no phase relation between any $g(q)$ and any $g(q')$, unless $q=q'$. It follows that

$$\langle s_1 s_1^*(X,\tau)\rangle = \frac{\exp(\tau-2X^2/3\tau)}{12\pi\tau}\int_{-\infty}^{\infty}\int_{-\infty}^{\infty}\frac{\langle g(q)g^*(q')\rangle\,dqdq'}{[\frac{1}{2}-i(q+\frac{1}{2}\sqrt{3})][\frac{1}{2}+i(q'+\frac{1}{2}\sqrt{3})]}$$

$$= \frac{\exp(\tau-2X^2/3\tau)}{12\pi\tau}\int_{-\infty}^{\infty}\frac{w(q)\,dq}{1+q\sqrt{3}+q^2}. \tag{47}$$

It only remains to express this result in terms of the internal motion of stream 1 before the collision. This is best described by means of a position coordinate ξ at rest in the stream, and the time coordinate τ. The linearized, dimensionless equations of the oscillation are

$$\partial v/\partial\tau = \mathscr{E} \qquad \text{(motion)}, \tag{48a}$$

$$\partial s/\partial\tau + \partial v/\partial\xi = 0 \quad \text{(continuity)}, \tag{48b}$$

$$\partial\mathscr{E}/\partial\xi = s \qquad \text{(Poisson)}. \tag{48c}$$

Hence $$\partial^2\mathscr{E}/\partial\tau^2+\mathscr{E} = 0,$$

and $$\mathscr{E} = G(\xi)e^{-i\tau} \tag{49}$$

in the complex notation. The form of the solution shows the well-known fact that the oscillations in the single stream have a frequency independent of the wave number, and so have zero group velocity. They cannot therefore propagate energy, and the part of stream 1 that has not yet collided remains unaffected by the part that has done so.

From (48a) and (49) it follows that

$$v = iG(\xi)e^{-i\tau}, \tag{50}$$

and from (48c) and (49) that

$$s = G'(\xi)e^{-i\tau}. \tag{51}$$

The average electrostatic energy per unit volume is

$$\frac{1}{16\pi}EE^* = \frac{1}{16\pi}\frac{m_0^2U^2}{\epsilon^2}\mathscr{E}\mathscr{E}^* = \tfrac{1}{4}Nm_0U^2GG^*(\xi),$$

and the average kinetic energy per unit volume of the electron gas relative to the stream as a whole is

$$\tfrac{1}{4}Nm_0uu^* = \tfrac{1}{4}Nm_0U^2vv^* = \tfrac{1}{4}Nm_0u^2GG^*(\xi).$$

The energy per unit volume of the electron plasma is therefore

$$\tfrac{1}{2}Nm_0U^2GG^*(\xi).$$

The input function for the motion in the region of counterstreaming is now $G'(\xi)e^{-i\tau}$, evaluated on the line $X(\equiv \tau-\xi) = -\tau$, or $\xi = 2\tau$, and is equal to $G'(2\tau)e^{-i\tau} \equiv f(\tau)$.

But the field in the incident stream may be represented by

$$G(\xi)e^{-i\tau} = e^{-i\tau}\int_{-\infty}^{\infty} \Gamma(l)\, e^{il\xi}\, dl; \tag{52}$$

if it is a random field there are no phase relations between any $\Gamma(l)$ and $\Gamma(l')$, unless $l = l'$. We have once again

$$\langle \Gamma(l)\Gamma^*(l')\rangle = [W(l)W(l')]^{1/2}\,\delta(l-l'), \tag{53}$$

and

$$\langle GG^*(\xi)\rangle = \int_{-\infty}^{\infty}\int_{-\infty}^{\infty} \langle \Gamma(l)\Gamma^*(l')\rangle\, dl dl'$$

$$= \int_{-\infty}^{\infty} W(l)\, dl. \tag{54}$$

The average internal energy per unit volume present in the dimensionless wave number range $(l, l+dl)$ is $\frac{1}{2}Nm_0U^2W(l)\,dl$; the total internal energy density of the plasma is

$$T_{\rm pl} = \tfrac{1}{2}Nm_0U^2\int_{-\infty}^{\infty} W(l)\, dl. \tag{55}$$

Further

$$G'(\xi)\,e^{-i\tau} = ie^{-i\tau}\int_{-\infty}^{\infty} l\Gamma(l)e^{il\xi}\, dl$$

and so

$$f(\tau) = ie^{-i\tau}\int_{-\infty}^{\infty} l\Gamma(l)e^{2il\tau}\, dl$$

$$\equiv i\int_{-\infty}^{\infty} (\tfrac{1}{4}q+\tfrac{1}{4})\Gamma(\tfrac{1}{2}q+\tfrac{1}{2})\, e^{iq\tau}\, dq. \tag{56}$$

We can now identify $g(q)$ with $i(\frac{1}{4}q+\frac{1}{4})\Gamma(\frac{1}{2}q+\frac{1}{2})$. Since there are no phase relations among the Γ's, there are none among the g's either, as required. It follows from (47) that

$$\langle s_1 s_1^*(X,\tau)\rangle = \frac{\exp(\tau-2X^2/3\tau)}{12\pi\tau}\,\frac{1}{16}\int_{-\tau}^{\tau}\int_{-\tau}^{\tau}\frac{(q+1)^2}{1+q\sqrt{3}+q^2}$$

$$\times\,\langle \Gamma(\tfrac{1}{2}q+\tfrac{1}{2})\Gamma^*(\tfrac{1}{2}q'+\tfrac{1}{2})\rangle\, dq dq'$$

$$= \frac{\exp(\tau-2X^2/3\tau)}{192\pi\tau}\int_{-\infty}^{\tau}\frac{(q+1)^2}{1+q\sqrt{3}+q^2}\,2W(\tfrac{1}{2}q+\tfrac{1}{2})\, dq$$

$$= \frac{\exp(\tau-2X^2/3\tau)}{48\pi\tau}\left\{\int_{-\infty}^{\tau} W(l)dl + O(1/\bar{l})\right\} \tag{57}$$

where $\bar{l}$ is the effective dimensionless wave number range of the internal oscillations. Now $\frac{1}{2}Nm_0U^2 = T_{\rm kin}$ is the initial kinetic energy of motion of the electrons in stream 1 relative to the (x,t) system of coordinates (which is symmetrical with respect to the two streams). It follows from (55) and (57) that

$$\langle s_1 s_1^*(X,\tau)\rangle = \frac{\exp(\tau-2X^2/3\tau)}{48\pi\tau}\,\frac{T_{\rm pl}}{T_{\rm kin}}. \tag{58}$$

It was one of the initial assumptions in setting up the linearized equations of motion that the condensation s_1 is much less than unity. Equation (58) shows that this is most probably no longer true when

$$\frac{\exp(\tau - 2X^2/3\tau)}{48\pi\tau} \geqslant \frac{T_{\rm kin}}{T_{\rm pl}}. \tag{59}$$

However, when s_1 is of order unity, the energy per unit mass of the plasma oscillations in the double stream will be comparable with the initial relative kinetic energy per unit mass of the two streams; since the former must grow at the expense of the latter it follows that the relative motion will by that time have been stopped to a large extent. The minimum value $\tau_{\rm crit}$ which satisfies (59) therefore leads to an estimate of the length of time for which the two streams can interpenetrate, and of the depth to which they can do so.

The smallest value of τ for which (59) holds occurs at $X = 0$, that is at the position where the two streams made first contact, and here

$$\frac{\exp(\tau_{\rm crit})}{48\pi\tau_{\rm crit}} = \frac{T_{\rm kin}}{T_{\rm pl}},$$

or

$$\tau_{\rm crit} \doteqdot \frac{a}{a-1}(a + \log a - 1), \tag{60}$$

where

$$a = \log\{48\pi(T_{\rm kin}/T_{\rm pl})\}. \tag{61}$$

To take some examples, when $T_{\rm pl}/T_{\rm kin} = 10^{-1}$, 10^{-3} or 10^{-5}, $\tau_{\rm crit} = 9{\cdot}6$, $14{\cdot}6$ or $19{\cdot}6$, respectively. The times corresponding to these values are given by

$$t_{\rm crit} = \frac{\tau_{\rm crit}}{\Omega} = \tau_{\rm crit}\sqrt{\left(\frac{m_0}{4\pi N\epsilon^2}\right)};$$

since $2U$ is the initial relative velocity of the streams the corresponding distances of penetration of stream 1 into stream 2 are given by

$$2Ut_{\rm crit} = 2\tau_{\rm crit}\sqrt{\left(\frac{m_0 U^2}{4\pi N\epsilon^2}\right)}. \tag{62}$$

Any plasma oscillation initially present in stream 2 will lead to a further contribution to the right-hand side of (58). If the oscillations in the two streams have roughly equal energies, the effect will be to multiply that side by 2, and this leads to a decrease by $\log_e 2 = 0{\cdot}69$ in the estimate for $\tau_{\rm crit}$.

The more accurate estimate for the distance of interpenetration of the streams, given in (62), only differs by the numerical factor $\sqrt{(2/\pi)}\tau_{\rm crit}$, from the earlier, cruder estimate given in (15). The numerical examples that have been quoted show that in any particular case $\tau_{\rm crit}$ depends, but only rather insensitively, on the ratio of the energies of the plasma oscillations present in the streams before collision to the energy of their relative motion.

References

Bostick, W. H. 1956 *Phys. Rev.* **104,** 292.

Kahn, F. D. 1955 Article in *Gas Dynamics of Cosmic Clouds* (ed. H. C. van de Hulst & J. Burgers), Ch. 20, p. 115. Amsterdam : North-Holland Pub. Co.

Lampert, M. A. 1956 *J. Appl. Phys.* **27,** 5.

Spitzer, L. 1956 *Physics of Fully Ionized Gases.* New York : Interscience Pub.

REVIEWS

Surveys in Mechanics: G. I. Taylor 70th Anniversary Volume, edited by G. K. BATCHELOR and R. M. DAVIES. Cambridge University Press, 1956. 475 pp. 50*s*. or $9.50.

It would be difficult to imagine a happier birthday present than a dedication volume of papers. The notion is not new, but few such volumes can have been so personally suited as this one is to Sir Geoffrey Taylor. Far from being an assortment of research progress reports by fellow scientists wishing to pay their respects, this is a limited collection of surveys of "fields of knowledge which he has made his own".

Following a biographical note by Sir Richard Southwell, the contents are as follows.

The mechanics of quasi-static plastic deformation in metals, by R. Hill
Dislocations in crystalline solids, by N. F. Mott
Stress waves in solids, by R. M. Davies
Rotating fluids, by H. B. Squire
The mechanics of drops and bubbles, by W. R. Lane and H. L. Green
Wave generation by wind, by F. Ursell
Viscosity effects in sound waves of finite amplitude, by M. J. Lighthill
Turbulent diffusion, by G. K. Batchelor and A. A. Townsend
Atmospheric turbulence, by T. H. Ellison
The mechanics of sailing ships and yachts, by K. S. M. Davidson

Readers of this Journal will not need to be told that this set of topics falls short of those to which G. I. Taylor has made central contributions. Isotropic turbulence dynamics (in fact, the very notion of isotropic turbulence), turbulent shear flow, propulsion at very small Reynolds numbers, flow past porous boundaries—these too could have been included. Like other fluid dynamicists, I have more than once had the experience of finding a pet idea stolen by G. I. Taylor decades before I even thought of it!

The singular talents of G. I. Taylor as a researcher need no more testimony than his own published—and unpublished—works. In an age of increasing dichotomy between theoretical and experimental research, a teacher can point to no better illustration of the benefits to be gained from combining the two.

The papers in this volume are of good quality and some are outstanding, though the group is variable in spirit and in purpose. My own limitations preclude pertinent comment on the solid mechanics work; perhaps a pardonable omission in this review. No single survey here is completely reportorial or completely critical, although the Lighthill, Ursell and Batchelor–Townsend contributions come closest to the latter.

Before taking up the individual fluid mechanics papers, I can't resist observing that Sir Geoffrey's direct descent from the mathematician Boole (mentioned in the pleasant biographical sketch by Sir Richard Southwell) in a sense runs counter to the old adage that scientific talent is handed down from father to son-in-law.

Rotating fluids

This is a clear, well-organized summary of work on disturbances in fluids which are basically in rigid body rotation. The chief headings are "1. Small disturbances", "2. A point source on the axis of rotation" and "3. Steady symmetric motions."

Part 2, apparently an improved version of a problem of Barua (*Quart. J. Mech. Appl. Math.* **8,** 1955), still has an *ad hoc* flavour. No criticism of the original paper is offered. Part 3, which includes the non-linear aspects, may treat them a bit more briefly than some specialists might prefer, but it does include some stimulating discussion.

Perhaps in the interest of brevity, the title seems more general than necessary; for example, there is much additional work on rotating fluids in the meteorological literature.

The mechanics of drops and bubbles

The topics treated here are: a particular kind of pendant drop, methods of producing drops, the behaviour of falling drops and their break-up, deposition of drops on obstacles, production of bubbles, and the dynamical behaviour of bubbles under various conditions.

This is a good job of assembling and organizing some remarkably dispersed groups of papers. As many readers will realize, the research literature in some of these areas is not only spread throughout a great assortment of professional journals, but is also presented from divergent points of view.

Since much of the work has been done with practical motivations, the publications often emphasize semi-empirical 'correlations' among parameters rather than a deductive approach based on fundamental fluid dynamics. In a sense these authors have continued the tradition by restricting themselves to reporting past work without pointing out the places where adverse criticism might be appropriate. Typical of this approach is the presentation of small Reynolds number droplet dynamics in impingement problems. Here the equations of motion are simply set down with the quasi-steady Stokes drag for a sphere already inserted. There is no hint of the considerable machinery of restriction and approximation which must be invoked.

Wave generation by wind

This is a gratifyingly critical article on a branch of hydrodynamics which seems on the verge of blossoming. The status of most of the older theoretical works is summarized in the following sentence. "Some hypotheses have thus remained without proof or disproof for many years, and through lapse of time are now taken more seriously than their authors would have wished." Quite apart from its merit as a piece of diplomacy, this sentence refers to a phenomenon noticeable elsewhere. Many engineers of the last 20 or 30 years have had far more literal faith in the 'mixing length' than did Taylor or Prandtl.

The general topics covered are as follows. Simple theory of stability of an interface, semi-empirical theories of wave generation, semi-empirical systems of wave forecasting, sea roughness, and surface slope due to wind.

There is an occasional lack of explicitness in describing experimental arrangements, especially noticeable where the traditionally aerodynamic concept of 'boundary layer' is involved.

The bibliography seems reasonable; perhaps the best known paper omitted is the extensive treatise of Hellström (*Ing. Vegen. Akad. Proc.* **158**, 1941).

Perhaps the most satisfying aspect of this paper is the emphasis on work that should be undertaken. It is not surprising to learn that well-defined laboratory experiments are given the highest priority. Research appears to be at the stage of evolution at which simplified laboratory studies aimed at an understanding of the basic mechanisms of phenomena are often dismissed as 'unrealistic' by professional oceanographers. This is presumably characteristic of any activity passing from a descripto-empirical stage to a scientific stage. In schools of oceanography in the United States, for example, it seems generally expected that even theoreticians should get their feet wet. How long is it since theoretical aerodynamicists were expected to hold pilot licences?

Atmospheric turbulence

Closely related to the problem of wind generated water waves is that of atmospheric turbulence. The general topics covered in this account are: mean profiles of wind, temperature and water vapour near the ground, experimental work on mean profiles, and turbulent fluctuations.

This is a generally good presentation, and is oriented more from meteorology than from fluid dynamics. The comparison of independent sets of data gives a critical aspect to the account. On the other hand, the invocation of traditional semi-empirical formulae is largely uncritical. For example, in discussion of the diffusion equation often used for heat and water vapour transport studies, Dr Ellison choses to omit mention of the apparent invalidity of the simple gradient transport concept here. A necessary condition for its applicability is that the characteristic convective scale (mean free path in kinetic theory, Lagrangian length scale here) be sufficiently small relative to the mean concentration field, and it is well known that this condition is not satisfied by conventional turbulent flows. Yet gradient transport calculations can often 'correlate' empirical data quite well, so we might say that this approach is not useful in principle, but merely in fact.

Although meteorologists seem more appreciative of laboratory experiments than do oceanographers, limitations of space apparently precluded coverage of the few but pertinent laboratory results on turbulent boundary layers over rough walls.

The mechanics of sailing ships and yachts

The first impression of this paper is that it has been written partly in some language other than English. Bewildered by the use of salty argot at crucial points in the exposition, I fortunately had a little-thumbed copy of *Shanty Men and Shanty Boys* by W. M. Doerflinger (New York: Macmillan, 1951). Having decoded the message, I found the story both fascinating and astonishing—fascinating because of what has been accomplished and recorded in the art of designing and operating sailing ships,

astonishing because so little use has been made up to the present time of scientific progress in fluid mechanics.

The latter fact suggests that the sailing ship is on the way out. Or perhaps the yacht racing set is less wealthy than is commonly believed. On the other hand, it is possible that the sea is a force for conservatism; there is no great evidence that design of motor driven ships has taken much advantage of modern fluid dynamics either.

In reference to the technical content, it might have been more appropriate to title this paper "the ***performance*** of sailing ships and yachts". The problem of sailing against the wind is very well expounded. On the other hand there is a lack of dynamical explanation for the speed figures tabulated. In general one gets the impression of an intriguing field of engineering in which the most exciting problems remain to be solved.

Turbulent diffusion

This is a general and authoritative survey of the field of turbulent dispersion, with particular emphasis on the authors' own contributions. Since this domain is somewhat closer to my line of work than the rest of the volume, I take the liberty of more explicit comments*.

This exposition has such good qualities of lucidity and logical organization that newcomers to the subject may get the impression of a more satisfactory current status for the turbulent diffusion problem than actually exists. A possible reason is some tendency toward de-emphasis of the distinctions among empirical facts, intuitive conjectures, and theoretical results.

Typical illustrations are as follows. (*a*) The authors point out (p. 356) that the transition probability Q, "if it is like other probability density functions relating to turbulent motion . . . , will not be too far from the normal or Gaussian form." Nothing in this text vicinity warns the reader that the Gaussian form of these other p.d.f.'s is a partly empirical fact and, furthermore, that very few kinds have ever been measured. (*b*) On pp. 358, 359, the unwary neophyte might get the impression that both particle displacement probability P and transition probability Q have been shown to satisfy classical diffusion equations. Of course, this is not a deductive result —as the authors point out on p. 360. (*c*) The reader is not warned that the method used to present the data on diffusion in decaying isotropic turbulence, although successful for existing data, is restrictive: it requires the Eulerian and Lagrangian lengths to be simply proportional during decay. Although this may be a good approximation during the 'initial period' of decay, the authors certainly would not wish to convey this as a general property of turbulence. (*d*) Reference on p. 392 to later "deductions" that the average product of the three principal strain rates is negative may imply to the literate reader that this is a purely theoretical result. In fact, it is partly empirical as of the publication date of the volume.

Another section for cautious reading is that on fluid line and surface stretching. The presentation here is as heuristic as the pioneering paper of Dr Batchelor. Having encountered a number of fluid dynamicists with the impression that the original paper *proved* that fluid lines stretch,

* S. Potter, *The Art of Reviewsmanship*, New York Times, 8 May, 1955.

I should like to observe that the authors make no such claim. The fluid line stretching is a conjecture (and inferentially an empirical result from vorticity behaviour). The exponential rate follows from quite intuitive assumptions.

The discussion of lateral diffusion in shear flow is a mixture of careful formalism and *ad hoc* simplifications. The derivation of equations through (3.19) is an improvement over earlier published work. Then the quasi-Gaussian postulate is invoked in a situation where the non-Gaussian character of the fluctuation field may well be crucial. With a bit of hand waving, it is likely that the consequent approximation, $\overline{u'v^3} \doteqdot 3\overline{u'v}\,.\,\overline{v^2}$, can be qualitatively justified : $\overline{v^2}$ is positive, and v^3 has the same sign as v. Whether it can be given any quantitative justification seems unclear. Somewhat more startling is the bland assumption that $\overline{u'v^2} \doteqdot \overline{u'v}\,.\,\overline{v^3}/\overline{v^2}$. It is not evident *a priori* that even the sign of this approximation is correct.

The brief discussion of the behaviour of a diffusive scalar field embedded in an isotropic turbulence ignores much of the existing work on the subject (Obukhov, *Izvest. Akad. Nauk, S.S.S.R., Ser. Geofiz.* **13**, 1949, and Corrsin, *J. Aero. Sci.* **18**, 1951; *J. Appl. Phys.* **27**, 1951).

There are at least two specific improvements over previous writings on these subjects by Drs Batchelor and Townsend. (A) Equation (5.1), expressing the rate of growth of a fluid surface element, is in more elegant form than in the original paper of Batchelor. (B) The turbulence behind a regular grid is no longer referred to as being isotropic. The non-isotropy of these flows has been known to turbulence researchers in the United States since perhaps 1942 (Corrsin, A.E. Thesis, Cal. Tech., 1942), but the great importance and volume of the published grid turbulence data coming from the Cavendish Laboratory has given a rather general impression that virtual isotropy prevails within 16 or 20 mesh length of the grid. The latest Cavendish data are apparently in better agreement with those that have been taken at other laboratories.

From a pedagogical viewpoint the only serious omission is perhaps a statement of the nature of the problem of relating Lagrangian dispersion statistics to Eulerian statistical information. This, after all, is a possible definition of 'the problem' of turbulent diffusion. Given the statistical properties of the Eulerian (space-time) velocity field $u_i(x_j, t)$, the Lagrangian velocity field is

$$v_i(\mathbf{a}, t) = u_i(\mathbf{X}(\mathbf{a}, t), t). \tag{1}$$

The fluid point displacement is

$$X_k(\mathbf{a}, t) = \int_0^t v_k(\mathbf{a}, t)\, dt, \tag{2}$$

and

$$a_j = X_j(\mathbf{a}, 0).$$

Each realization of the Lagrangian time variation following a tagged fluid point (a_i = constant) is thus the variation along a trajectory through a member of the ensemble of Eulerian fields. The central difficulty of the problem is indicated by noting that each irregular 'sampling trajectory' is analytically related to the field it samples. Therefore we must deal with a stochastic integral equation. Putting (1) in (2) gives

$$X_k(\mathbf{a}, t) = \int_0^t u_k(\mathbf{X}(\mathbf{a}, t_1), t_1)\, dt_1. \tag{3}$$

The Lagrangian two-point correlation tensor is

$$L_{ik} = \overline{v(\mathbf{a}, t)v_k(\mathbf{a}+\boldsymbol{\alpha}, t+\tau)}$$
$$= \overline{u_i(\mathbf{X}(\mathbf{a}, t), t)u_k(\mathbf{X}(\mathbf{a}+\boldsymbol{\alpha}, t+\tau), t+\tau)}.$$

For stationary fields, this depends on $(\boldsymbol{\alpha}, \tau)$ only. Taylor expressed the mean square particle displacement in terms of the Lagrangian time correlations $L_{11}(0, \tau)$.

The theory of correlation functions obtained by sampling with random intervals over an ensemble of functions appears to be new to probability theory, even for the degenerate case in which the individual intervals are unrelated to the individual members of the ensemble being sampled. Yet we face here the still more complicated case in which each member of the function ensemble determines its own sampling interval through the integral operation (3).

Viscosity effects in sound waves of finite amplitude

This is a condensed 100 page review which treats virtually all phases of the title subject. Especially noteworthy are the careful clarification and correction of the various traditional approximations, and the use of Burgers' equation (where it is really appropriate), designed originally as a 'model' of turbulence. Equally appealing is the author's consistent emphasis on the Reynolds numbers of the various kinds of waves. The principal subject headings are as follows. The physical mechanism of viscosity and other diffusion effects in gases, attenuation of sound due to relaxation effects, classical theory of shock wave formation, structure of stronger shock waves, more general theory of plane shock wave formation, interiors of unsteady shock waves, formation and decay of non-plane shock waves, sound waves of moderate Reynolds number, relaxation effects in sound waves of finite amplitudes.

The remarkable coverage of this review will undoubtedly make it a standard reference for a long time to come. There are perhaps two other facets that could be included to round out the subject. Chapter two, on the physical mechanism, stops short of statistical mechanics. At the phenomenological level of the fluid dynamicist, the underlying physical mechanism resides in the molecular dynamics. Professor Lighthill has chosen to omit discussion of the challenging and poorly understood problem of how the probability density of molecular velocities changes from one form to another in a few mean free paths through a shock wave. It might have been appropriate to make special mention of the measurements of F. S. Sherman, giving profiles through a shock wave (*Nat. Adv. Comm. Aero., Wash., Tech. Note* no. 3298, 1955).

In conclusion, this volume is an impressive tribute to one of the great engineering scientists of this century. The only Taylor-associated writings I expect to enjoy more are the research papers he will publish himself in the future!

S. Corrsin

INDEX

Alpher, Ralph A. The Saha equation and the adiabatic exponent in shock wave calculations, 123.

Bakke, P. An experimental investigation of a wall jet, 467.

Benjamin, T. Brooke Wave formation in laminar flow down an inclined plane, 554.

Bennett, F. D. *See* **Steininger and Bennett.**

Binnie, A. M. Experiments on the onset of wave formation on a film of water flowing down a vertical plane, 551.

Case, K. M. and Parkinson, W. C. Damping of surfaces waves in an incompressible liquid, 172.

Chisnell, R. F. The motion of a shock wave in a channel, with applications to cylindrical and spherical shock waves, 286.

Cox, R. N. A cross-flow theory for the normal force on inclined bodies of revolution of large thickness ratio, 446.

Crane, L. J. and Pack, D. C. The laminar and turbulent mixing of jets of compressible fluid. Part I. Flow far from the orifice, 449.

Crapper, G. D. An exact solution for progressive capillary waves of arbitrary amplitude, 532.

Dumas, R. *See* **Favre, Gaviglio and Dumas.**

Ellison, T. H. Turbulent transport of heat and momentum from an infinite rough plane, 456.

Favre, A., Gaviglio, J. J. and Dumas, R. Space-time double correlations and spectra in a turbulent boundary layer, 313.

Feldman, Saul On the hydrodynamic stability of two viscous incompressible fluids in parallel uniform shearing motion, 343.

Freeman, N. C. On the stability of plane shock waves, 397.

Gadd, G. E. An experimental investigation of heat transfer effects on boundary layer separation in supersonic flow, 105.

Gaviglio, J. J. *See* **Favre, Gaviglio and Dumas.**

Glauert, M. B. A boundary layer theorem, with applications to rotating cylinders, 89.

Grant, H. L. and Nisbet, I. C. T. The inhomogeneity of grid turbulence, 263.

Hay, J. S. and Pasquill, F. Diffusion from a fixed source at a height of a few hundred feet in the atmosphere, 299.

Hayes, Wallace D. The vorticity jump across a gasdynamic discontinuity, 595.

Jahn, Robert G. Transition processes in shock wave interactions, 33.

Kahn, F. D. The collision of two ionized streams, 601.

Keller, Joseph B. and Weitz, Mortimer L. Upward ' falling ' jets and surface tension, 201.

Kovásznay, Leslie S. G. An electronic analogue for supersonic flow, 383.

Lighthill, M. J. Dynamics of a dissociating gas. Part I. Equilibrium flow, 1.

Lighthill, M. J. Corrigenda to " Drift ", 311.

Lighthill, M. J. Contributions to the theory of the Pitot-tube displacement effect, 493.

Lock, R. C. A note on the application of the supersonic area rule to the determination of the wave drag of rectangular wings, 575.

Milne-Thomson, L. M. A general solution of the equations of hydrodynamics, 88.

Moore, D. W. The flow past a rapidly rotating circular cylinder in a uniform stream, 541.

Morton, B. R. Buoyant plumes in a moist atmosphere, 127.

Nisbet, I. C. T. *See* **Grant and Nisbet.**

Owen, P. R. and Zienkiewicz, H. K. The production of uniform shear flow in a wind tunnel, 521.

Pack, D. C. *See* **Crane and Pack.**

Parkinson, W. C. *See* **Case and Parkinson.**

Pasquill, F. *See* **Hay and Pasquill.**

Payne, R. B. A numerical method for a converging cylindrical shock, 185.

Pearson, J. R. A. *See* **Proudman and Pearson.**

Phillips, O. M. On the generation of waves by turbulent wind, 417.

Proudman, Ian and Pearson, J. R. A. Expansions at small Reynolds numbers for the flow past a sphere and a circular cylinder, 237.

Proudman, J. Oscillations of tide and surge in an estuary of finite length, 371.

Scorer, R. S. Experiments on convection of isolated masses of buoyant fluid, 583.

Smith, F. B. The diffusion of smoke from a continuous elevated point-source into a turbulent atmosphere, 49.

Steininger, D. H. and Bennett, F. D. Interferometric test for *N*-wave flow, 209.

Thomas, D. B. and Townsend, A. A. Turbulent convection over a heated horizontal surface, 473.

Townsend, A. A. *See* **Thomas and Townsend.**

Weitz, Mortimer L. *See* **Keller and Weitz.**

White, Donald R. On the existence of higher than normal detonation pressures, 513.

Whitham, G. B. A new approach to problems of shock dynamics. Part I. Two-dimensional problems, 145.

Wood, W. W. Boundary layers whose streamlines are closed, 77.

Wooding, R. A. Steady state free thermal convection of liquid in a saturated permeable medium, 273.

Zienkiewicz, H. K. *See* **Owen and Zienkiewicz.**

REVIEWS

Theory of Combustion Instability in Liquid Propellant Rocket Motors, by Luigi Crocco and Sin-I Cheng, 100.

Momentum Transfer in Fluids, by W. H. Corcoran, J. B. Opfell and B. H. Sage, 204.

Relaxation Methods in Theoretical Physics, Volume II, by R. V. Southwell, 412.

Proceedings of the 8th International Congress on Theoretical and Applied Mechanics (*Istanbul* 1952), 416.

Viscous Flow Theory, I—Laminar Flow, by Shih-I Pai, 515.

Molecular Flow of Gases, by G. N. Patterson, 518.

Surveys in Mechanics: G. I. Taylor 70th Anniversary Volume, edited by G. K. Batchelor and R. M. Davies, 616.

Beginning with Volume 3, Part 1

JOURNAL OF FLUID MECHANICS

will be published by

CAMBRIDGE UNIVERSITY PRESS

Orders and subscriptions for Volume 3 should be sent through agents or booksellers, or direct, to :

CAMBRIDGE UNIVERSITY PRESS
Bentley House, 200 Euston Road, London, N.W.1

or, in the U.S.A. and Canada, to

CAMBRIDGE UNIVERSITY PRESS
American Branch
32 East 57th Street, New York 22, N.Y., U.S.A.

JOURNAL OF FLUID MECHANICS
Volume 2, Part 6 August 1957

CONTENTS

The production of uniform shear flow in a wind tunnel
by P. R. OWEN and H. K. ZIENKIEWICZ 521

An exact solution for progressive capillary waves of arbitrary amplitude
by G. D. CRAPPER 532

The flow past a rapidly rotating circular cylinder in a uniform stream
by D. W. MOORE 541

Experiments on the onset of wave formation on a film of water flowing down a vertical plane
by A. M. BINNIE 551

Wave formation in laminar flow down an inclined plane
by T. BROOKE BENJAMIN 554

A note on the application of the supersonic area rule to the determination of the wave drag of rectangular wings
by R. C. LOCK 575

Experiments on convection of isolated masses of buoyant fluid
by R. S. SCORER 583

The vorticity jump across a gasdynamic discontinuity
by WALLACE D. HAYES 595

The collision of two ionized streams
by F. D. KAHN 601

Reviews 616

Index to Volume 2 622

9075